ENGINEERING MESENCHYMAL STROMAL CELL CONSTRUCTS TO ENHANCE IMMUNOMODULATION

A Dissertation
Presented to
The Academic Faculty

By

Joshua A. Zimmermann

In Partial Fulfillment
Of the Requirements for the Degree
Doctor of Philosophy in Biomedical Engineering

Georgia Institute of Technology

August 2016

ENGINEERING MESENCHYMAL STROMAL CELL CONSTRUCTS TO ENHANCE IMMUNOMODULATION

Approved by:

Dr. Todd McDevitt, Advisor
Gladstone Institute of Cardiovascular Disease
Gladstone Institutes

Dr. Andrés García
Department of Mechanical Engineering
Georgia Institute of Technology

Dr. Ed Mocarksi
Department of Microbiology and Immunology
Emory University

Dr. Krishnendu Roy
Department of Biomedical Engineering
Georgia Institute of Technology

Dr. Susan Thomas
Department of Mechanical Engineering
Georgia Institute of Technology

Date Approved: 5/6/2016

ACKNOWLEDGEMENTS

I would like to start by thanking my advisor, Dr. Todd McDevitt, for his constant support and encouragement through graduate school. Todd was a great mentor who allowed me to develop my own project and taught me how to think critically, which has made a significant impact on my development as a scientist and an engineer. I would also like to thank my committee members, Dr. Ian Copland, Dr. Andrés García, Dr. Edward Mocarski, Dr. Krishnendu Roy, and Dr. Susan Thomas, for their insight into my project and all the helpful suggestions they provided over the years. The numerous members of the McDevitt have also provided so much help, advice, and support over the years. I want to particularly thank Dr. Melissa Kinney and Dr. Tracy Hookway for being fantastic leaders and role models of the group over the years. I also want to thank Dr. Jenna Wilson and Marian Hettiaratchi for always being there to discuss science in the lab and for being such great friends outside of lab. I want to also want to thank the other graduate students from my year, Torri Rinker, Denise Sullivan, Reggie Tran, and Ariel Kniss-James for being great friends throughout graduate school. Finally, I want to thank my parents, Frank and Nancy, and my brothers, Zack and Jacob, for all their love and support over the years.

TABLE OF CONTENTS

LIST OF TABLES

LIST OF FIGURES

LIST OF SYMBOLS AND ABBREVIATIONS

1-MT	1-Methyl-Tryptophan
ADSC	Adipose Derived Stem Cell
aMΦ	Activated Macrophage
APS	Ammonium Persulfate
BSA	Bovine Serum Albumin
CCM	Complete Culture Medium
DC	Dendritic Cell
DSS	Dextran Sodium Sulfate
ELISA	Enzyme Linked Immunosorbent Assay
FBS	Fetal Bovine Serum
GAG	Glycosaminoglycan
GvHD	Graft Versus Host Disease
HGF	Hepatocyte Growth Factor
HPL	Human Platelet Lysate
IDO	Indoleamine 2,3-Dioxygenase
IFN-γ	Interferon Gamma
IL-1β	Interleukin-1 Beta
IL-6	Interleukin-6
IL-10	Interleukin-10
LPS	Lipopolysaccharide
M-CSF	Macrophage Colony-Stimulating Factor

MP	Microparticle
MSC	Mesenchymal Stem/Stromal Cell
NFκB	Nuclear Factor Kappa B
OPG	Osteoprotegerin
PBMC	Peripheral Blood Mononuclear Cell
PBS	Phosphate Buffered Saline
PCR	Polymerase Chain Reaction
PGE_2	Prostaglandin E_2
PLGA	Poly-Lactic-Co-Glycolic Acid
PMA	Phorbol-12 myristate 13-acetate
RANK	Receptor Activator of Nuclear Factor κB
RANKL	RANK Ligand
TEMED	Tetramethylethylenediamine
TGF-β1	Transforming Growth Factor Beta 1
Th	T-helper cell
TLR3	Toll-Like Receptor 3
TLR4	Toll-Like Receptor 4
TNBS	Trinitrobenzenesulfonic Acid
TNF-α	Tumor Necrosis Factor Alpha
TRAP	Tartrate Resistant Acid Phosphatase
Treg	Regulatory T-cell
TSG-6	TNF Stimulated Gene 6
VEGF	Vascular Endothelial Growth Factor

SUMMARY

Mesenchymal stem/stromal cells (MSCs) are potent modulators of inflammatory and immune responses due to their ability to secrete soluble paracrine factors that regulate both innate and adaptive immunity and repolarize cells from pro-inflammatory to anti-inflammatory or pro-resolving phenotypes. Since the initial discovery that MSCs suppress T-cell proliferation and activation *in vitro*, MSCs have been demonstrated to regulate numerous leukocyte populations including T-cells, macrophages, dendritic cells, and natural killer cells. This ability of MSCs to modulate multiple components that contribute to the complexity of an immune response further motivated the use of MSCs to treat diseases such as graft-versus host disease, inflammatory bowel disease, and autoimmune disorders. In order to modulate immune response, multiple paracrine and immunomodulatory factors are expressed by MSCs that mediate suppression of immune cells and the coordinated action of the immunomodulatory secretome of MSCs is necessary to regulate complex immune responses. Importantly, these immunomodulatory factors are not constitutively expressed by resting MSCs and their expression is strongly induced by exposure of MSCs to inflammatory cytokines. Thus, MSC immunomodulation is highly dependent on the local inflammatory milieu to activate immunomodulatory factor expression. Due to the dependency of MSC immunomodulation on the local cytokine milieu, the efficacy of MSC-based cellular therapies is highly dependent on the *in vivo* environment they are exposed to after injection. The environment may be highly variable based on the individual and disease being treated, the stage of inflammation, and the site of MSC transplantation. For

example, high concentrations of inflammatory cytokines that often accompany acute inflammatory responses stimulate MSC immunomodulation. However, the low levels of cytokines observed in chronic inflammation may not be sufficient to induce MSC immunomodulatory activity, thereby limiting the ability of MSCs to regulate inflammation of certain disease states. Furthermore, MSCs are typically infused intravenously and the majority of cells are entrapped within the capillary beds of the lung tissue, distant from sites of inflammation. Entrapped MSCs are then rapidly cleared from the body within several days, limiting their residency time and effective window for immunomodulatory activity. Therefore, the objective of this dissertation was to develop strategies to enhance intrinsic MSC immunomodulatory activity to improve cellular therapies for the treatment of inflammatory and immune diseases. Three-dimensional MSC constructs offer a promising approach to control the microenvironment and thereby the immunomodulatory activity of MSCs while also enhancing acute cell survival and persistence after transplantation *in vivo*. Furthermore, engineering the physical and chemical elements of the MSC construct microenvironment through biomaterial-based approaches serves as a novel route to regulate the temporal presentation of inflammatory factors in order to sustain immunomodulatory activity *in vivo*. Altogether, this strategy offers a novel translatable means of controlling MSC paracrine activity post-transplantation and therefore, improve the efficacy of MSC-based treatment strategies for inflammatory and immune diseases.

CHAPTER 1

INTRODUCTION

The initial discovery that mesenchymal stem/stromal cells (MSCs) potently inhibit T-cell proliferation and activation upon T-cell receptor (TCR) stimulation *in vitro* motivated the use of MSCs as a potential therapeutic agent in inflammatory and immune diseases dominated by a pathogenic T-cell response and spurred research to better understand the interactions of MSCs and the immune system. Since then, MSCs have been demonstrated to regulate numerous leukocyte populations of both innate and adaptive immune systems, including T-cells, B-cells, macrophages, dendritic cells, and natural killer (NK) cells. Through the expression of numerous immunomodulatory factors in response to the inflammatory cytokine milieu, MSCs can modulate multiple signaling pathways and cell types that contribute to the complex pathogenesis of inflammatory and immune diseases that is currently unachievable with available drug treatment regimens. While the immunological mechanisms of MSCs are still actively under investigation, the demonstration of immunomodulatory effects in animal models has encouraged the investigation of MSCs as cell therapies in clinical trials for treatment of graft-versus host disease, inflammatory bowel diseases, and autoimmune disorders. However, positive therapeutic outcomes of MSC therapies in these clinical trials have not been consistently achieved; the variable responses have been attributed to donor-dependent variability of MSCs, environmental host factors, and limited cell survival and retention resulting from standard systemic intravenous delivery methods. More importantly, MSC

immunomodulation is critically dependent on the cellular microenvironment and the composition and concentration of the inflammatory cytokine milieu. High concentrations of inflammatory cytokines, such as interferon gamma (IFN-γ), which often accompany acute inflammatory responses, stimulate MSC expression of immunomodulatory factors. However, the low levels of cytokines observed in chronic inflammation may not be sufficient to induce MSC immunomodulation, limiting the ability of MSCs to regulate inflammation in these disease states. To address these critical challenges impeding the translation of MSC-based therapies, three-dimensional MSC constructs offer a promising approach to control the microenvironment and thereby the immunomodulatory activity of MSCs while also enhancing acute cell survival and persistence after transplantation *in vivo*. Furthermore, engineering the physical and chemical elements of the MSC construct microenvironment through biomaterial-based approaches serves as a novel route to regulate the temporal presentation of inflammatory factors in order to sustain immunomodulatory activity *in vivo*.

The *long term goal* that motivated the work of this dissertation was to develop strategies to enhance intrinsic MSC immunomodulatory activity to improve cellular therapies for the treatment of inflammatory and immune diseases. The **primary objective** of this work was to characterize the immunomodulatory secretome of MSCs in response to aggregation and inflammatory cytokines, in order to engineer transplantable stem cell constructs to enhance the extent and temporal kinetics of MSC immunomodulatory paracrine secretion to. The **central hypothesis** was that biomaterial-based presentation of MSC immunomodulation stimuli within 3D spheroids will result in the sustained and increased secretion of

immunomodulatory activity. The rationale for this work is that local presentation of inflammatory cytokines directly within the MSC 3D microenvironment may provide an additional level of control to promote persistent paracrine factor expression by regulating the spatial and temporal presentation of cytokines to transplanted MSC constructs. The central hypothesis was tested by the following specific aims:

Specific Aim 1: Determine the effects of aggregation and cytokine stimulation on MSC immunomodulation. The *working hypothesis* of this aim was that the MSC secretome can be manipulated by altering environmental conditions, such as three-dimensional aggregation and cytokine treatment, to enhance inherent immunomodulatory activity. The impact of the culture format (2D monolayer or 3D spheroids) and biochemical environment (culture media and cytokine milieu) on MSC immunomodulation was assessed by quantification of MSC paracrine factors and suppression of activated macrophages and T-cells in peripheral blood mononuclear cell (PBMCs) co-cultures. Furthermore, we more broadly assessed the effects of aggregation on the MSC secretome. From this analysis, we identified a highly differentially expressed secreted soluble factor, osteoprotegerin, and determined its functional role in suppressing T-cell proliferation and osteoclast differentiation.

Specific Aim 2: Engineer MSC/microparticle constructs to enhance immunomodulatory activity. The *working hypothesis* of this aim was that the presentation of biochemical stimuli of MSC immunomodulation within MSC spheroids can serve as a method of enhancing and sustaining inherent MSC immunomodulatory

activity that is applicable to cellular therapies for inflammatory diseases. The interaction between heparin microparticles and IFN-γ was investigated in order to deliver inflammatory cytokines directly within the spheroidal MSC microenvironment. The effects of microparticle incorporation within MSC aggregates on enhancing and sustaining immunomodulatory activity was evaluated by assessing paracrine factor secretion and suppression of activated macrophage and T-cells in PBMC co-cultures *in vitro*.

This project is *innovative* because it examines the ability to engineer the physical and biochemical elements of transplantable MSC constructs in order to direct MSC paracrine factor secretion and enhance immunomodulation. Through the completion of this project, we have demonstrated the ability to precisely engineer the environment of transplantable MSC multicellular aggregates in order to induce sustained immunomodulatory activity. This work establishes a novel and translatable approach that can be used to improve current MSC-based therapies for inflammatory and immune disorders and potentially expand the use of MSCs to disease states where current MSC strategies are ineffective. Finally, the results of this project have yielded novel scientific insights into the mechanisms governing the effects aggregation plays on MSC paracrine activity.

CHAPTER 2

BACKGROUND

2.1 Mesenchymal Stem/Stromal Cells

The origins of mesenchymal stem/stromal cell (MSC) research dates back to the 1960s with the identification of "colony-forming fibroblasts" within the bone marrow stroma that were capable of forming new bone after transplantation to an ectopic site [1, 2]. These cells were later termed "mesenchymal stem cells" and were described as a proliferative, plastic adherent cell population with a potential for differentiation to the cells of skeletal tissue, in particular osteoblasts, adipocytes, and chondrocytes [3, 4]. Since these initial discoveries, cell populations that exhibit similar phenotypes and differentiation potential have been isolated from numerous tissues in addition to bone marrow, most notably in adipose [5], umbilical cord [6]. Due to the use of "mesenchymal stem cell" to describe cell populations derived from different tissue sources using different isolation and expansion methods, the International Society for Cellular Therapy designated minimal criteria for defining human "multipotent mesenchymal stromal cells" in an attempt to standardize MSC research. These criteria include: 1) adherence to tissue culture plastic, 2) surface antigen expression profile, and 3) tri-lineage differentiation potential to osteogenic, adipogenic, and chondrogenic lineages [7]. Specifically, *in vitro* culture expanded MSCs should express the surface markers CD105, CD73, CD90 and be negative for the endothelial and hematopoietic cell markers CD34, CD45, CD14, CD11b, CD79α, CD19, and HLA-DR. Furthermore, culture expanded MSC cultures are a heterogeneous population and individual cells do not all have the same multilineage potential [8, 9]. Therefore, the use of “stromal cell” instead of “stem

cell" more accurately describes MSCs as the stem cell properties (i.e. *in vivo* self-renewal and clonal multipotency) of most MSC preparations are untested.

Despite the heterogeneous nature of MSC preparations, rare self-renewing progenitor cells capable of differentiating into cells of skeletal tissue have been identified among human bone marrow MSCs [10]. However, one of the challenges of studying this stem cell population is that no unique phenotypic marker of bone marrow mesenchymal stem cell exists. The surface markers CD73, CD90, and CD105 are not specific to MSCs and are commonly expressed by stromal cells and fibroblasts of various tissues [11]. Furthermore, only CD105 has been shown to be expressed on uncultured human MSCs capable of generating CFU-F and both CD73 and CD90 expression are acquired during *in vitro* culture expansion [12]. CD44, which is highly expressed on culture expanded MSCs, actually selects for the bone marrow fraction with little CFU-F activity while the $CD44^-$ fraction contains the population with multilineage differentiation potential [13]. Additionally, several surface markers of fresh MSCs that have been demonstrated to enrich for CFU-F activity are downregulated in cell culture, such as STRO-1 or CD271 [14, 15] expression in human MSCs and Nestin expression in mouse MSCs [16]. Despite the lack of individual surface markers that precisely mark MSC populations, researchers have taken combinatorial approaches to select for cell populations that enrich for CFU-F and stem cell activity. Isolation of the $CD146^+CD45^-$ population from bone marrow yielded a population of self-renewing progenitor cells containing all the CFU-F activity and capable of forming a heterotopic bone marrow niche in a subcutaneous transplantation model [10]. Alternatively, another study demonstrated that the $CD271^+$ fraction of bone marrow

contained all the CFU-F activity, although $CD271^{+}CD146^{+}$ co-expressing cells enriched for CFU-F activity compared to $CD271^{+}CD146^{-}$ population [17]. Numerous other markers have also been demonstrated to enrich for CFU-F activity or differentiation potential alone or in combination with CD271, CD146, CD90, CD73, and CD105 [18]. Despite these attempts to better define the heterogeneous MSC population, much work still needs to be done to precisely define and standardize phenotypic markers of the stem and progenitor cell population amongst MSCs in order to better understand which cells are responsible for the biological effects observed *in vitro* and after injection of MSCs.

The lack of unique markers of MSC populations also makes it difficult to determine the extent to which cells from various tissue sources differ in their phenotype and functionality. In the case of many of tissues, these MSC-like populations are not stromal cells but reside in a perivascular niche, such as in bone marrow [10, 16], fat [19], and skeletal muscle [20]. It is hypothesized that MSCs in these tissues may actually be perictyes, a cell population that lies on the abluminal side of blood vessels and wrap around endothelial cells [21]. Cultured pericytes share a similar morphology to MSCs [22], can differentiate into osteoblasts, adipocytes, and chondrocytes [23–25], and express similar surface antigens to MSCs [26]. Within the mouse bone marrow, several perivascular stromal cell populations exist that display MSC-like characteristics, including CXCL12-abundant reticular (CAR) cells and nestin-expressing cells [16, 27]. These bone marrow stromal cell populations play a critical role not only in supporting bone tissue repair and homeostasis but in supporting hematopoietic stem cell function as well. CAR cells were identified in mice by knocking in GFP into the *Cxcl12* locus and were found to be co-localized with HSCs within the bone

marrow [27]. These CAR cells expressed high levels of CXCL-12, also known as stromal derived factor 1 (SDF-1), an important paracrine factor that aids in retaining HSCs in hematopoietic organs [28]. Furthermore, investigators identified a subset of CXCL-12 expressing stromal cells that express GFP under the Nestin promoter [16]. In addition to CXCL-12, Nestin-GFP^{+} cells highly expressed the HSC regulatory paracrine factors angiopoietin-1 and stem cell factor (SCF) as well as the adhesion protein VCAM-1. Nestin-GFP+ cells were located in close proximity to HSCs within the bone marrow and generated ectopic bone and bone marrow after transplantation. Additionally, depletion of Nestin-GFP+ cells from the bone marrow by diphtheria toxin injection in Nes-Cre^{ERT2}; iDTR mice led to loss of HSCs. Another subset of perivascular stromal cells, CXCL-12 expressing cells were also identified by the Leptin receptor (LepR) [29]. These LepR^{+} cells also expressed high levels of SCF, highly enriched for CFU-F, produced new osteoblasts and adipocytes in adult bone marrow, and could form ossicles that support hematopoiesis. Furthermore, conditional deletion of SCF in LepR^{+} cells led to depletion of HSCs while deletion of CXCL-12 in LepR^{+} cells led to HSC mobilization, demonstrating the importance of the paracrine activity of these progenitor cells in the HSC niche. However, it remains unclear whether these cell populations, identified in the mouse, are equivalent to human CD45^{-}CD146^{+} cells that are also capable of reconstituting hematopoietic activity after ectopic transplantation. While the differences in bone marrow MSCs and MSC-like populations from other tissues sources remains unclear, recent evidence suggests that the stromal cell population of bone marrow contains perivascular progenitor cell populations responsible not only for the maintenance of bone and bone marrow stroma but also regulating HSC function through the secretion of paracrine factors.

While the importance of bone-marrow MSC populations in regulating components of the hematopoietic system *in vivo* have recently been demonstrated, no clear link has yet to been established between the immunomodulatory paracrine capabilities of culture expanded MSCs and their *in vivo* function. Interestingly, recent studies have begun to examine the interaction between MSC populations in the bone marrow and the differentiated progeny of HSCs that make up the immune system. In one example, CAR cells and Nestin-GFP$^+$ MSCs were found to regulate the egress and retention of monocytes in the bone marrow in response to microbial challenge [30]. After systemic injection of a low-dose of lipopolysaccharide (LPS), MSCs upregulated expression of CC-chemokine ligand 2 (CCL2/MCP1) which promoted egress of monocytes from the bone marrow into the blood system. In another study, MSCs function was found to be regulated by components of the immune system within the bone marrow environment. CD169$^+$ macrophages within the bone marrow were found to promote Nestin-GFP$^+$ MSC expression of HSC maintenance factors [31]. While the exact mechanism by which CD169$^+$ macrophages promoted MSCs paracrine activity were not elucidated, insulin like growth factor 1 (IGF-1), interleukin 1 (IL-1), interleukin 10 (IL-10), and TNF-α were not responsible. Importantly, this ability of MSCs to respond to the local environment and environmental factors (i.e. immune cells, cytokines, TLR ligands) is a characteristic also shared by culture expanded MSCs. MSCs respond to inflammatory cytokines including IFN-γ, TNF-α, IL-1β, and IL-17 [32–36] as well as TLR3 and TLR4 agonists (dsRNA and LPS, respectively) [37, 38] by increasing their production of anti-inflammatory paracrine factors. However, it remains unclear if MSCs use the same mechanisms *in vivo* to respond to inflammation and regulate the

immune response. Further understanding of the interactions between MSCs and components of the hematopoietic and immune systems, especially during inflammatory disease states, may provide further insight into the mechanisms of culture expanded MSC immunomodulation.

2.2 MSC Immunomodulation

The finding that *in vitro* culture expanded bone-marrow derived MSCs suppress T-cell proliferation *in vitro* [39, 40], has led a rapid increase in the investigation of MSCs as potential immunomodulatory agents for the treatment of inflammatory and immune diseases. Since these initial discoveries, the ability of MSCs to suppress the activation and function of cellular components of both innate and adaptive immunity, including neutrophils, macrophages, dendritic cells, natural killer cells, T lymphocytes, and B lymphocytes have been extensively investigated [41]. These studies have demonstrated that paracrine signaling plays a critical role in MSC immunomodulation and a single cytokine, chemokine, or growth factor alone is not responsible for the broad immunomodulatory effects on numerous immune cell populations. Furthermore, MSC immunosuppression has been found to be dependent on the coordinated modulation of myeloid and lymphoid populations simultaneously in order to promote the resolution of inflammation. Because of the multifaceted approach used to regulate the complex inflammatory milieu, MSCs offer a potent alternative to conventional drug treatment regimens. Therefore, MSCs are being explored clinically as a potent alternative approach to the treatment of diseases such as graft-versus-host disease [42–45], multiple sclerosis [46–49], inflammatory bowel disease [50–53], and systemic lupus erythematosus [54, 55].

Clinically, intravenous (I.V.) delivery of MSCs was initially thought to result in migration of MSCs to sites of inflammation and injury by following chemotactic signals and upon arrival, impart their immunomodulatory action through secretion of soluble paracrine signals without engrafting within the host tissue. However, in actuality, the vast majority of I.V. infused MSCs are entrapped within the lung (>60% in lung, 10% in liver, and <5% in other tissues) and do not survive for more than a few days [56, 57]. Despite minimal homing to inflamed tissue and poor survival post-infusion, a growing list of clinical studies have provided evidence that MSC infusion can improve the clinical condition of patients [58, 59]. However, lack of standardization of MSC isolation, culture, and delivery to patients as well as the variability in the environment between different patients and diseases treated by MSCs has limited the ability of researchers to precisely determine the critical mechanisms mediating MSC immunomodulation *in vivo* and disease states in which MSC-based therapies are most effective.

Over the past ten years, significant progress has been made in understanding the molecular mechanisms governing MSC immunomodulation *in vitro* and *in vivo*. The production of soluble secreted factors such as prostaglandin E2 (PGE_2), transforming growth factor beta 1 (TGF-β1), TNF-α stimulated protein 6 (TSG-6), hepatocyte growth factor (HGF), heme oxygenase-1 (HO-1), human leukocyte antigen G5 (HLA-G5), and interleukin-6 (IL-6), as well as the intracellular enzyme indoleamine 2,3-dioxygenase (IDO) have all been identified as important components of paracrine-mediated MSC immunomodulation of both innate and adaptive immunity [60–66]. Furthermore, blocking studies have demonstrated that inhibition of individual factors, such as PGE_2 [67], IDO [67, 68], TGF-

β1 [61], IL-6 [62], HGF [65], and IL-10 [69], can significantly reduce the potency of MSC immunomodulation in mixed lymphocyte reactions or in animal models. These studies demonstrate that a complex cocktail of paracrine factors are necessary for MSCs to regulate immune responses and therefore, delivery of individual factors alone is unlikely to recapitulate the immunomodulatory capacity of MSCs. While MSC expression of these immunomodulatory paracrine factors suppress inflammatory responses of numerous leukocyte populations including macrophages [70], dendritic cells [71, 72], B lymphocytes [73, 74], T lymphocytes [75, 76], and natural killer (NK) cells [77], these MSC-secreted paracrine factors can also induce anti-inflammatory and tolerogenic phenotypes, including M2 macrophages [78, 79], tolerogenic dendritic cells (DC) [80], and regulatory T cells (Tregs) [68, 81]. Thus, the potential of MSCs to not only suppress inflammatory responses but also induce immune cells towards anti-inflammatory and tolerogenic phenotypes suggests MSCs may provide an effective means of establishing endogenous cell populations capable of regulating inflammatory responses to prevent or resolve chronic inflammation.

In order to elicit immunomodulation, MSCs must be stimulated by signals in the local microenvironment in order to secrete immunomodulatory paracrine factors that alter immune cell responses [41]. The inflammatory cytokine milieu, including interferon gamma (IFN-γ), tumor necrosis factor alpha (TNF-α), interleukin 1 beta (IL-1β), and interleukin-17 (IL-17) regulates MSC immunomodulatory function by activating MSC expression of immunomodulatory factors such as IDO, PGE_2, and hepatocyte growth factor (HGF) [32–36]. Additionally, ligands for toll-like receptors TLR-3 and TLR-4 can regulate

MSC immunomodulation by altering paracrine factor secretion of MSCs [37, 38]. However, IFN-γ has been demonstrated to be a key inducer of MSC immunosuppressive activity. Wild-type MSCs prevented graft-versus-host disease and delayed-type hypersensitivity (DTH) in mice but MSCs lacking the IFN-γ receptor (IFNγR1$^{-/-}$ MSCs) or co-delivered with an anti-IFN-γ neutralizing antibody actually enhanced the immune response [33]. In human MSCs, IFN-γ priming induces expression of IDO, a key component of MSC regulation of adaptive immune responses [67, 82, 83], and the International Society for Cellular Therapy has recommended that the expression of IDO in response to IFN-γ be a key property to assess the immunomodulatory characteristics of MSC populations [84]. Furthermore, both the composition and concentration of the inflammatory cytokine milieu are critically important for MSC immunomodulation. Low concentrations of IFN-γ upregulate MSC expression of chemokines without induction of immunomodulatory factors, such as IDO, resulting in recruitment of lymphocytes without suppression of inflammation [85]. Additionally, antigen-pulsed MSCs stimulated with a low concentration of IFN-γ can act as antigen-presenting cells and activate antigen-specific CD8+ T-cells [86, 87]. Thus, strong inflammatory signals stimulate MSC immunosuppression while weak inflammation can actually enhanced the immune response [88]. Taken together, these studies demonstrate the importance of inflammatory signals in initiating MSC immunomodulatory factor expression.

2.2.1 MSCs and Monocytes and Macrophages

Monocyte migration into tissues and differentiation into macrophages plays a crucial role in the inflammatory response and in subsequent resolution of inflammation and tissue

regeneration [89]. Through the secretion of paracrine factors, MSCs can modulate the monocyte/macrophage response by recruiting monocytes to sites of inflammation and repolarizing macrophages from inflammatory anti-microbial M1 to pro-resolving M2 phenotypes, thereby supporting resolution of inflammation and wound healing. As described above, mouse MSC-like populations in the bone marrow regulate monocyte egress from the bone marrow in response to microbial challenges through a CCL2/MCP1 dependent mechanism [30]. Furthermore, MSCs at sites of inflammation can recruit monocytes and macrophages into inflamed tissue by secretion of the chemokines CCL3, CXCL2 (MIP2), and CCL12 (MCP5) [90]. Upon recruitment of macrophages, MSCs are thought to promote polarization of macrophages to M2-like phenotypes that promote tissue repair and enhance clearance of apoptotic cells. *In vitro*, co-culture of MSCs with monocytes induces M2 polarization of macrophages that have high IL-10 expression, low TNF-α, IFN-γ, and MHC class II expression, and phagocytic activity [79, 91, 92]. MSC regulation of macrophage phenotype has been demonstrated to be dependent on several mechanisms including IDO and PGE_2 expression [78, 79]. Priming of MSCs by IFN-γ, TNF-α, or LPS further enhances MSC induction of M2 macrophages by increasing MSC expression of PGE_2 and IDO. *In vivo*, MSCs reprogramming of macrophage phenotype was first demonstrated in a sepsis model in which injection of mouse MSCs decreased lethality by inducing IL-10 producing M2 macrophages that blocked excessive neutrophil infiltration into the peritoneum [70]. Similar results were observed in an endotoxin-induced lung injury model, in which local delivery of mouse MSCs decreased the production of M1 cytokines TNF-α and CXCL2 and increased the production of the M2 cytokine IL-10 by alveolar macrophages [93]. Finally, in a zymosan-induced peritonitis model, infused

human MSC expression of TSG-6 interfered with TLR2 and downstream NF-κB signaling that inhibited M1 polarization of macrophages [94]. Altogether, MSCs can aid in the resolution of inflammation through the recruitment of monocytes and polarizing macrophages to pro-resolving phenotypes.

2.2.2 MSCs and Natural Killer Cells

Natural killer (NK) cells also play an important role in innate immunity by eliminating virus-infected and stressed cells and secreting pro-inflammatory cytokines such as IFN-γ and TNF-α [95]. MSC interactions with NK cells have been found to be dependent on the activation state of both the MSCs and NK cells. MSCs inhibit IL-2 and IL-15 induced proliferation of freshly isolated, resting NK cells, but have reduced inhibition of proliferation on IL-2 activated NK cells [77]. Additionally, MSCs can decrease NK cell cytotoxic activity, cytokine production, granzyme B release, and the expression of activating receptors NKp30, NKp44, and NKG2D [77, 96]. These effects are mediated through cell-cell contact, PGE_2, IDO, TGF-β, and soluble HLA-G5 [64, 97]. However, the decreased inhibition of activated NK cell proliferation may be due, at least in part, to the ability of activated NK cells to lyse autologous and allogeneic MSCs. Expression of the ligands for activating NK receptors, ULBPs, CD155, and Nectin-2, were found to be responsible for NK cell lysis of MSCs [98]. However, when MSCs are stimulated with IFN-γ prior to co-culture, NK-mediated lysis is inhibited [99], which may be in part due to upregulation of HLA class I by MSCs [77, 83] and downregulation of ULBP3 [100]. While the interaction between MSCs and isolated NK cells *in vitro* has been investigated, there is little information on how MSCs interact with NK cells *in vivo.* However, it is speculated

that resilience of IFN-γ activated MSCs may allow transplanted MSCs to elude NK-mediated lysis in inflammatory environments and plays a role in the decreased immunogenicity of allogeneic MSCs [101].

2.2.3 MSCs and Dendritic Cells

Dendritic cells (DCs) serve as a link between the innate and adaptive immune responses by both producing cytokines and by acting as potent antigen-presenting cells. Upon activation, DCs upregulate MHCs, increase expression of co-stimulatory molecules, and migrate to secondary lymphoid tissue in order to prime T-cells for an adaptive immune response. Additionally, DCs produce cytokines that direct downstream T cell effector function. In both *in vitro* culture and *in vivo* animal models, MSCs have been demonstrated to interfere with many of these functions of DCs. For example, *in vitro* MSCs inhibit DC endocytosis, decrease expression of MHC and co-stimulatory molecules CD40, CD80, CD83, and CD86 during DC maturation, and decrease expression lymph node homing chemokine receptor CCR7 [71, 102, 103]. Furthermore, DCs differentiated in the presence of MSCs have a reduced ability to stimulate naive T cell proliferation. Infused MSCs also inhibit DC function *in vivo* by suppressing DC maturation, cytokine secretion, and migration to lymph nodes. Infusion of MSCs decreased the number of CCR7 and CD49dβ1, markers of DC activation, expressing DC in draining lymph nodes and decreased antigen priming to ovalbumin-specific CD4+ T-cells [80]. The mediators of MSC modulation of DC function include IL-6, which partially contributes to MSC inhibition of DC differentiation and downregulation of maturation markers [62]. Additionally, contact-dependent Notch signaling has also been demonstrated to be

important for MSC-dependent inhibition of DC differentiation and maturation [104] and may be mediated through MSC expression of the Notch ligand Jagged-2 [105]. Altogether, infused MSCs may significantly impair the development of an adaptive immune response by inhibiting DC migration, maturation, and antigen presentation.

Similarly to the effects of MSC on repolarization macrophages from pro-inflammatory to anti-inflammatory or pro-resolving phenotypes, MSCs can alter the phenotype of DCs from a lymphocyte stimulatory DC into a tolerogenic DC. *In vitro*, co-cultures of MSCs with DCs, increases DC production of IL-10 and TGF-β, decreases production of pro-inflammatory cytokines IL-12 and TNF-α, and increases phagocytic activity [106, 107]. Furthermore, DCs generated in the presence of MSCs *in vitro* do not activate $CD4^+$ T-cells [108] but do promote the generation of antigen-specific Tregs [109]. Both MSC expression of PGE_2 and Notch ligands, such as Jagged-2, have been implicated in converting mature DCs into a regulatory phenotype [110, 111]. Furthermore, MSCs have been found to generate tolerogenic DCs through an IL-10 dependent activation of suppressor of cytokine signaling-3 (SOCS-3) signaling [106]. However, it is unclear whether these pathways and mechanisms are responsible for MSC generation of tolerogenic DCs after infusion *in vivo* that have been shown to inhibit delayed-type hypersensitivity responses [106, 107] and aid in heart and skin allograft survival in the presence of low-dose immunosuppression [112]. Thus, transplanted MSCs may regulate immune responses, not only by inhibiting DC antigen presentation and subsequent activation of T-cells, but also induce tolerogenic DC phenotypes that can actively aid in resolving inflammation and induce tolerance to transplanted tissue.

2.2.4 MSCs and T-Cells

T-cells play a critical role in adaptive immunity and become activated in response to antigen presented by professional antigen presenting cells [113]. Activation of naïve T-cells results in proliferation and differentiation to distinct phenotypes with characteristic cytokine profiles dependent on the cytokine milieu during activation. MSC suppression of activated T-cell proliferation *in vitro* [39, 40] initially sparked the investigation of MSCs as potential immunomodulatory agents. *In vitro*, MSCs have consistently been reported to suppress both $CD4^+$ T-helper (Th) cells and $CD8^+$ cytotoxic T cell proliferation and activation [114]. Both mitogen- and antigen-stimulated proliferation of T-cells is inhibited by MSCs and results in arrest of T-cells in the G_0/G_1 phase of the cell cycle [115]. MSC suppression of T-cell proliferation has largely been attributed to the expression of IDO which inhibits T-cell proliferation through depletion of tryptophan [77, 116]. Additionally, metabolites derived from IDO catabolism of tryptophan, including kynurenine, also aid in suppression of T-cell proliferation through activation of the stress response kinase GCN2 [117, 118]. In addition to IDO, other MSC-expressed paracrine factors can aid in suppression of T-cell proliferation, including PGE_2 [60, 119], HLA-G5 [64], and TGF-β1 [120].

In addition to the suppression of T-cell proliferation, MSCs are capable of altering the balance of $CD4^+$ helper T-cell phenotypes. Numerous studies have demonstrated that MSCs can shift the balance of $CD4^+$ T-cells from a pro-inflammatory IFN-γ and TNF-α expressing Th1 phenotype to an IL-4, IL-5, IL-10, and IL-3 expressing Th2 phenotype both

in vitro [121] and *in vivo* [122, 123]. Th1 cells are involved in clearance of intracellular pathogens and delayed-type hypersensitivity and play an important role in inflammatory and autoimmune diseases such as type 1 diabetes mellitus and Crohn's disease. MSCs have been demonstrated to attenuate cutaneous DTH in mice by reducing infiltration of Th1 cells at the challenge site and promoting apoptosis of activated T-cells in the draining lymph nodes [124]. In another example, MSCs reduced disease scores in an TNBS-induced experimental colitis model by reducing IFN-γ production by Th1 cells and increasing the number of FoxP3+ Tregs [125]. Finally, MSCs have also been shown to suppress Th1-mediated diabetes mellitus in rats and mice [126, 127]. However, an opposite effect on Th populations is observed in the context of Th2 driven pathologies; MSCs promote the Th1 phenotype and cytokine profile and inhibit Th2 cytokine expression [44, 128]. Th2 responses are associated with host defense against extracellular parasites and recruitment of eosinophils and play an important role in allergic diseases. In an example of MSC suppression of Th2 responses, MSC treatment in an ovalbumin-induced airway inflammation model reduced the number of infiltrating eosinophils and reduced IL-4 and IL-13 production [129]. Additionally, an increase in IL-10 expression and $FoxP3^+$ cells was observed, suggesting that MSCs induced Tregs that mediated aided in suppression of the Th2 response. Similarly, MSC infusion in human subjects with chronic GvHD was reported to reduce IL-4 and IL-10 and increase IL-2 and IFN-γ producing T-cells [44]. Finally, MSCs can also inhibit Th17 differentiation [81, 130]. Through expression of IDO and PGE_2, MSCs suppress expression of the Th17 transcription factor RORγt and upregulate expression of the Treg transcription factor Foxp3 [131]. Th17 are characterized by their secretion of IL-17A, IL-21, and IL-22 and play a pathogenic role in several

diseases including rheumatoid arthritis, multiple sclerosis, and inflammatory bowel diseases. Several studies have demonstrated that MSC treatment can improve the disease state in experimental autoimmune encephalitis (EAE) models by suppression of IL-17 production and Th17 activity as well as upregulation of TGF-β and IL-4 in the central nervous system [132–134]. Like in MSC suppression of Th1 and Th2 responses, induction of Tregs has been associated with amelioration of Th17 inflammation in models of type 1 diabetes mellitus, collagen-induced arthritis, and EAE [61, 135]. Altogether, these studies demonstrate the ability of MSCs to shift the balance of Th phenotypes in multiple disease contexts, partially mediated by induction of regulatory T-cells that aid in MSC immunomodulation.

Tregs are a subset of CD4+ T-cells that display regulatory or suppressor functions and are thought to prevent autoimmunity and aid in resolution of inflammation. Tregs are characterized by their expression of CD25 and the transcription factor FoxP3 and can regulate the activation of Th cells and other immune cells. Initial studies demonstrated that co-culture of MScs with CD4+ T-cells induced a population of $CD25^{+}FoxP3^{+}$ Tregs that, when purified, displayed suppressive activity in a mixed lymphocyte reaction [136, 137]. Several mechanisms have been demonstrated to be involved in MSC induction of Treg populations. MSC IDO expression, in response to IFN-γ, induce naive $CD4^{+}CD25^{-}$ T-cell differentiation into $CD4^{+}CD25^{+}$FoxP3+ regulatory T-cells (Tregs) [138] and aids in the induction of immune tolerance *in vivo* [139]. MSC expression of TGF-β1 also play a critical role in the induction of inducing antigen-specific Treg phenotypes [140, 141]. Additionally, MSC expression of PGE_2 [136], HLA-G5 [64], HO-1 [66], CCL2 [134], and

Fas ligand [142] have all been demonstrated to play a role in MSC induction of Tregs *in vitro* and *in vivo*. Through these molecular mechanisms, MSC induction of Tregs has been strongly associated with protection from or alleviation of alloreactive [143, 144], autoimmune [61, 127, 142, 145], and allergic diseases [129, 146]. Therefore, Treg-mediated induction and maintenance of tolerance to self- or allo-antigens is thought to be a critical mechanisms by which MSCs can ultimately be beneficial in treating these diseases even when MSCs themselves do not persist in the patient over time.

Finally, in addition to $CD4^+$ T-cells, MSCs can also inhibit $CD8^+$ cytotoxic T-cells (CTLs) which are responsible for inducing cell death upon secondary encounter of antigen expressed on cells and are responsible for the extensive tissue damage in diseases such as graft-versus-host disease. MSC can suppress CTLs directly or indirectly by inhibiting Th responses which aid in activation of CTLs. Furthermore, MSCs are resistant to CTL lysis, even after pulsing MSCs with a high dose of synthetic peptide at high concentrations, despite expressing MHC class I [147]. Furthermore, MSCs did not upregulate CD25 or IFN-γ and TNF-α expression in CTLs. Similarly, CTL formation is inhibited in mixed lymphocyte cultures when MSCs are added to the culture [148]. However, while MSCs can prevent CTL activation during the primary stimulation phase, MSCs are not able to suppress already activated CTLs [149]. Interestingly, MSCs have little effect on T-cell responses to viruses compared to allo-antigen *in vitro* [150], suggesting that transplanted MSCs may be useful in suppressing pathogenic immune responses without impairing host defense against viral challenge.

2.3 Three-Dimensional Culture of MSCs

Self-assembled, scaffoldless, spheroidal aggregates of tightly packed MSCs have been proposed in order to improve or maintain MSC properties during *ex vivo* expansion by better recreating the three dimensional nature of the MSC niche[151, 152]. This 3D aggregation approach have been commonly applied to other stem cell and cancer cell populations to more closely recapitulate the three dimensional structure of tissues (i.e. cell-cell and cell-matrix interactions) [153]. For example, embryoid body culture has been a common technique for culturing pluripotent embryonic stem cells as a model of morphogenic events that occur during embryonic development [154]. Tumorspheres are another commonly used *in vitro* model to study cancer biology and potential therapeutics in a system that more closely mimics the physical structure of tumors *in vivo* [155]. Furthermore, aggregation of cells has been demonstrated to enhance the maintenance and culture of stem cell populations *ex vivo*. Neural stem cells are typically cultured as 3D "neurospheres" which aids in preserving their progenitor cell phenotype [156]. Similarly, when applied to the culture of MSCs, aggregation enhanced the intrinsic regenerative potential of MSCs by maintaining their differentiation capacity, increasing the secretion of angiogenic and immunomodulatory paracrine factors, and improving cell retention and survival post-transplantation [157].

Techniques such as hanging drop, forced aggregation, and culture on non-adherent surfaces are commonly used to confine MSCs in a high density in order to increase cell-cell contact and promote self-assembly [151]. By spatially confining cells, aggregation of MSCs can occur through cadherin mediated self-assembly of 3D spheroids. Several studies have

demonstrated that ethylenediaminetetraacetic acid (EDTA), a calcium-chelator, inhibits the ability of bone marrow and umbilical cord MSC to self-assemble into aggregates [158] by interfering with calcium-dependent cadherin binding [159]. Furthermore, MSCs are capable of forming spheroids in serum-free media with no supplemental ECM adhesion molecules, further suggesting that cadherin molecules are responsible for initial MSC aggregation [160, 161]. However, the specific cadherins mediating self-aggregation may be dependent on the cell source as well as the aggregation method. Bone marrow derived MSCs predominately express N-cadherin and cadherin-11 [162] whereas E-cadherin was found to be the primary cadherin mediating aggregation of umbilical cord derived MSCs [159]. Differential expression of cadherin expression is thought to mediate the ultrastructure of MSC aggregates, with high cadherin expression will be found at the interior of the aggregate while low cadherin expressing cells will be found at the exterior to minimize the surface free energy. Furthermore, cadherins play an important role in interfacing with the cytoskeleton and mediating cytoskeletal tension. As a result of aggregation, cells at the interior of the aggregate are rounded in shape due to decreased cortical tension from multiple cell-cell connections whereas MSCs at the exterior are spread due to the increased tension at the aggregate-medium interface [163–166]. Since biophysical changes in the cytoskeletal have been demonstrated to influence MSC differentiation and function [167, 168], these physical changes achieved by 3D aggregation of MSCs may play a role in the increased regenerative potential of aggregated MSCs.

As the trophic effects of MSCs are a key component of the regenerative potential of MSCs, it is unsurprising that the overall paracrine activity of MSCs is increased when MSCs are

aggregated into three dimensional spheroids. Secretion of the angiogenic factors VEGF, FGF-2, HGF, EGF, SDF-1, and angiogenin have all been found to be increased in MSC aggregate culture compared to adherent monolayer cultures [169–171]. Cadherins in particular have been found to be critically important in mediating the increased expression of angiogenic factors by MSC spheroids. For example, activation of N- and E-cadherin through cell-cell interactions regulate VEGF secretion in cord blood and umbilical cord derived MSCs, respectively [159, 172]. Furthermore, the immunomodulatory activity of MSCs is greater when MSCs are aggregated as spheroids. Secretion of the immunomodulatory factors TNF-α stimulated protein 6 (TSG-6) and PGE_2 are both increased in MSC aggregate cultures compared to adherent monolayer cultures [173, 174]. Upregualtion of TSG-6 and PGE_2 secretion in response to aggregation was dependent on activation of caspase signaling resulting in upregulation of IL-1α and IL-1β expression [175]. MSC expression of IL-1s was subsequently responsible for self-activation of NF-κB signaling resulting in increased expression of TSG-6 and PGE_2. Additionally, inhibition of Notch signaling through γ-secretase inhibitors resulted in decreased PGE_2 expression, suggesting that Notch signaling may also play a role in the increased immunomodulatory factor expression by MSC aggregates. The increased secretion of PGE_2 by MSC aggregates resulted in increased suppression of inflammatory cytokine secretion of LPS activated macrophages *in vitro* and polarized these macrophages to an M2-like phenotype [174]. Furthermore, MSC spheroids injected intraperitoneally (I.P.) in a zymosan-induced peritonitis mouse model resulted in a decreased inflammatory response (i.e. decreased inflammatory cytokines and secreted neutrophil myeloperoxidase in lavage fluid) compared to injection of adherent cultures MSCs or no MSC treatment. Additionally,

intraluminal injection of MSC spheroids improved disease scores and decreased inflammatory cytokine expression in a mouse model of colitis [176]. Altogether, these results demonstrate that several signaling pathways (cadherin, caspase, NF-κB, Notch) are involved in enhancing paracrine activity of MSCs upon aggregation.

The increased secretion of paracrine factors by aggregated MSCs has also been attributed to improved differentiation efficiency of MSCs cultured as spheroids. Culture of MSCs as large pellets (typically > 250,000 per aggregate) enhances the osteochondral differentiation potential of MSCs that is thought to be a result of the formation of a hypoxic core within the pellets [177, 178]. However, enhanced differentiation potential towards osteogenic, chondrogenic, and adipogenic fates has been demonstrated in smaller MSC spheroids (< 200 μm in diameter [179–181]), below the threshold of aggregate size at which oxygen gradients are expected to develop [182]. Alternatively, the increased differentiation potential of MSC aggregates may be due to the enhanced secretion of growth factors and ECM proteins observed in spheroid culture. For example, increased expression of fibroblast growth factor 2 (FGF-2) [169] and bone morphogenic protein 2 (BMP-2) [183] have been observed in MSC spheroid culture and both of these growth factors regulate MSC proliferation and differentiation towards osteochondral fates [184]. Furthermore, increased expression of ECM molecules such as fibronectin, collagens, and glycosaminoglycan [169, 185, 186] by MSCs cultured as spheroids may further aid in promoting differentiation and aid in locally presenting and retaining growth factors to further support MSC differentiation.

Importantly, differentiation of MSCs in aggregate culture requires the supplementation of differentiation cues into the culture medium to direct differentiation, suggesting that aggregate cultures alone does not induce spontaneous differentiation of MSCs. Instead of inducing differentiation, spheroid culture better maintains the multipotency of MSCs compared to adherent culture [187]. MSC spheroids cultured for over two weeks in growth medium did not differentiate toward adipogenic or osteogenic lineages but maintained their capacity for differentiation when transferred to mediums containing the necessary biochemical cues for differentiation [179]. Additionally, clonal aggregates of Nestin^{+} perivascular stromal cells that contain all the CFU-F activity within mouse bone marrow self-renew and generate heterotopic bone ossicles with hematopoietic activity after serial transplantations [16, 188], indicating that multipotency and hematopoietic activity is maintained in spheroid culture. Furthermore, spheroid culture may not only support maintenance of MSCs but also induce dedifferentiation of MSCs to an early mesendoderm-like state [189]. Since formation of a compact mesenchymal blastema and subsequent dedifferentiation is necessary for limb regeneration in zebrafish, xenopus, and newts, Pennock et al. sought to mimic these conditions by generating 3D spheroids of human MSCs. Aggregation of MSCs was found to reverse cell hypertrophy, increase expression of reprogramming factors (Oct4, Nanog, and Sox2) and early mesendoderm markers, and increase *in vivo* mesodermal tissue generation. Finally, an autophagic response of MSCs cultured as spheroids was observed and promoted cytoplasmic remodeling, mitochondrial regression, and a switch from oxidative phosphorylation to anaerobic metabolism suggesting a dedifferentiated state. Altogether, aggregation of MSCs improves biological activity by better maintaining or perhaps even inducing a more multipotent state.

Infusion or transplantation of single-cell suspensions of MSCs results in little retention and engraftment within desired tissues. For example, when systemically administered, the vast majority of cells are entrapped within the capillary beds of lung tissue and cleared from the tissue within a few days. Alternatively, transplantation of pre-formed cellular aggregates can improve cellular engraftment and viability [190]. In addition to the increased expression of angiogenic and ECM proteins that can aid in protecting transplanted cells from cytotoxic injury or inflammatory sites, maintenance of cell-cell interactions and ECM components of spheroids prior to implantation prevents anoikis and associated cell loss, yielding better engraftment in host tissue [159, 169, 186]. This improved cell-survival of MSC aggregates has been attributed to improved regenerative capacity in several wound healing models. For example, increased cell survival of MSC aggregates improved bone healing in heterotopic and orthotopic sites compared to single-cell MSC suspensions [191]. Furthermore, improved retention of MSC aggregates after transplantation of MSCs in cardiac and skeletal muscle was observed due to physical entrapment within the tissue due to aggregate size [159, 192]. Entrapment of MSC aggregates within cardiac tissue resulted in increased retention of cells and increased paracrine activity that ultimately improved cardiac function and reduced fibrosis in myocardial infarction in rodent models [185]. Altogether, transplantation of 3D MSC aggregates may be a means of improving retention and survivability of MSCs at sites of transplantation and thereby increasing the duration that transplanted MSCs can secrete therapeutic paracrine factors.

CHAPTER 3

AGGREGATION AND CYTOKINE PRE-CONDITIONING TO ENHANCE MESENCHYMAL STEM CELL IMMUNOMODULATORY ACTIVITY[1]

3.1 INTRODUCTION

Mesenchymal stem/stromal cell (MSC) immunomodulation and paracrine factor secretion is highly regulated by the local microenvironment of the cells [41]. In particular, the inflammatory cytokine milieu, including interferon gamma (IFN-γ), tumor necrosis factor alpha (TNF-α), and interleukin 1 beta (IL-1β), regulates MSC immunomodulatory function by activating MSC expression of immunomodulatory factors such as PGE_2, IDO, and HGF [32–34]. Furthermore, ligands for toll-like receptors TLR3 and TLR4 can regulate MSC immunomodulation by altering paracrine factor secretion of MSCs [37, 38]. Interestingly, 3D aggregation of MSCs also enhances immunomodulatory paracrine factor secretion, including PGE_2 and TNF-α stimulated gene/protein 6 (TSG-6), which aid in MSC suppression of macrophage inflammatory cytokine production [173–175]. While hypoxic conditioning due to transport limitations of oxygen within the 3D cellular structure has largely been implicated in the increased paracrine secretion observed in MSC spheroid cultures [169, 193], it is currently unclear what role 3D aggregation plays in enhancing MSC immunomodulation in small cellular aggregates where transport of oxygen is not a limitation. Furthermore, while the exact mechanisms and interplay of environmental parameters, including 3D aggregation and cytokine stimulation, on the regulation of MSC

[1] Modified from: Zimmermann JA, Mcdevitt TC. Pre-conditioning mesenchymal stromal cell spheroids for immunomodulatory paracrine factor secretion. *Cytotherapy*. 2014;16(3):331-345.

immunomodulation are not yet fully understood, variability in the biochemical or physical components of the local inflammatory environment may contribute to the success or failure of MSC-based therapies. Thus, understanding the specific effects of the local microenvironment regulating MSC immunomodulation activity may provide new insights into components of the microenvironment that can be utilized to enhance MSC immunomodulatory therapies that are broadly applicable to an array of inflammatory and immune diseases.

While MSCs have been investigated as cell therapies for the treatment of inflammatory and immune diseases, reproducibility of positive patient responses to MSC treatments in clinical trials has not been clearly demonstrated between studies with differences in patient populations, donor cells, culture conditions, and treatment regimens. The lack of a robust therapeutic response in these immune and inflammatory diseases has largely been attributed to inconsistent numbers of MSCs at sites of inflammation due to a lack of cell engraftment or insufficient cell homing [194, 195]. Additionally, discrepancies between studies have been attributed to variability in processing and culture conditions including growth medium and passage number, resulting in highly variable starting cell populations for transplantation [196]. Since MSC immunomodulatory factor secretion can be induced by environmental stimuli, culturing MSCs in a defined environment containing activating signals, such as with 3D aggregation or pro-inflammatory cytokine stimulation, may be a means of priming cells to increase immunomodulatory activity. MSCs that display increased immunomodulatory factor secretion immediately upon transplantation could enhance the therapeutic potential of MSCs during the relatively short resident times after

transplantation. Therefore, development of pre-conditioning strategies could maximize MSC immunomodulatory potential and thereby increase the effectiveness of MSC-based cell therapies for inflammatory and immune diseases.

The objective of this study was to systematically determine whether environmental culture conditions, such as three dimensional aggregation and pro-inflammatory cytokine stimulation, modulate endogenous MSC paracrine factor secretion and pre-condition MSCs to enhance their immunomodulatory activity. Human MSCs were cultured either as adherent monolayers or 3D spheroids formed via forced-aggregation in microwells with a prescribed number of cells per aggregate. Additionally, subsets of MSC cultured in monolayer and as spheroids were cultured in medium supplemented with the pro-inflammatory cytokines IFN-γ and TNF-α. The impact of spheroid culture and pro-inflammatory cytokine treatment on immunomodulatory paracrine factor secretion and pre-conditioning of MSCs was analyzed by morphological and phenotypic analysis as well as by evaluating suppression of inflammatory responses through co-culture with activated macrophages. Furthermore, the ability of MSC spheroids to suppress T-cell proliferation *in vitro* was evaluated. The results of this study demonstrate that 3D aggregation and pro-inflammatory cytokine treatment modulate MSC paracrine factor secretion and work synergistically to enhance MSC immunomodulation. Additionally, the results provide a translatable approach to pre-condition MSCs through 3D aggregation and pro-inflammatory cytokine pre-treatment to enhance their inherent immunomodulatory properties and thereby improve the efficacy of MSC-based treatments of inflammatory diseases and immune disorders.

3.2 MATERIALS AND METHODS

3.2.1 Cell Culture and Expansion

Human bone marrow-derived MSCs were obtained from the Texas A&M College of Medicine Institute for Regenerative Medicine and expanded according to established protocols [197]. Approximately $1x10^6$ cryopreserved MSCs were seeded onto a 15-cm tissue culture dish in 20 mL MSC complete culture medium (CCM, Minimal Essential Medium Alpha (MEMα, VWR, Radnor, PA) supplemented with 16.5% fetal bovine serum (FBS, Hyclone, Logan, UT), 2mM L-glutamine (Corning cellgro, Manassas, VA), 100 U/mL penicillin and 100 µg/mL streptomycin (Corning cellgro)). After overnight incubation, adherent MSCs were washed with phosphate-buffered saline (PBS, Invitrogen, Carlsbad, CA) and detached from the plate using 0.25% trypsin and 1 mM EDTA in Hanks' Balanced Salt Solution (Corning cellgro). Dissociated cells were counted using a hemocytometer and plated onto 15-cm tissue culture dishes at a density of 60 cells/cm^2 in 20 mL CCM per dish. Media was completely exchanged every 3 days until cells reached approximately 70% confluence. Cells were trypsinized, counted, and either re-plated for monolayer expansion cultures or used for experiments after passage 4. MSCs from Texas A&M College of Medicine Institute for Regenerative Medicine were used for evaluation of cell viability and histology, immunomodulatory factor quantification, and THP-1 cell co-cultures described below.

Human bone marrow-derived MSCs were also obtained from RoosterBio Inc. (Frederick, MD) and expanded according to the manufacturer's protocols. Briefly, 10^7 cryopreserved MSCs were plated in twelve T225 flasks in 42 mL of RoosterBio High Performance Media

and incubated at 37°C for 7 days in a humidified 5% CO_2 incubator. Media was exchanged after 4 days of culture. Cultures were passaged at 80% confluency by washing with 10 mL PBS followed by incubation with 10 mL of TrypLE at 37 ºC. An equal volume of RoosterBio High Performance Media was added to quench TrypLE activity. Dissociated cells were then collected and centrifuged at 200xg. Cells were frozen in CryoStor CS5 cell cryopreservation media (STEMCELL Technologies, Vancouver, BC, Canada) prior to expansion for experiments. MSCs were expanded for one or two passages from frozen stocks by plating $0.5x10^6$ cells in RoosterBio High Performance Media in 15 cm tissue culture treated dishes. Media was exchanged every three days and cells were passaged at 80% confluency. MSCs from RoosterBio Inc. were used in peripheral blood mononuclear cell co-cultures described below.

3.2.2 Spheroid Formation and Culture

Forced-aggregation of single cell suspensions of MSCs was used to generate MSC spheroids. Spheroids were formed overnight in 400 µm agarose microwells for a high throughput method of generating homogenous cell aggregates [198]. Briefly, $1.2x10^6$, $3x10^6$, or $6x10^6$ MSCs were added to 6-well microwell inserts containing approximately 6,000 wells and centrifuged at 200xg for 5 min to force aggregation of spheroids with approximately 200, 500, or 1000 cells per aggregate, respectively. After 18h in the microwells, spheroids were removed and transferred to suspension culture in 100 mm bacteriological grade Petri dishes at equivalent total cell densities (~300,000 cells per plate; 1500 200-cell spheroids, 600 500-cell spheroids, 300 1000-cell spheroids). Spheroids were cultured in suspension on a rotary orbital shaker for up to 4 days at 65 RPM. Additionally,

adherent MSC controls were plated in 10-cm tissue culture dishes at a density of ~1300 cells/cm^2. MSC spheroids and adherent controls were cultured in 10 mL of either CCM or the serum-free defined MesenCult-XF medium (STEMCELL Technologies, Vancouver, Canada). Furthermore, 10 ng/mL IFN-γ, 10 ng/mL TNF-α, or 5 ng/mL of both IFN-γ and TNF-α (R&D, Minneapolis, MN) were supplemented on day 1 cultures of 500-cell spheroids and adherent controls in both CCM and MesenCult medium. After 4 days of culture, MSCs and conditioned media were collected for histological analysis as well as cell counts and immunomodulatory factor quantification.

3.2.3 Cell Viability and Histological Analyses

Cell viability of MSC spheroids treated with IFN-γ and/or TNF-α was analyzed via LIVE/DEAD staining (Invitrogen) after 4 days of culture. Samples were incubated in PBS containing 1 µM calcein AM and 2 µM ethidium homodimer I for 1 hour at 4º C. Samples were washed 3 times in PBS and immediately imaged using confocal microscopy (Zeiss LSM700-405, Germany). MSC spheroids were washed twice with PBS and fixed in 10% formalin for 20 minutes for histological analyses. After fixation, spheroids were washed three times with PBS, paraffin processed, embedded, and sectioned at 5 µm. Histological sections were de-paraffinized and stained with either hematoxylin and eosin (H&E), Toluidine Blue, Safranin O, or Masson's Trichrome and coverslipped with mounting media. A Nikon 80i upright microscope equipped with a SPOT Flex camera (Diagnostic Instruments, Sterling Heights, MI) was used to capture brightfield images of samples.

3.2.4 Cell Number and Immunomodulatory Factor Quantification

MSCs cultured as monolayers or spheroids with or without inflammatory cytokine treatment were cultured for 4 days and evaluated for total cell number and immunomodulatory factor secretion. The number of starting cells and after 4 days of culture were quantified for each culture condition using a CyQUANT assay (Invitrogen) according to the manufacturer's protocol. Collected cells were lysed and total DNA was measured and compared to a standard curve of known cell densities to determine cell numbers of each sample. PGE_2 in conditioned media was quantified using a Prostaglandin E2 Parameter Assay Kit (R&D). Human TGFβ1 and IL6 concentrations in conditioned media were quantified using DuoSet ELISA kits (R&D). Total secreted PGE_2, TGF-β1, and IL-6 was determined by subtracting cytokine concentrations in culture media controls incubated for 4 days in 100 mm Petri dishes. Total secreted PGE_2, TGFβ1, and IL6 were normalized to the average cell number over the 4-day culture period for each condition.

3.2.5 THP-1 Co-Culture Assay and Analysis

The human monocyte THP-1 cell line (ATCC) was expanded in growth media (RPMI-1640 with 10% FBS, 100 U/mL penicillin, and 100 µg/mL streptomycin and 0.05 mM 2-mercaptoethanol) and differentiated in growth media supplemented with 100 ng/mL phorbol-12 myristate 13-acetate (PMA, Sigma Aldrich) to induce macrophage differentiation. After 2 days in PMA-supplemented growth media, adherent cells were rinsed and cultured in growth media with 100 ng/mL of lipopolysaccharide (LPS) and 40 ng/mL IFN-γ for 2 days to activate the macrophages. Activated macrophages ($8x10^5$) and MSCs ($1x10^5$) were co-cultured for 16 hours in 0.4 µm pore transwells and 12-well tissue culture treated polystyrene plates (Corning), respectively. Adherent monolayer and

spheroid MSC cultures were pre-treated with or without 5 ng/mL IFN-γ and 5 ng/mL TNF-α for 4 days prior to being rinsed in PBS and transferred to 12-well plates. MSCs were cultured in the 12-well plates for 6 hours in RPMI-1640 with 10% FBS, 100 U/mL penicillin, and 100 µg/mL streptomycin and 0.05 mM 2-mercaptoethanol before addition of activated macrophages cultured in the transwells. Non-activated and activated macrophages were cultured in transwells without MSCs as controls. Human TNF-α was quantified from culture media after 16 hours using a DuoSet ELISA kit (R&D). Secreted TNF-α was determined by subtracting the concentration of TNF-α in media-only controls incubated for 16 hours in a 12-well plate.

3.2.6 IDO Detection and Peripheral Blood Mononuclear Cell Co-culture Assays

To evaluate MSC spheroid expression of IDO, RoosterBio MSCs were passaged and either plated in 10-cm plates (300,000 cells per plate) or aggregated into 500-cell spheroids. A subset of adherent and spheroid MSCs were stimulated with 20 ng/mL IFN-γ for 24 hours. After 24 hours, untreated and IFN-γ stimulated adherent and spheroid MSCs were lysed and RNA collected for quantitative real-time PCR (qRT-PCR) to measure IDO gene expression. RNA was extracted using an E.Z.N.A. Total RNA kit (OMEGA Bio-Tek, Norcross, GA) kit and cDNA was subsequently synthesized (300 ng RNA per sample) using an iScript cDNA synthesis kit (Bio-Rad, Hercules, CA). Forward and reverse primers for *IDO1* (Forward: AGCTTCGAGAAAGAGTTGAGAAG; Reverse: GTGATGCATCCCAGAACTAGAC) and *18S* (Forward: CTTCCACAGGAGGCCTACAC; Reverse: CTTCGGCCCACACCCTTAAT) were designed using Primer-Blast (www.ncbi.nlm.nih.gov) and purchased from Invitrogen

(Carlsbad, CA). *IDO1* gene expression was calculated with respect to untreated MSCs and normalized to *18S* expression using the ΔΔCT method.

To assess MSC suppression of T-cell proliferation, PBMCs were isolated from whole blood obtained with IRB approval from healthy volunteers via Ficoll (Sigma-Aldrich) density gradient separation. Isolated PBMCs were cultured at 400,000 cells per well in 24-well plates with adherent (1:9, 1:6, and 1:3 MSC-to-PBMC ratios) and spheroid MSCs (1:3, 1:1, and 3:1 MSCs-to-PBMC ratios) stimulated with 20 ng/mL IFN-γ for 24 hours prior to co-culture. In a subset of cultures, PBMCs were added to the upper well of a 0.4 μm pore polycarbonate transwell (Corning) and co-cultured with IFN-γ pre-treated adherent and spheroid MSCs. At the start of co-cultures, 0.2 μg/mL of anti-human CD3 and CD28 antibodies were added to the co-cultures to induce T-cell proliferation and activation. For all PBMC co-cultures, T-cell proliferation was assessed 4 days later by flow cytometry analysis of CD3 (FITC-conjugated mouse anti-CD3 IgG; BD Biosciences, East Rutherford, NJ) and Ki67 (PE-conjugated mouse anti-Ki67 IgG; BD Biosciences) double positive stained cells. T-cell activation was also assessed after 4 days by measuring the amount of IFN-γ in spent media supernatants by ELISA (R&D).

3.2.7 Statistical Analysis and Hierarchical Clustering

Statistical analyses were performed using Systat (Systat Software, Chicago, IL). Data are presented as mean ± standard error (n=6). Comparisons between multiple experimental groups were conducted using analysis of variance (ANOVA) and Box-Cox transformation followed by Tukey post hoc analysis to determine statistically significant differences ($p <$

0.05). The Genesis software package was used to produce heat maps of cell growth, immunomodulatory factor expression, and suppression of activated macrophage TNF-α secretion and to calculate and visualize two-dimensional hierarchical clustering between measured parameters and culture format, medium, and cytokine treatment groups, based on Euclidian distance and average linking clustering.

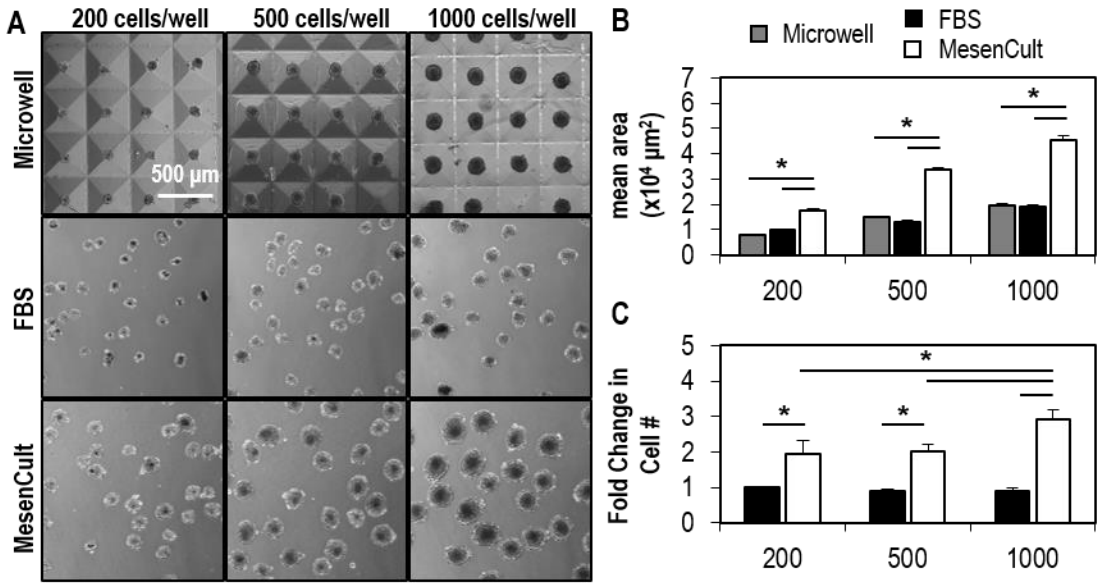

Figure 3.1. MSC spheroid formation and suspension culture. (A) MSC spheroids of distinct sizes were aggregated in agarose microwells overnight and subsequently cultured on a rotary orbital shaker (65 rpm) in either FBS or MesenCult™ medium. (B) After 4 days, spheroids cultured in MesenCult™ medium were larger than their initial size whereas spheroids in FBS medium maintained their original size. (C) Spheroid cultures in MesenCult™ medium exhibited a greater fold change in cell number over 4 days of culture compared to spheroids cultured in FBS medium and was greatest in 1000-cell spheroids. * = $p < 0.05$. Scale bar = 500 µm.

3.3 RESULTS

3.3.1 Impact of Spheroid Culture on MSC Phenotype

MSC spheroids with approximately 200, 500, or 1000 cells were formed via forced aggregation in 400 μm microwells by modulating the number of cells seeded into each well. After overnight incubation in the microwells, MSCs aggregated into relatively uniform spheroids of distinct sizes (**Figure 3.1A**) and were transferred to suspension culture to prevent surface attachment and agglomeration of individual aggregates. To determine if media composition altered the immunomodulatory secretion of MSCs, culture in traditional MEMα media supplemented with 16% FBS as well as serum-free, defined MesenCult medium, both of which support proliferation of monolayer MSC cultures was investigated. Spheroids cultured in MesenCult medium appeared larger after four days of culture compared to those cultured in FBS media, suggesting enhanced growth in these conditions. Morphometric analysis of spheroid projected area and quantification of cell numbers was performed to quantify aggregate size. After 4 days of culture, 200-, 500-, and 1000-cell spheroids cultured in MesenCult medium had significantly greater mean areas (1.8-, 2.6-, and 2.4- fold increase respectively, $p < 0.001$) compared to spheroids of the same initial cell number cultured in FBS medium (**Figure 3.1B**). In FBS media, no change in the total number of cells in spheroid cultures occurred after 4 days, indicating no significant expansion in MSCs over the culture period. However, a 1.9-, 2.0-, and 2.9-fold change in the total number of cells was observed in 200-, 500-, and 1000-cell spheroid cultures, respectively, in MesenCult media after 4 days (**Figure 3.1C**). H&E staining of 200, 500, and 1000 cell spheroids after microwell formation and after four days of culture in FBS or MesenCult medium revealed distinct differences in spheroid structure (**Figure**

3.2). Spheroids cultured in FBS media were consistently smaller than those cultured in MesenCult medium. The distribution of cells within the aggregates was more uniform in spheroids cultured in FBS whereas, with the exception of 1000 cell spheroids, MSCs clustered at the outer edges of spheroids cultured in MesenCult medium. Together, these results indicate that MSCs cultured as spheroids in MesenCult medium continue to grow whereas cell spheroids in FBS-supplemented medium fail to do so over the same period of time.

3.3.2 Spheroid Culture Increases Immunomodulatory Factor Secretion

To determine the impact of spheroid culture and medium on the secretion of immunomodulatory paracrine factors, conditioned media was collected and analyzed to determine MSC secretion of the immunomodulatory factors PGE_2, TGF-β1, and IL-6. When cultured as spheroids, MSCs in FBS medium secreted greater amounts of PGE_2, TGF-β1, and IL-6 (**Figure 3.3A-C**) compared to those cultured in MesenCult medium. In comparison to adherent monolayer cultures, MSCs cultured as 500-cell spheroids in FBS medium secreted a 4-fold greater amount of PGE_2 ($p < 0.001$), similar to previously described results [174], as well as a 1.7- and 3.2-fold increase in TGF-β1 and IL-6 secretion ($p = 0.041$ and 0.001, respectively). However, in MesenCult medium, no difference in PGE_2 was observed between adherent monolayer and spheroid cultures, and spheroid cultures actually secreted less TGF-β1 ($p < 0.001$). Only IL-6 secretion was observed to be increased in spheroid cultures in MesenCult medium compared to adherent monolayers, which did not secrete detectable levels of IL-6. Overall, there was little difference in the secretion of immunomodulatory paracrine factors between spheroids of different sizes, but

the most abundant paracrine factor secretion was consistently observed in 500-cell spheroids, thus 500-cell spheroids were chosen for further analysis of immunomodulatory paracrine factor secretion.

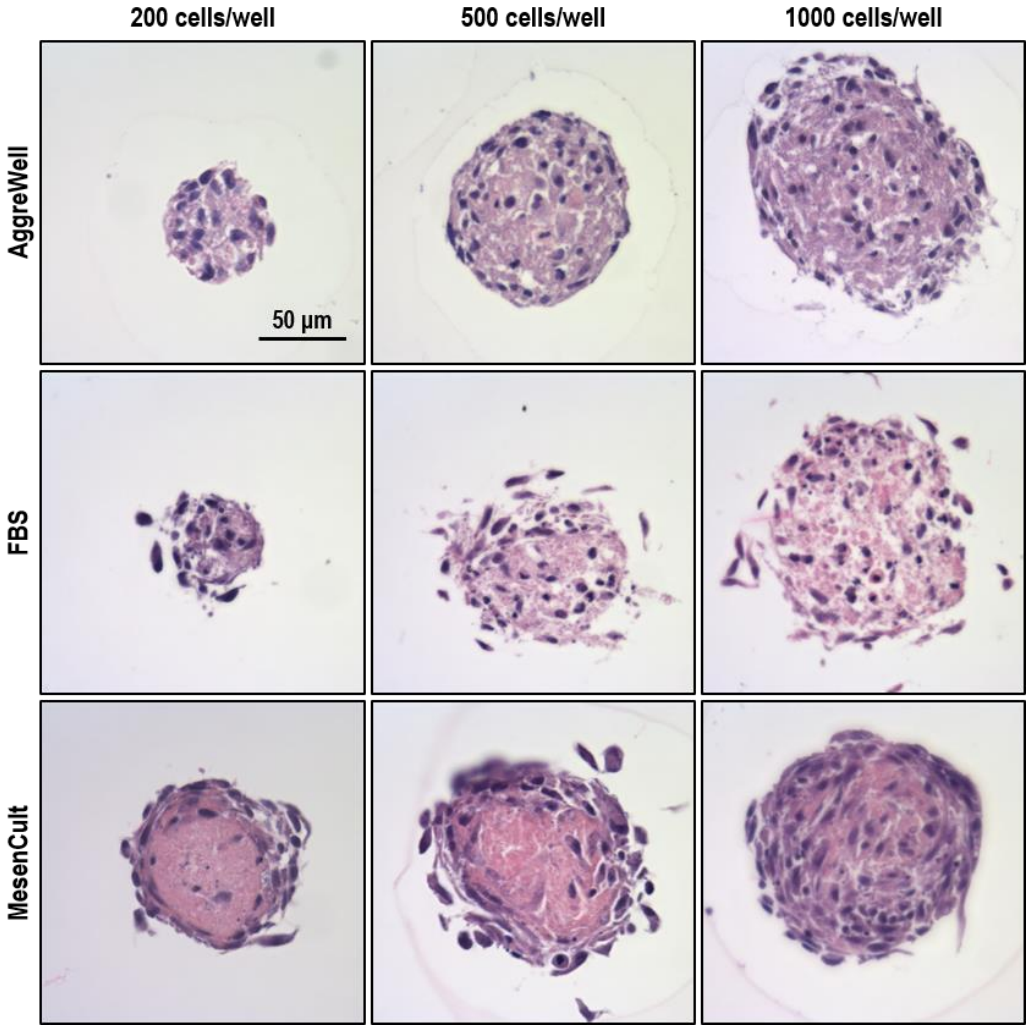

Figure 3.2. Histological analysis of MSC spheroids of varied size and culture medium. MSCs initially aggregated overnight to form compact spheroid structures with approximately 200, 500, and 1000 cells (top row). After 4 days, MSCs cultured as spheroids in MesenCult™ medium appeared more compact than spheroids cultured in FBS medium (middle row). MSCs cultured as 200- and 500-cell spheroids in MesenCult™ media appeared to be distributed primarily towards the exterior of spheroids whereas MSCs were distributed more uniformly throughout 1000-cell spheroids in MesenCult™ medium (bottom row). Scale bar = 50 µm.

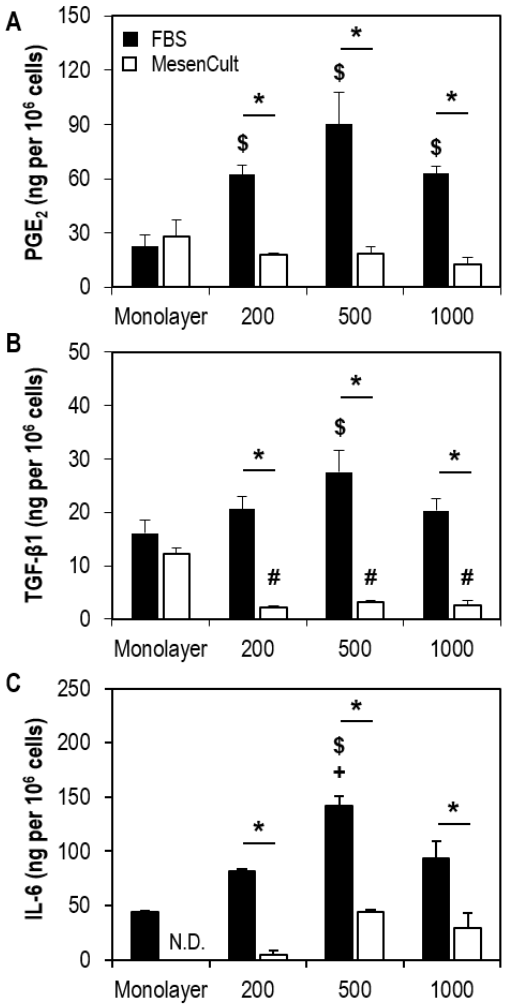

Figure 3.3. Immunomodulatory factor expression of MSCs. Differential secretion of the immunomodulatory factors (A) PGE_2, (B) TGF-β1, and (C) IL-6 was observed after 4 days of MSC culture in monolayer and spheroid formats, as well as in different culture media. Spheroids with approximately 500 cells in FBS supplemented medium exhibited the greatest secretion of these three immunomodulatory factors while comparable numbers of MSCs in MesenCult medium tended to secrete less of each factor. (D) IDO activity, measured by the amount of kynurenine, was greater in cells cultured in FBS medium but was not impacted by culture format. * indicates $p < 0.05$ by groups denoted by bar; $ indicates $p < 0.05$ (FBS) compared to adherent monolayer culture; # indicates $p < 0.05$ (MesenCult) compared to adherent monolayer culture; + indicates $p < 0.05$ (FBS) compared to 200-cell spheroid culture; ND = not detectable.

3.3.3 Cytokine Conditioning of MSCs is Dependent on Culture Medium

To investigate the effects of cytokine treatment of MSC spheroids, 500-cell spheroids were cultured in FBS and MesenCult mediums supplemented with 10 ng/mL IFN-γ, 10 ng/mL TNF-α, or 5 ng/mL of each cytokine, for 4 days in suspension culture. Although MSCs cultured in MesenCult medium secreted lower levels of immunomodulatory factors, treatment with pro-inflammatory cytokines was hypothesized to stimulate MSC immunomodulatory activity even in MesenCult medium. Whereas the size of spheroids cultured in FBS medium did not vary when treated with different cytokines, the size of spheroids cultured in MesenCult medium was modulated by cytokine treatment (**Figure 3.4A**). Spheroids treated with TNF-α alone were larger, while spheroids exposed to IFN-γ (alone or in combination with TNF-α) yielded smaller spheroids after 4 days compared to untreated controls (**Figure 3.4B**). However, an increase in cell number after 4 days of culture was observed in spheroid cultures in MesenCult medium compared to FBS medium and cell expansion was not inhibited by IFN-γ or TNF-α treatment alone (**Figure 3.4C**), suggesting that differences in spheroid size reflected differences in spheroid structure or individual cell size. Additionally, no difference in cell numbers was observed between spheroids treated with both IFN-γ and TNF-α in either FBS or MesenCult medium, suggesting that this cytokine combination inhibits the cell growth observed in spheroids cultured in MesenCult medium alone.

Histological analysis of spheroids cultured in FBS and MesenCult medium with pro-inflammatory cytokine treatment revealed similar spheroid structures and cell distributions as untreated controls (**Figure 3.5A**). Histological analysis to determine the cellular and

extracellular composition of spheroids after 4 days of culture indicated little matrix deposition within the cores of the spheroid structures as assessed by Toluidine blue, Safranin O, and Masson's Trichrome staining (**Figure 3.5B-C**). Furthermore, viability of cells within spheroids did not appear to be significantly affected by cytokine treatment (**Figure 3.6**). However, MSC spheroids cultured in MesenCult medium and treated with IFN-γ alone or in combination with TNF-α displayed more uniformly distributed cells throughout the spheroid structure that were less densely packed, similar to the multicellular organization of spheroids cultured in FBS medium alone.

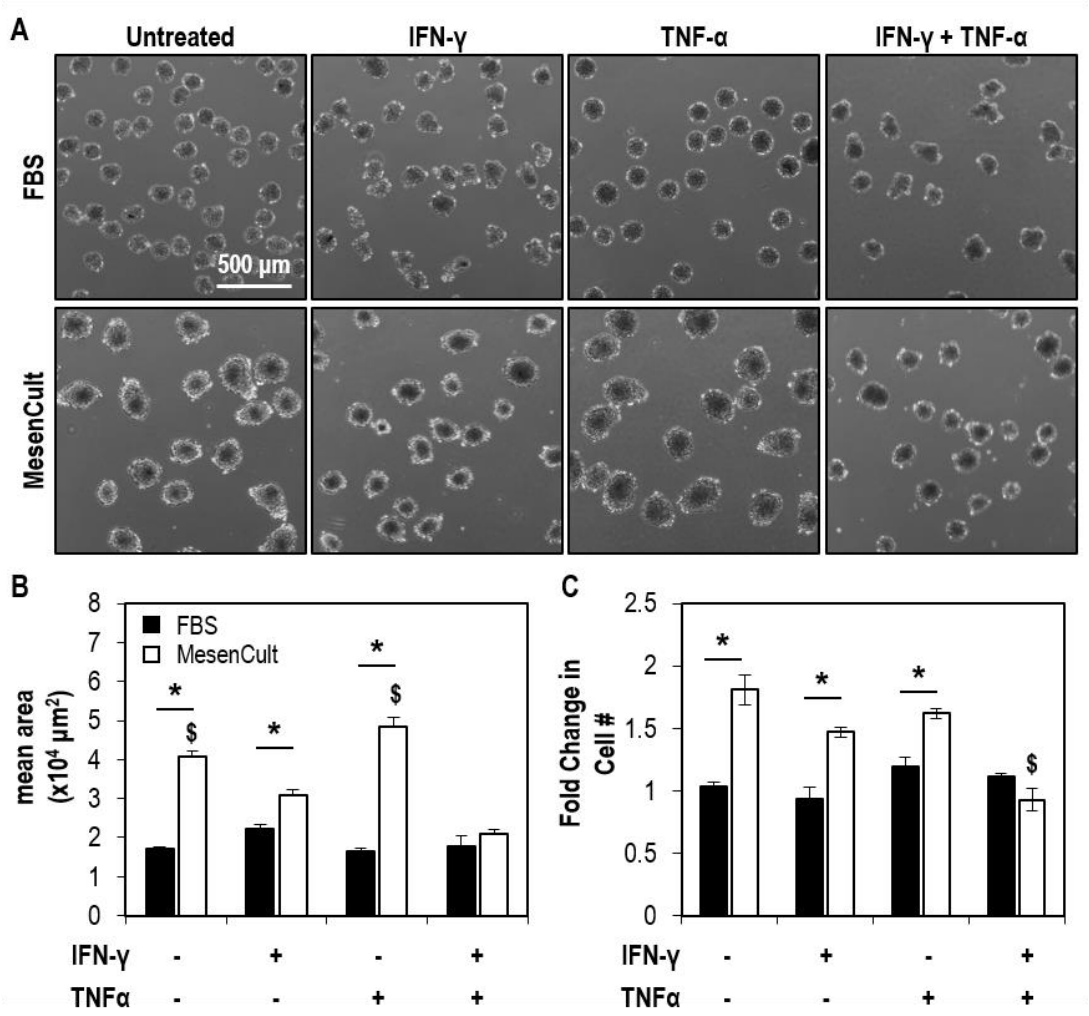

Figure 3.4. IFN-γ and TNF-α conditioning of 500-cell MSC spheroids. (A) MSC spheroids were cultured in FBS and MesenCult medium supplemented with 10 ng/mL IFN-γ, 10 ng/mL TNF-α, or 5 ng/mL of both cytokines for 4 days. Scale bar = 500 µm. (B) Differences in aggregate size were observed after the 4 day culture period and IFN-γ treatment (alone or in combination with TNF-α) appeared to inhibit the increase in spheroid size observed in spheroids cultured in MesenCult medium. (C) Treatment with both IFN-γ and TNF-α inhibited the expansion of cell numbers in MesenCult medium and resulted in a comparable cell number similar to spheroids cultured in FBS medium. * indidcates $p < 0.05$ compared between FBS and MesenCult medium; $ indicates $p < 0.05$ (MesenCult) compared to all cytokine treatment groups; # indicates $p < 0.05$ (FBS) compared to TNF-α treated group.

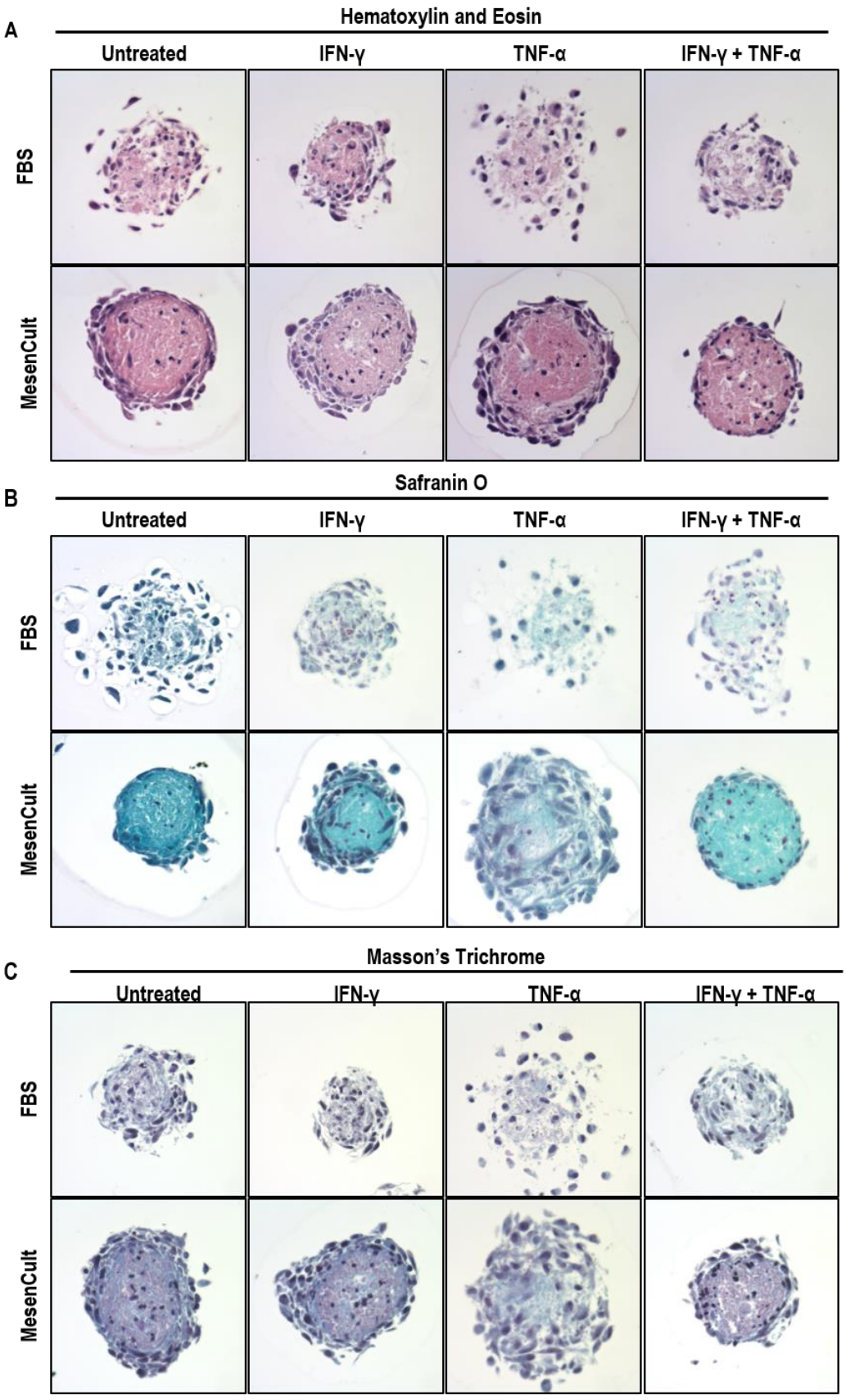

Figure 3.5. Histological analysis of MSC spheroids treated with IFN-γ and TNF-α. (A) Spheroids (500 cells initially) cultured for 4 days of culture in FBS medium (top row) supplemented with IFN-γ alone (10 ng mL^{-1}) or in combination with TNF-α (5 ng mL^{-1} of each cytokine) appeared similar in structure to untreated controls whereas spheroids treated with TNF-α alone (10 ng mL^{-1}) appeared to be less densely packed. Spheroids cultured in MesenCult medium (bottom row) supplemented with IFN-γ and TNF-α alone had similar structures to untreated controls. However, spheroids treated with both IFN-γ and TNF-α appeared smaller in size with less cellularity. Spheroids in both FBS and MesenCult displayed very little GAG (B) or collagen (C) deposition over 4 days suggesting that MSC spheroids lack significant amounts of extracellular matrix after short culture periods. While the spheroid cellular structure was modulated by cytokine treatment, IFN-γ and TNF-α treatment did not alter GAG or collagen matrix deposition over 4 days of culture in either FBS or MesenCult media. Scale bar = 50 μm.

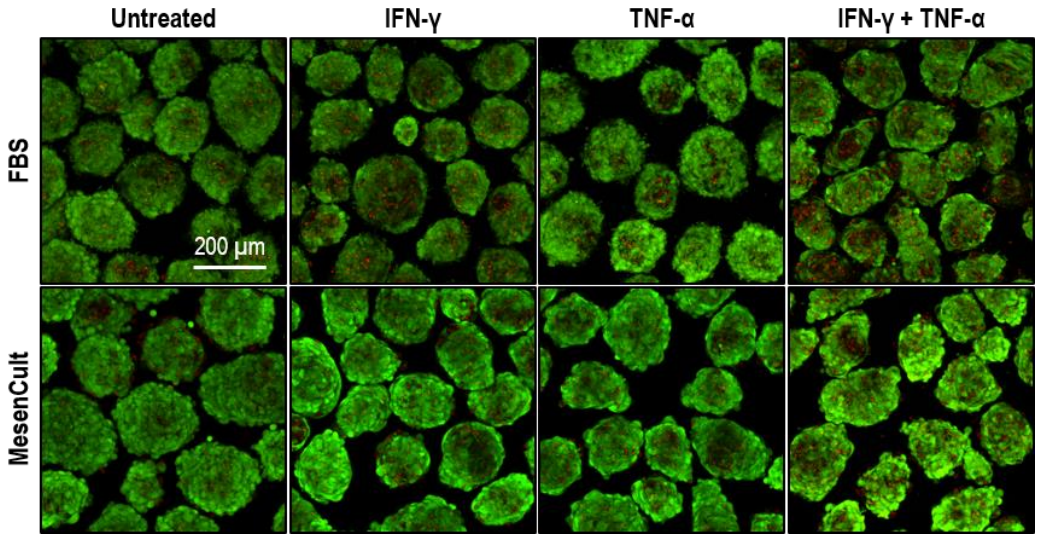

Figure 3.6. Cell viability analysis of MSC spheroids treated with IFN-γ and TNF-α. Spheroids cultured in FBS or MesenCult media with or without supplementation with 10 ng mL^{-1} IFN-γ or TNF-α were stained with calcein AM and ethidium homodimer to evaluate the ratio and distribution of live and dead cells. MSCs were predominately stained with calcein AM with only a few dead cells distributed throughout the spheroid. Additionally, cell viability did not appear to be affected by cytokine treatment with either IFN-γ or TNF-α.

Analysis of immunomodulatory paracrine factors produced in response to treatment with pro-inflammatory cytokines revealed cytokine-specific variation in individual immunomodulatory paracrine factor secretion dependent on the culture medium. PGE_2 secretion was found to be greater in spheroids cultured in FBS medium compared to spheroids cultured in MesenCult (**Figure 3.7A**). Treatment with TNF-α alone (10 ng/mL) in FBS resulted in a 2.8-fold increase in PGE_2 secretion compared to untreated spheroid controls. Furthermore, TNF-α treatment of spheroids in FBS resulted in a 4.2-fold increase in PGE_2 secretion compared to TNF-α treated monolayer cultures in FBS. However, spheroids treated with both TNF-α and IFN-γ (5 ng/mL each) did not exhibit significantly different PGE_2 secretion compared to either non-treated controls or IFN-γ treated spheroids. IFN-γ treatment alone or with TNF-α did not impact MSC TGF-β1 secretion in FBS medium, while TNF-α treatment alone suppressed secretion of TGF-β1 (**Figure 3.7B**). IL-6 secretion by MSC monolayers and spheroids was increased by individual cytokine treatment in both FBS and MesenCult medium. Furthermore, treatment with IFN-γ and TNF-α together appeared to synergistically increase IL-6 secretion by MSC spheroids as the greatest IL-6 secretion (23.2-fold increase compared to untreated spheroid controls) was observed in spheroids treated with the combination of both cytokines (**Figure 3.7C**). Cytokine treatment in MesenCult medium stimulated secretion of PGE_2 only in monolayer culture when treated with both cytokines. Additionally, IL-6 secretion was increased in both monolayer and spheroid cultures with treatment of both IFN-γ and TNF-α. Finally, TGF-β1 secretion was suppressed in all spheroid treatment groups compared to untreated spheroid controls. These results demonstrate that treatment with pro-inflammatory

cytokines can enhance immunomodulatory paracrine factor secretion of MSC spheroids depending on the composition of the culture media.

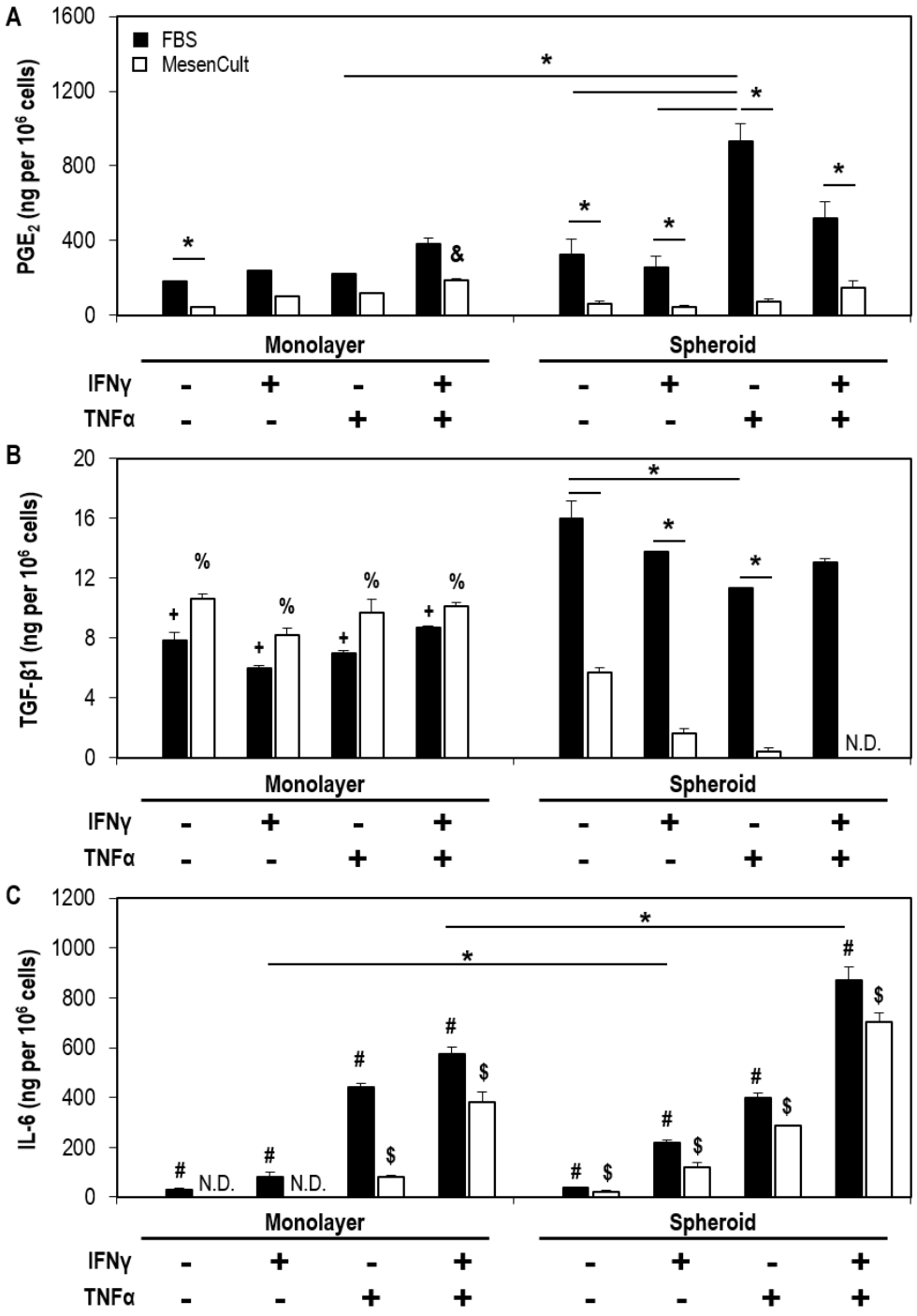

Figure 3.7. Immunomodulatory factor expression of IFN-γ and TNF-α conditioned MSC monolayer and spheroid cultures. Increased secretion of (A) PGE_2 was observed in spheroids treated with TNF-α and cultured in FBS media whereas (B) TGF-β1 secretion of spheroids decreased with TNF-α treatment. (C) IL-6 secretion was greatest in 500-cell spheroids treated with both IFN-γ and TNF-α in FBS media. * = $p < 0.05$ compared between groups denoted by bars; & = $p < 0.05$ compared to untreated of same culture format and medium; + = $p < 0.05$ compared to spheroid culture in FBS media with the same cytokine treatment; % = $p < 0.05$ compared to spheroid cultures in MesenCult media with the same cytokine treatment; # = $p < 0.05$ compared to all cytokine treatment groups in FBS medium; $ = $p < 0.05$ compared to all cytokine treatment groups in MesenCult medium; N.D. = not detectable.

3.3.4 Pre-conditioning MSC Spheroids to Enhance Immunomodulation

Having demonstrated that culture environment parameters alter the secretion of immunomodulatory paracrine factors, pre-conditioned MSC spheroid suppression of the inflammatory response of activated macrophages (aMΦ) was next determined. Since PGE_2 secretion was greatest with TNF-α treatment alone, and IL-6 secretion was greatest with both IFN-γ and TNF-α treatment, the ability of pre-treatment with TNF-α ± IFN-γ to enhance MSC immunomodulation in macrophage co-cultures was determined. In co-culture studies, adherent monolayers of MSCs suppressed macrophage TNF-α secretion less than comparable numbers of MSCs as spheroids (**Figure 3.8A**). Pre-conditioning spheroids with both IFN-γ and TNF-α, but not TNF-α alone, further increased suppression of macrophage TNF-α secretion compared to untreated spheroids. Since MSCs cultured in MesenCult medium secreted lower levels of immunomodulatory factors, whether this culture medium impaired the immunomodulatory capabilities of MSCs in an *in vitro* model of an inflammatory environment (i.e. co-culture with activated macrophages) was examined. However, no difference in suppression of macrophage TNF-α secretion was observed between MSC spheroids cultured in FBS or MesenCult medium after being

transferred to macrophage co-culture. However, pre-conditioning spheroids with IFN-γ and TNF-α in MesenCult medium was unable to further reduce macrophage TNF-α expression. Altogether, these results demonstrate that pre-conditioning MSCs by manipulation of culture parameters can enhance immunomodulatory secretion to suppress inflammatory responses of activated macrophages that is dependent on the composition of the culture medium.

3.3.5 Effects of Aggregation of MSCs on Suppression of T-cell Proliferation

To further investigate the effects of aggregation and cytokine treatment on MSC immunomodulation, the ability of MSC spheroids to suppress T-cell proliferation was determined in co-cultures with CD3/CD28 activated PBMCs. Since expression of IDO in response to IFN-γ stimulation is critical for the suppression of T-cell proliferation, MSC expression of IDO from two different sources of MSCs (Texas A&M and RoosterBio MSCs) first evaluated in adherent and spheroid cultures. When treated with 20 ng/mL IFN-γ, gene expression of *IDO1* was massively upregulated (>10^4 fold induction of IDO) in both adherent and spheroid MSCs from both commercial sources (**Figure 3.9**). Additionally, MSC spheroids expressed greater levels of *IDO1* when stimulated with IFN-γ compared to adherent MSCs. In Texas A&M MSCs, gene expression of *IDO1* was 1.5-fold greater ($p = 0.019$) in spheroids stimulated with IFN-γ compared to adherent MSCs stimulated with IFN-γ. Similarly, in RoosterBio MSCs, gene expression of *IDO1* was 4-fold greater ($p < 0.001$) in spheroids stimulated with IFN-γ compared to adherent MSCs.

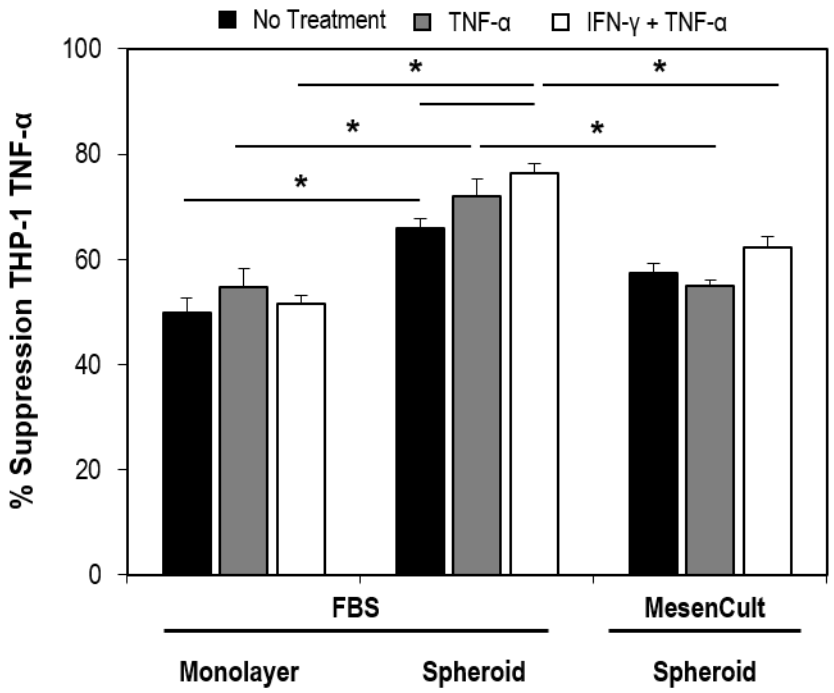

Figure 3.8. MSC suppression of THP-1 TNF-α secretion. MSCs cultured as monolayers and spheroids in FBS medium suppressed aMΦ secretion of TNF-α, however, TNF-α secretion was significantly reduced more by co-culture with spheroids compared to monolayer cells. However, spheroids cultured in MesenCult prior to co-culture did not differ in suppression of aMΦ TNF-α secretion compared to spheroid cultures in FBS culture medium. Pre-treating spheroids with 5 ng/mL of both IFN-γ and TNF-α, but not 10 ng/mL of TNF-α alone, in FBS medium further enhanced suppression of aMΦ TNF-α secretion. However, addition of IFN-γ and TNF-α to MesenCult medium did not enhance the subsequent immunosuppressive effects of MSC spheroids on aMΦ. * = $p < 0.05$ compared between all other experimental groups.

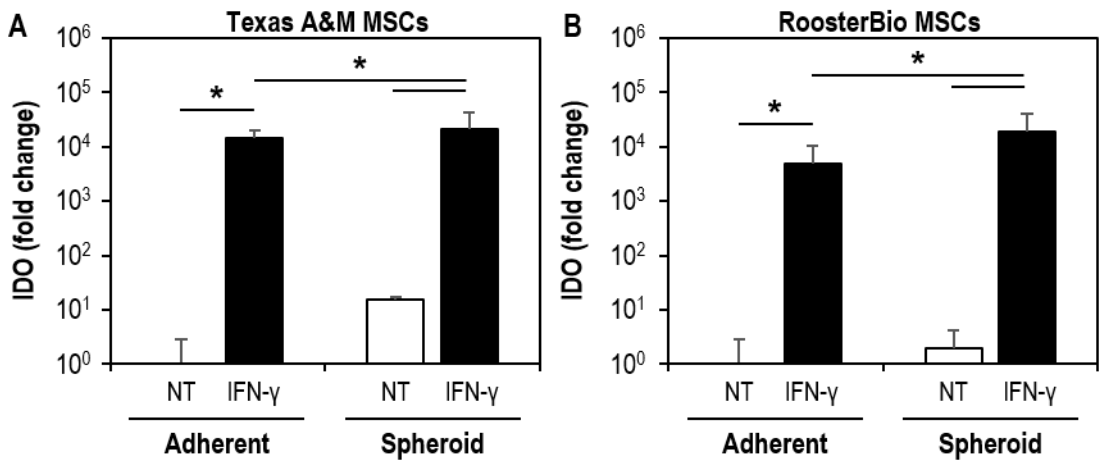

Figure 3.9. IDO expression in IFN-γ stimulated adherent and spheroid MSCs. (A) *IDO1* expression by Texas A&M MSCs was significantly upregulated in response to IFN-γ stimulation in both adherent and spheroid cultures. (B) Likewise, *IDO1* expression was similarly upregulated in RoosterBio MSCs in response to IFN-γ treatment. * indicates $p < 0.05$ between groups denoted by bars.

Despite MSCs from both commercial sources expressing IDO in response to IFN-γ, only IFN-γ stimulated MSCs from RoosterBio were capable of inhibiting T-cell proliferation in co-culture with CD3/CD28 activated PBMCs (**Figure 3.10A**). When co-cultured at a 1:3 MSC:PBMC ratio, adherent RoosterBio MSCs significantly reduced the number of $Ki67^+$ T-cells (~23% $Ki67^+$) compared to activated PBMCs alone (~87% $Ki67^+$; $p < 0.001$). However, in co-cultures with Texas A&M MSCs at a 1:3 MSC:PBMC ratio, no significant difference was found in the percentage of Ki67+ T-cells compared to PBMCs alone (68% $Ki67^+$; $p = 0.331$). A similar trend in PBMC expression of IFN-γ was observed in co-cultures; RoosterBio MSCs had significantly greater suppression of IFN-γ expression compared to Texas A&M MSCs at an equivalent MSC:PBMC ratio (**Figure 3.10B**). However, it is important to note that the Texas A&M MSCs used were expanded and cryopreserved several years prior to experiments, whereas RoosterBio MSCs were ordered

new and expanded prior to the start of these experiments. Cryopreservation has previously been demonstrated to interfere with the immunomodulatory capability of MSCs [199, 200]. Since only RoosterBio MSCs were found to suppress T-cell proliferation, these cells were used for all further experiments.

To compare suppression of T-cell proliferation by adherent and spheroid MSCs, varying ratios of MSCs-to-PBMCs were investigated. Surprisingly, a greater dose of MSCs were needed to suppress T-cell proliferation when MSCs were aggregated despite MSC spheroids expressing greater amounts of IDO. Co-culture of PBMCs with adherent MSCs at a 1:3 MSC:PBMC ratio significantly reduced the percentage of $Ki67^+$ T-cells (**Figure 3.11A**; ~32% $Ki67^+$ compared to ~87% in PBMC only cultures, $p = 0.014$) and T-cell IFN-γ expression (**Figure 3.11B**; ~2.4 ng/mL IFN-γ compared to 9.6 ng/mL in PBMC only cultures, $p < 0.001$). However, at an equivalent dose of MSC spheroids (1:3 MSC:PBMC ratio) no significant difference in percentage of $Ki67^+$ T-cells (**Figure 3.11C**) or IFN-γ expression (**Figure 3.11D**) was observed between co-cultures and PBMC only controls. Instead, nearly a 10-fold increase in the number of MSCs was necessary to begin to observe suppression of T-cell proliferation by MSC spheroids. Co-culture of PBMCs with spheroid MSCs at a 3:1 MSC:PBMC ratio significantly reduced the percentage of $Ki67^+$ T-cells (**Figure 3.11C**; ~21% $Ki67^+$ compared to ~65% in PBMC only cultures, $p < 0.001$) and T-cell IFN-γ expression (**Figure 3.11D**; ~1.2 ng/mL IFN-γ compared to ~10.2 ng/mL in PBMC only cultures, $p < 0.001$). Altogether, MSC spheroids were less effective at suppressing T-cell proliferation *in vitro* compared to an equivalent amount of MSCs plated as adherent monolayers.

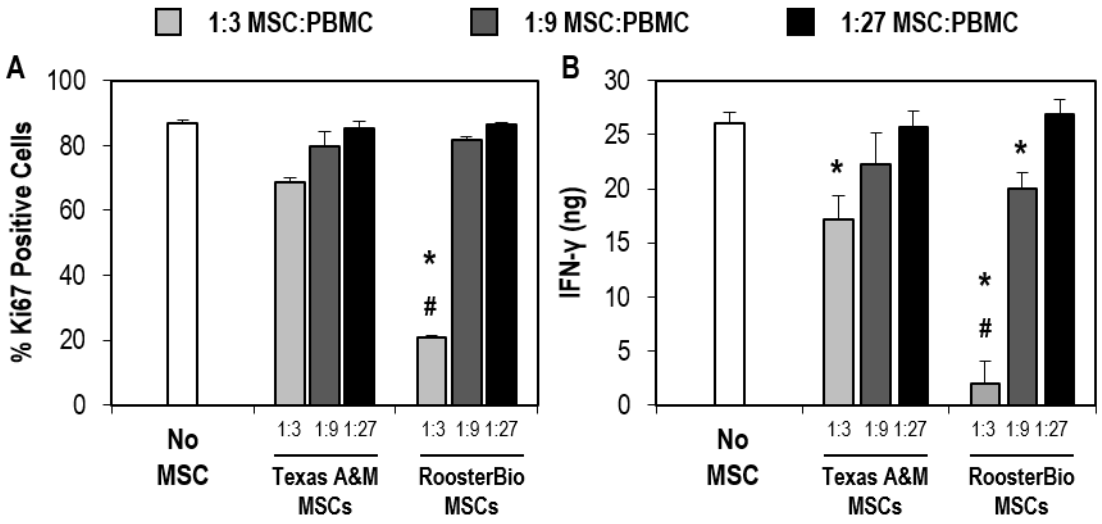

Figure 3.10. **Suppression of T-cell proliferation and activation by Texas A&M and RoosterBio MSCs.** (A) Adherent MSCs from RoosterBio but not Texas A&M significantly reduced proliferation of T-cells in PBMC co-cultures as determined by $Ki67^{+}$ T-cells. (B) While both MSCs from RoosterBio and Texas A&M decreased T-cell secretion of IFN-γ at a 1:3 MSC:PBMC ratio, suppression of IFN-γ secretion was significantly greater in co-cultures with RoosterBio MSCs. * indicates $p < 0.05$ compared to "No MSC" group; # indicates $p < 0.05$ compared to co-cultures with Texas A&M MSCs at the equivalent MSC:PBMC ratio.

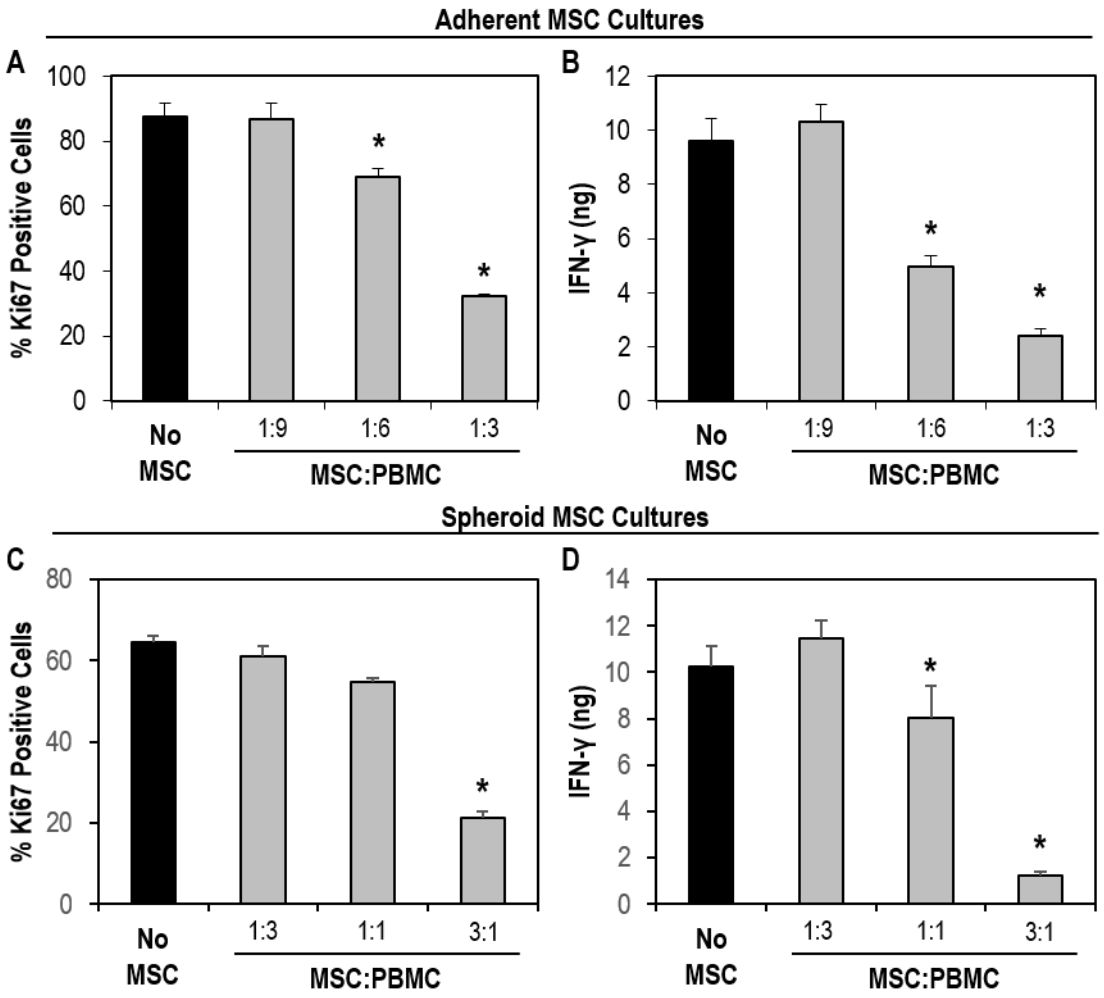

Figure 3.11. A greater dose of MSCs is needed to suppress T-cell proliferation when MSCs are aggregated. (A) Co-culture of CD3/CD28 activated PBMCs with adherent MSCs at multiple MSC:PBMC ratios demonstrated that adherent MSCs were effective at suppressing T-cell proliferation, as determined by the percentage of $Ki67^{+}$ T-cells, at a 1:3 MSC:PBMC ratio. (B) Similarly, T-cell expression of IFN-γ was significantly reduced by adherent MSCs at a 1:6 and 1:3 MSC:PBMC ratio. However, when aggregated into spheroids, a 3:1 MSC:PBMC ratio was necessary to suppress (C) T-cell proliferation and (D) IFN-γ expression. * indicates $p < 0.05$ compared to "No MSC" group.

To investigate why more MSCs were required to suppress T-cell proliferation in spheroid culture, cell-contact dependent mechanisms were first examined. Cell-contact dependent signaling has been demonstrated to aid in adherent MSC suppression of T-cell proliferation [142, 201] and MSC spheroids have reduced surface area for cell-cell contacts. We hypothesized that MSC spheroids rely solely on paracrine mechanisms, such as IDO expression, to suppress T-cell proliferation and not direct cell contact and therefore, more cells are required to suppress T-cell proliferation. To investigate the role of direct cell contact, MSCs and PBMCs were cultured using a transwell co-culture system. Adherent and spheroid MSCs were co-cultured with PBMCs at MSC:PBMC ratios found to inhibit T-cell proliferation (1:3 MSC:PBMC for adherent MSCs, 3:1 MSC:PBMC for spheroid MSCs). As expected, physical separation of adherent MSCs and PBMCs significantly reduced the ability of MSCs to suppress T-cell proliferation (**Figure 3.12A**; ~11% $Ki67^+$ T-cells in direct co-culture compared to ~35% $Ki67^+$ T-cells in transwell co-cultures, $p = 0.002$) and suppress IFN-γ expression (**Figure 3.12B**; ~1.6 ng/mL IFN-γ in direct co-culture compared to ~7.0 ng/mL IFN-γ in transwell co-culture, $p < 0.001$). Similarly, transwell co-culture also reduced the ability of MSC spheroids to suppress T-cell proliferation (~35% $Ki67^+$ T-cells in direct co-culture compared to ~75% $Ki67^+$ T-cells in transwell co-cultures, $p = 0.022$) and IFN-γ expression (~1.7 ng/mL IFN-γ in direct co-culture compared to ~5.5 ng/mL IFN-γ in transwell co-culture, $p < 0.001$). Altogether, direct cell-contact plays a role in both adherent and spheroid MSC suppression of T-cell proliferation yet both adherent and spheroid MSCs were still capable of suppressing T-cell proliferation in transwell co-cultures.

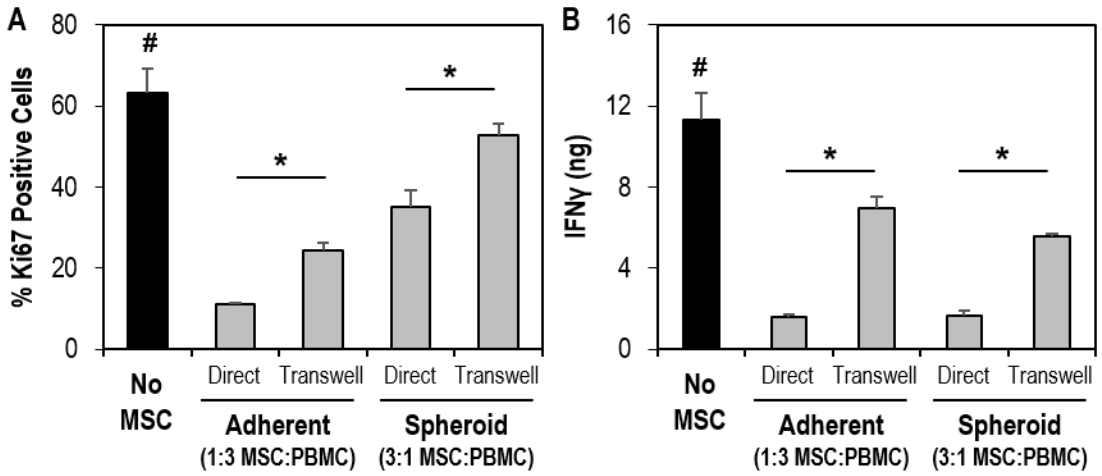

Figure 3.12. Transwell co-culture reduces the ability of both adherent and spheroid MSCs to suppress T-cell proliferation. (A) Co-culture of CD3/CD28 activated PBMCs with adherent and spheroid MSCs in transwell co-culture reduced the ability of MSCs to suppress T-cell proliferation as determined by percentage of $Ki67^+$ T-cells. (B). Similarly, transwell co-culture reduced the ability of MSCs to suppress T-cell expression of the effector cytokine IFN-γ. * indicates $p < 0.05$ compared to groups denoted by bars. # indicates $p < 0.05$ compared to all MSC co-cultures.

3.4 DISCUSSION

These results demonstrate that 3D aggregation of MSCs increases endogenous immunomodulatory factor secretion that is dependent on medium composition and pro-inflammatory cytokine treatments. Furthermore, pre-conditioning MSCs via culture conditions can enhance inherent secretory properties and improve the suppression of pro-inflammatory macrophages. In medium supplemented with FBS, MSCs cultured as 500-cell spheroids secreted greater levels of the immunomodulatory factors PGE_2, TGF-β1 and IL-6 compared to monolayer cultures. Interestingly, 200- and 1000-cell spheroids did not yield significantly increased secretion of TGF-β1 and IL-6 compared to monolayer cultures, which may be due to differences in the number or distribution of cell-cell contacts

in 200-cell spheroids or 1000-cell spheroids. However, striking differences in cell phenotypes of MSCs cultured as spheroids were observed in FBS (no cell growth, high paracrine secretion) and MesenCult (significant cell growth, low paracrine secretion) culture mediums (**Figure 3.13**). PGE_2 and IL-6 secretion as well as IDO activity were increased by cytokine treatment in FBS medium, whereas only IL-6 secretion was induced by cytokine treatment in MesenCult medium. Upon transferring MSC spheroids to activated macrophage co-cultures, both FBS and MesenCult culture media altered the immunomodulatory capacity of MSCs pre-conditioned with the pro-inflammatory cytokines IFN-γ and TNF-α, but did not affect the immunomodulatory capacity of untreated spheroids. Pre-treatment of MSCs with both cytokines in FBS medium increased suppression of macrophage TNF-α secretion compared to monolayer and untreated spheroid cultures while pre-treatment of MSCs in MesenCult did not increase suppression of macrophage TNF-α secretion compared to untreated spheroids. Altogether, these results suggest that environmental parameters, including spheroid culture, media composition, and cytokine conditioning, can modulate the secretion of anti-inflammatory molecules by MSCs.

Three dimensional aggregation of MSCs enhanced secretion of immunomodulatory factors and suppression of activated macrophage TNF-α secretion, similar to previously published results [174]. However, previous studies reported enhanced secretion of the immunomodulatory factors PGE_2 and TSG-6, from much larger MSC aggregates comprised of approximately 25,000 cells per aggregate [174]. Since oxygen gradients arise in cell aggregates above a critical size threshold (~300 μm diameter) [182], oxygen

availability to cells within spheroids may differ significantly between aggregates grown above and below this size threshold. Furthermore, adipose derived stromal cells (ADSCs) cultured as spheroids with diameters greater than 100 μm expressed more hypoxia induced survival factors such as hypoxia-inducible factor (HIF)-1α and paracrine factors, such as HGF and vascular endothelial growth factor (VEGF), compared to monolayer cultures [169]. Additionally, hypoxic culture of ADSCs enhanced the suppression of CD4+ and CD8+ T cell proliferation but did not affect the expression of IDO [193]. Therefore, oxygen transport limitations may play a role in the regulation of MSC immunomodulatory factor secretion in spheroid cultures. In large MSC aggregates, enhanced immunomodulation was attributed to MSCs responding to signals released from stressed and apoptotic cells induced by aggregation [174]. The authors demonstrated that caspase, NFκB, and IL1 signaling, which are involved in mediating the cellular stress response, were involved in PGE_2 secretion from MSC aggregates [174, 175]. However, MSC spheroids examined in this current study contained approximately 1,000 or fewer cells per aggregate and thus the largest sized aggregates remained below the threshold for limited oxygen transport. Furthermore, formation of necrotic regions in the interior of cell aggregates was not observed in any of the histological analyses performed in this study. Therefore, the increase in immunomodulatory factor expression observed in MSC spheroids with fewer than 1,000 cells per spheroid may be due to another mechanism other than hypoxia induced stress. For example, increased MSC immunomodulatory activity may be due to increased cell contact dependent signaling and intercellular adhesions, which have been implicated in the enhanced paracrine activity of MSC aggregates. Contact-dependent Notch signaling has also been demonstrated to play a role in mediating MSC secretion of PGE_2, as well as

suppression of macrophage TNF-α secretion [175]. Additionally, 3D aggregation of MSCs was found to upregulate E-cadherin expression, which in turn was responsible for enhanced vascular endothelial growth factor (VEGF) secretion via the ERK/AKT signaling pathway [159]. Thus, although the mechanism(s) responsible for increased immunomodulatory factor expression by MSCs cultured as 3D spheroids remains unclear, aggregation of MSCs represents a rather simple, yet effective means of enhancing the immunomodulatory potential of MSCs prior to transplantation.

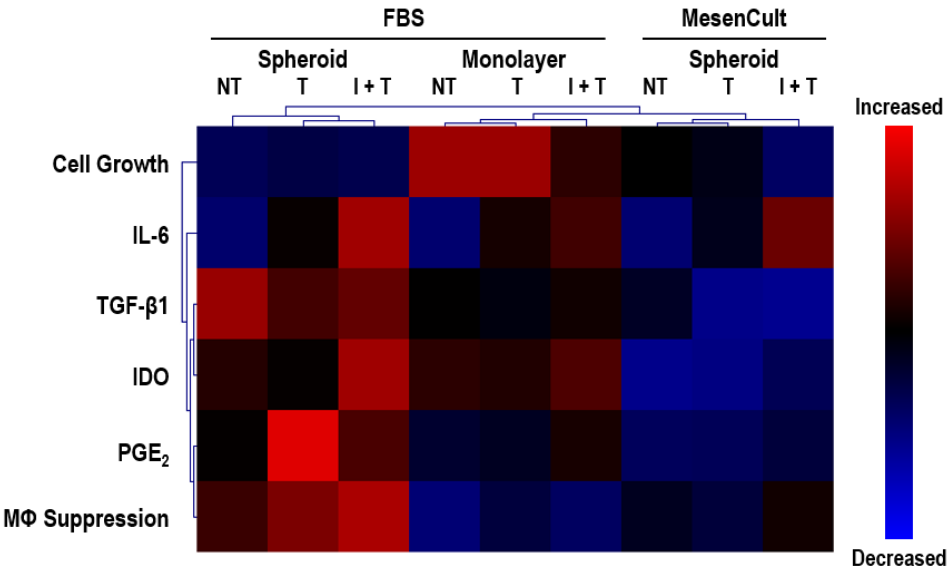

Figure 3.13. Heatmap visualization of MSC growth, cytokine secretion, and activated mΦ suppression. Hierarchical clustering illustrated the differences in MSC phenotype between cells cultured as monolayers or spheroids in either FBS or MesenCult media. Spheroids cultured in FBS medium displayed greater immunomodulatory factor expression and activated mΦ suppression but decreased cell growth. Alternatively, spheroids cultured in MesenCult media and monolayers cultured in FBS clustered together and displayed lower immunomodulatory factor expression and activated mΦ suppression but increased cell growth. Finally, cytokine treatment tended to enhance immunomodulatory factor expression and macrophage suppression while decreasing cell growth. NT = no treatment; T = 10 ng/mL TNF-α treatment; I + T = 5 ng/mL IFN-γ and 5 ng/mL TNF-α treatment.

The development of culture media with defined components and/or xenogen-free supplements, such as human platelet lysate (HPL), are desired for MSC therapies in order to reduce the inherent batch-to-batch variability of FBS and address safety concerns about the potential transfer of animal-derived proteins as well as zoonotic agents [202]. However, few studies to date have examined the effects of media composition on subsequent MSC immunomodulation. In this dissertation, culture media was found to drastically influence immunomodulatory paracrine factor secretion. Culture in MEMα supplemented with FBS induced paracrine factor secretion but limited MSC growth in spheroids, whereas culture in MesenCult medium suppressed immunomodulatory paracrine factor secretion but promoted MSC growth in spheroids. Compared to MSC spheroids cultured with FBS-containing media, addition of pro-inflammatory cytokines to MesenCult medium did not pre-condition spheroids to secrete increased PGE_2 or increase IDO activity and did not enhance the suppression of TNF-α secretion by activated macrophages. Similar to our results, MSCs expanded as adherent monolayers in medium supplemented with HPL displayed enhanced proliferation and expansion potential, yet decreased PGE_2 production and impaired inhibition of T-cell proliferation [203]. In addition, although MSCs cultured in FBS or HPL media inhibited T-cell proliferation comparably in mixed lymphocyte reactions, inhibition of B cell proliferation was greater when co-cultured with MSCs expanded with FBS instead of HPL [204]. Furthermore, differences in the cytokine secretion of lymphocytes were noted in co-cultures with MSCs expanded in either FBS- or HPL-containing media. Altogether, these studies demonstrate that the soluble components of MSC culture medium can significantly impact immunomodulatory function. Therefore, a systematic determination of appropriate culture media that enhances the paracrine

secretion capabilities of MSCs may be critical for stimulating immunomodulatory phenotypes in MSC cultures for translational applications. Recently, several groups have taken this approach to begin to systematically determine chemically-defined xeno-free culture medium to culture MSC spheroids and stimulate immunomodulatory factor expression [205, 206].

The addition of the pro-inflammatory cytokines IFN-γ and TNF-α to FBS culture media further enhanced immunomodulatory paracrine factor secretion and suppression of activated macrophages by MSC spheroids, demonstrating that 3D aggregation and cytokine treatment can work synergistically to enhance MSC immunomodulation. IFN-γ and TNF-α are critical components of the inflammatory milieu, capable of stimulating MSC immunomodulatory paracrine factor secretion. PGE_2 secretion by adherent mouse MSCs can be induced by IFN-γ and TNF-α treatment [32, 35]. PGE_2 aids in suppression of T-cell activation and proliferation [60, 119], modulates CD4+ T-cell differentiation [81], and regulates macrophage phenotypes by suppression of M1 and induction of M2 phenotypes [70, 79]. PGE_2 secretion from MSC spheroids appears to be more responsive to TNF-α treatment since treatment with 10 ng/mL TNF-α alone resulted in greater PGE_2 secretion compared to untreated and IFN-γ-treated spheroids, whereas treatment with 5 ng/mL of both IFN-γ and TNF-α did not significantly alter PGE_2 secretion compared to untreated or TNF-α-treated spheroids. IFN-γ induces human MSC expression of IDO [67, 82, 83], which inhibits proliferation of T- and natural killer (NK) cell proliferation through tryptophan depletion [77, 116], induces naive CD4+CD25- T-cell maturation into CD4+CD25+FOXP3+ Tregs [138], and can aid in the induction of immune tolerance [139].

Additionally, IDO-derived tryptophan metabolites, including kynurenine, can suppress T-cell proliferation [117]. MSC spheroids were responsive to IFN-γ and had greater IDO expression compared to adherent cultures. In MSC spheroid cultures, stimulation with IFN-γ and TNF-α in FBS culture media resulted in the greatest secretion of IL-6. Secretion of IL-6 has been implicated in regulating maturation of dendritic cell (DC) populations by suppressing monocyte differentiation [62]. Additionally, mouse MSC suppression of inflammation in an arthritis model was primarily mediated by IL-6 dependent secretion of PGE_2, suggesting that increased IL-6 secretion may be a mechanism by which MSCs are self-activated to secrete PGE_2 that can impart other immunomodulatory effects [135]. In contrast to the increases of PGE_2, IDO, and IL-6, secretion of TGFβ1, which has been demonstrated to be involved in inducing Treg phenotypes [61, 140, 141], was not enhanced by cytokine treatment of spheroid cultures in either FBS or MesenCult media. Taken together, while MSC spheroid formation increased the secretion of several immunomodulatory factors, pro-inflammatory cytokine treatment could further augment secretion of several paracrine factors responsible for MSC immunomodulation.

Several *in vitro* pre-conditioning strategies have been explored as a means to stimulate MSCs to elicit a desired response when transplanted *in vivo*. For example, hypoxic conditioning of MSCs has frequently been used to stimulate angiogenic paracrine factor production for MSC-based treatments for ischemia [207–209]. Additionally, there is some evidence that pre-conditioning MSCs with activating signals can enhance MSC immunomodulation as pre-treatment of adherent MSCs with IFN-γ and TNF-α [131] or TLR3 and TLR4 ligands [34,35] can regulate MSC immunomodulation *in vitro*. In our

study, aggregation of MSCs and pre-treatment with IFN-γ and TNF-α in FBS medium, but not MesenCult medium, enhanced the suppression of macrophage TNF-α secretion. Pre-conditioning may therefore provide a potential means of enhancing MSC immunotherapies by priming the cells to secrete immunomodulatory paracrine factors immediately upon transplantation. However, the success of this strategy to enhance MSC immunomodulatory paracrine factor secretion may be dependent on specific culture parameters, such as media composition and cell culture format (i.e. spheroid culture).

Interestingly, despite the increased expression of several immunomodulatory factors known to be involved in MSC-mediated suppression of T-cells, IFN-γ pre-treated MSC spheroids displayed a reduced ability to suppress T-cell proliferation and activation compared to an equivalent amount of adherent MSCs. While previous studies have found a strong correlation between MSC expression of IDO and the ability to inhibit T-cell proliferation [78], this correlation was not consistent with MSC spheroid cultures. The difference in surface area between and adherent and spheroid cultures was initially hypothesized to reduce the efficacy of MSC suppression of T-cells due to reduced contact with immunosuppressive membrane-bound ligands such as PDL1, PDL2, or FasL [142, 201]. However, physical separation of MSCs from PBMCs using a transwell co-culture significantly reduced, but did not eliminate MSC suppression of T-cell proliferation of both adherent and spheroid cultures. Therefore, other mechanisms independent from direct cell-cell contact are likely responsible for the observed differences in MSC suppression of T-cells when MSCs are cultured as adherent monolayers or aggregated spheroids. Interestingly, other groups have found that aggregated MSCs self-activate caspase-

dependent IL-1 signaling [175]. The expression of IL-1α and IL-1β by MSCs in response to aggregation resulted in downstream autocrine signaling that stimulated MSC expression of the anti-inflammatory factors PGE_2 and TSG-6. While the authors found the concentrations of IL-1α and IL-1β to be relatively low (4-10 pg/mL in hanging drops), expression of IL-1 or other inflammatory cytokines by MSCs in response to aggregation could potentially reduce the effectiveness of MSC suppression of T-cell proliferation *in vitro*. However, despite the reduced capacity of MSC spheroids to suppress T-cells *in vitro*, aggregation of MSCs after intravenous or intraperitoneal injection does not impair the immunomodulatory capabilities of transplanted MSCs [173, 174, 210]. Ultimately, a broader understanding of the anti- and pro-inflammatory factors expressed by MSCs through transcriptomic or proteomic analysis may provide better insight into the response MSCs have to not only aggregation but cytokine treatment as well. These broader analyses could aid in elucidating the mechanisms regulating MSC immunomodulatory function *in vitro* to better inform therapeutic strategies aimed at using MSCs to modulate immune responses *in vivo*.

3.5 CONCLUSION

MSCs offer a promising approach for cell-based therapies of inflammatory and immune diseases due to their inherent ability to modulate responses of cell populations involved in both innate and adaptive immunity. While MSC-based treatments in animal models and clinical trials of inflammatory and immune diseases have yielded variable results, the development of robust translatable strategies to enhance MSC immunomodulation may provide a simple means of improving such therapies and enable translation to the clinical

setting. The results of this study demonstrate that 3D aggregation enhances MSC immunomodulatory factor secretion and that the biochemical medium composition, including the presence of pro-inflammatory cytokines, can additionally increase endogenous MSC immunomodulatory properties. More broadly, pre-conditioning MSCs via environmental parameters can enhance inherent secretory properties that may improve the potency and efficacy of MSC-based therapies for the treatment of inflammatory diseases and immune disorders.

CHAPTER 4

OSTEOPROTEGERIN IS DIFFERENTIALLY EXPRESSED BETWEEN ADHERENT AND SPHEROID CULTURES OF MSCS

4.1 INTRODUCTION

Current mesenchymal stem/stromal cell (MSC) therapeutic strategies aim to use MSC-secreted soluble paracrine factors to modulate immune responses and promote tissue repair. As previously discussed, the quantity of paracrine factors secreted by MSCs, such as PGE_2, TGF-β1, and IL-6, can be enhanced by aggregation of MSCs into 3D spheroids [211]. However, the profile of paracrine factors expressed by MSCs is also altered in spheroid culture; expression of specific factors can be entirely induced or inhibited by aggregation of MSCs. For example, osteoprotegerin (OPG) is a secreted soluble factor that is highly differentially expressed between adherent and spheroid cultured MSCs (see **Figure 4.1**). OPG has been studied extensively in bone biology and plays a critical role in bone homeostasis by inhibiting osteoclast differentiation and maturation, thereby maintaining the balance of bone matrix deposition and resorption [212]. However, OPG has not been extensively explored in the context of the immune system, and the close relationship between osteoclasts and macrophages suggests that MSC-expressed OPG may also play a role in modulation of monocyte/macrophage populations and thereby contribute to the immunomodulatory activity of MSCs.

OPG (also known as TNFRSF11B) is a secreted 60 kDa protein and is a member of the tumor necrosis factor (TNF) receptor superfamily [213]. OPG acts as a soluble decoy receptor for the Receptor Activator of Nuclear Factor Kappa B Ligand (RANKL). Binding of OPG to RANKL inhibits the interaction between RANKL and its receptor, RANK, thereby inhibiting downstream activation of NF-κB and other transcription factors [214]. In bone, osteoclast generation from myeloid hematopoietic precursor cells is dependent on RANKL as well as the growth factor M-CSF [215, 216]. M-CSF stimulates osteoclast precursor survival and induces osteoclast precursor expression of RANK. Subsequent stimulation of osteoclast precursors with RANKL, typically by osteocytes and bone marrow stromal cells under homeostatic conditions [217, 218], results in expression of the transcription factors c-fos [219] and NFATc1/NFAT2 [220] and induces expression of genes necessary for osteoclast function including tartrate-resistant acid phosphatase (TRAP), cathepsin-K, calcitonin receptor, and c-myc [221]. Thus, OPG production, primarily by bone marrow stromal cells, regulates the generation of osteoclasts by binding to RANKL and inhibiting the RANK/RANKL interaction. Knockout of OPG in mice models results in the development of osteoporosis [222], illustrating the critical role of OPG in regulating the balance of osteoclast resorptive activity.

Outside its role as a critical mediator of bone homeostasis, the RANK/RANKL/OPG signaling axis has also been demonstrated to play a role in the immune system. RANKL is expressed by T-cells, B-cells, and γδT-cells while RANK is expressed by DCs, macrophages, and monocytes [223]. Additionally, OPG expression can be induced in B cells and DCs in response to CD40L [224]. RANKL expressed by T-cells promotes the

survival and function of DCs during immune responses [225–227] and stimulation of DCs with RANKL *in vitro* enhances cell survival, cytokine production, and antigen presentation [228]. Furthermore, dendritic cells in OPG-null mice are more effective in stimulating allogeneic T-cells [229] demonstrating an important two-way communication between T-cell and DCs through RANK/RANKL/OPG signaling. In addition to interactions with DCs, RANKL expression on T-cells can also induce differentiation of osteoclasts from monocytes [230]. Under inflammatory conditions, the cytokines IL-1, TNF-α, and IL-6 upregulate expression of RANKL in T-cells resulting in increased differentiation of osteoclasts and ultimately osteoporosis [231]. Altogether, interactions between RANKL expressed by lymphoid cells (i.e. T-cells) and RANK expressed by myeloid cells (i.e. DCs/monocytes) increase the immune response of these cell populations. Interestingly, MSC expression of OPG has not previously been investigated in relation to RANK/RANKL signaling between T-cells and myeloid cell populations and could potentially be a mechanism by which MSCs suppress immune responses.

Because of the multiple roles OPG plays in both maintaining bone homeostasis by regulating osteoclast differentiation and regulating immune responses, we sought to evaluate the functional role OPG expression plays in MSC suppression of T-cell proliferation and osteoclast differentiation *in vitro*. Previous studies have demonstrated that OPG expressed by adherent cultures of MSCs can inhibit osteoclast differentiation and maturation *in vitro* but no work has investigated the effect of aggregated MSCs on osteoclast differentiation [232]. Furthermore, the mechanisms governing OPG expression by MSCs in adherent and spheroid cultures is unclear. In osteoblasts, OPG expression is

regulated by a wide array of signaling molecules. For example, TGF-β, IL-1, IL-6, TNF-α, estrogen, and Wnt ligands all upregulate OPG expression while PGE_2 and glucocorticoids downregulate expression [233]. Wnt signaling, in particular, appears to play a critical role in mediating OPG expression by osteoblasts and osteoclast activity *in vivo* [234]. Activation of the canonical Wnt pathway results in dephosphorylation of β-catenin and subsequent nuclear translocation where β-catenin, along with T-cell factor (Tcf) and lymphoid-enhancing factor (Lef), can regulate transcription of target genes. However, β-catenin localization is also mediated by cell-cell cadherin interactions where it can be sequestered at adherens junctions. Since cadherins play a critical role in mediating self-aggregation of MSC spheroids [158, 159], we hypothesized that β-catenin is sequestered to adherens junctions at the cell membrane in spheroid cultures thereby inhibiting nuclear translocation of β-catenin and downstream transcription of OPG. Altogether, a better understanding of the functional role of MSC paracrine factors, such as OPG, and the mechanisms that regulate their expression may provide insight into new applications for MSC paracrine-based therapies and approaches to engineer systems to modulate MSC paracrine activity.

4.2 METHODS AND MATERIALS

4.2.1 MSC Expansion and Culture

Human bone marrow-derived MSCs were obtained from both Texas A&M Institute for Regenerative Medicine and RoosterBio Inc., and expanded according to the manufacturer's protocols as previously described (See *Chapter 3*). MSCs were expanded from 3 donors (1 Texas A&M Institute for Regenerative Medicine, 2 RoosterBio) and were passaged with

0.25% Trypsin and 1 mM EDTA upon reaching 80% confluency. To generate adherent and spheroid MSC cultures, MSCs were either plated overnight on tissue culture treated plastic or aggregated into 500-cell spheroids by addition of MSCs to 400 μm agarose microwells, as described previously (See *Chapter 3*).

4.2.2 Antibody Cytokine Arrays and Analysis

In order to more broadly examine MSC cytokine expression, 80 target cytokine antibody arrays were purchased from AbCam (ab133998; Abcam, Cambridge, UK) (species listed in **Table 4.1**). To generate conditioned medium for cytokine analysis, 300,000 adherent or spheroid MSCs were cultured for four days in 10 mL of RPMI-1640 medium supplemented with 10% FBS, 1% L-Glutamine, and 1% Penicillin/Streptomycin. Samples of conditioned medium were stored at -20 ºC prior to cytokine detection with antibody arrays. Arrays were developed according to the manufacturer's protocol using undiluted media samples and subsequently imaged using a Li-Cor Odyssey Fc imager equipped with a CCD camera. Semi-quantitative cytokine expression levels were determined by densitometry analysis using ImageJ software.

OPG and RANKL expression was also analyzed directly through qRT-PCR and ELISA analysis to quantify gene and protein expression, respectively. Adherent and spheroid MSCs were lysed 24 hours after plating and aggregation and RNA was collected for qRT-PCR, as previously described. Forward and reverse primers for *OPG* (Forward: GCTAACCTCACCTTCGAGCA; Reverse: TCAGGATCTGGTCACTGGGT), *RANKL* (Forward: CCAGGTTGTCTGCAGCGT; Reverse: TGACTCTCCAGAGTTGTGTCT),

and *18S* (Forward: CTTCCACAGGAGGCCTACAC; Reverse: CTTCGGCCCACACCCTTAAT) were designed using Primer-Blast (www.ncbi.nlm.nih.gov) and purchased from Invitrogen (Carlsbad, CA). *OPG* and *RANKL* gene expression was calculated with respect to untreated MSCs and normalized to *18S* expression using the ΔΔCT method. Additionally, the amount of secreted OPG and soluble RANKL was examined in adherent and spheroid conditioned medium after 4 days of culture via ELISA (R&D), according to the manufacturer's protocol. Finally, to examine the dynamics of OPG expression, MSCs were cultured as adherent monolayers, spheroids in suspension culture, spheroids dissociated to a single cell suspension with 0.25% Trypsin and 1mM EDTA and plated on tissue culture plastic, or spheroids plated directly onto tissue culture plastic. Medium was sampled every day for four days and secreted OPG was quantified using an ELISA.

Table 4.1: Protein species on cytokine antibody arrays

80 Target Cytokine Array										
Positive Control	Positive Control	Positive Control	Positive Control	Negative Control	Negative Control	ENA-78	GCSF	GM-CSF	GRO	GRO-α
I-309	IL-1α	IL-1β	IL-2	IL-3	IL-4	IL-5	IL-6	IL-7	IL-8	IL-10
IL-12 p40/p70	IL-13	IL-15	IFN-γ	MCP-1	MCP-2	MCP-3	MCSF	MDC	MIG	MIP-1b
MIP-1δ	RANTES	SCF	SDF-1	TARC	TGF-β1	TNF-α	TNF-β	EGF	IGF-1	Angiogenin
Oncostatin M	Thrombo-poietin	VEGF	PDGF-BB	Leptin	BDNF	BLC	Ck β 8-1	Eotaxin	Eotaxin-2	Eotaxin-3
FGF-4	FGF-6	FGF-7	FGF-9	Flt-3 Ligand	Fractalkine	GCP-2	GDNF	HGF	IGFBP-1	IGFBP-2
IGFBP-3	IGFBP-4	IL-16	IP-10	LIF	LIGHT	MCP-4	MIF	MIP-3α	NAP-2	NT-3
NT-4	Osteo-pontin	Osteo-protegerin	PARC	PIGF	TGF-β2	TGF-β3	TIMP-1	TIMP-2	Positive Control	Positive Control

4.2.3 Peripheral Blood Mononuclear Cell Co-culture Assays

PBMCs were isolated from whole blood obtained with IRB approval from healthy volunteers via Ficoll (Sigma-Aldrich) density gradient separation. Isolated PBMCs were cultured at 400,000 cells per well in 24-well plates with adherent and spheroid MSCs spheroids at a 3:1 MSCs-to-PBMC ratios. At the start of co-culture, 0.2 μg/mL of anti-human CD3 and CD28 antibodies were added to the co-cultures to induce T-cell proliferation and activation. Additionally, a range of concentrations (0.1-2.5 μg/mL) of an OPG blocking antibody (R&D) was added to a subset of co-cultures with adherent MSCs. Furthermore, a range of soluble recombinant OPG (20-500 ng/mL OPG; R&D) was added to a subset of spheroid cultures. For all PBMC co-cultures, T-cell proliferation was assessed 4 days later by flow cytometry analysis of CD3 (FITC-conjugated mouse anti-CD3 IgG; BD Biosciences) and Ki67 (PE-conjugated mouse anti-Ki67 IgG; BD Biosciences) double positive stained cells. T-cell activation was also assessed after 4 days by measuring the amount of IFN-γ in co-culture spent media supernatants by ELISA (R&D).

4.2.4 Osteoclast Differentiation and Analysis

Osteoclasts were differentiated according to previously published protocols. Briefly, $5x10^5$ PBMCs per well were plated in 96-well plates in MEMα medium supplemented in 10% FBS with 1% Pen/Strep and 1% L-Glutamine. After 1.5 hours to allow for attachment of monocytes, wells were washed three times with PBS to remove non-adherent cells. Fresh MEMα medium or conditioned medium collected from adherent or spheroid MSC cultures was then added to monocytes. For all osteoclast differentiations, recombinant human M-

CSF (25 ng/mL; R&D) and RANKL (50 ng/mL; Santa Cruz Biotech) were supplemented into basal MEMα medium, adherent conditioned medium, and spheroid conditioned medium. Additionally, where indicated, 100 ng/mL of recombinant human OPG (R&D) was added to either basal MEM medium or spheroid conditioned medium. Monocytes were cultured for two weeks to allow for osteoclast differentiation with medium exchanged every 3 days with fresh M-CSF, RANKL, and OPG.

To evaluate OPG differentiation, cells were fixed with 4% paraformaldehyde after 14 days of differentiation. A subset of fixed cells were stained with 1 µM DAPI and 1 µM phalloidin for 30 minutes to examine cell morphology and quantify the number of multinucleated cells. Fluorescent imaging of DAPI and phalloidin stained osteoclasts were acquired using an inverted Axio Observer Zeiss microscope. Additionally, a subset of fixed osteoclasts were stained for TRAP expression using a TRAP staining kit (Sigma) according to the manufacturer's instructions. Briefly, fixed cells were incubated with a solution of Naphthol AS-Bl phosphates, Fast Garnet GBC, and L-tartrate. Naphthol AS-Bl is released by acid phosphates resistant to tartrate and combine with Fast Garnet GBC to form insoluble maroon dye deposits where TRAP is expressed. TRAP stained cells were also counterstained for 2 minutes with Gill's Hematoxylin solution (Newcomer Supply, Middleton, WI). TRAP and hematoxylin stained cells were imaged with an upright Axio Imager A2 Zeiss microscope.

In order to evaluate functional activity of osteoclasts differentiated in the presence of MSC soluble factors, bone resorption activity was measured by differentiating osteoclasts on

fluoresceinated calcium phosphate-coated plates (CosmoBio, Tokyo, Japan). Seven days after initial plating of cells, medium from plates was sampled every other day and the fluorescent intensity at 488nm was measured using a SpectraMax i3 plate reader to determine the amount of fluorescein released from the calcium-phosphate coating by osteoclast resorptive activity. Fluorescence intensity at each day was normalized to medium samples from control wells with no cells. After 14 days of differentiation, cells were removed from the plates using a 5% bleach solution. Phase contrast images of the remaining calcium-phosphate coating were obtained using an upright Axio Imager A2 Zeiss microscope. Resorption pit area was quantified using ImageJ software.

4.2.5 Evaluation of β-catenin Localization in Adherent and Spheroid MSC Cultures

For determination of β-catenin localization, MSCs were plated at 10,000 cells/cm^2 (equivalent to density used in monolayer cultures) or aggregated into 500-cell spheroids. After 18 hours to allow for cell attachment to plates or aggregation of spheroids, MSCs were fixed with 4% paraformaldehyde. Cells were stained with a mouse anti-human β-catenin primary antibody (BD Bioscience) and donkey anti-mouse IgG Alex Fluor 488 conjugated secondary antibody (Life Technologies). Cells were subsequently stained with Hoechst (1:100 dilution) and CellMask (1:1000 dilution) to label nuclei and cell membranes, respectively. For adherent MSCs, fluorescent microscopy images were acquired with an inverted Zeiss Axio Observer microscope. For spheroid MSCs, 3D fluorescent images were acquired using a Zeiss light sheet microscope.

4.2.6 Statistical Analysis

Statistical analyses were performed using GraphPad Prism 6 software (Graphpad Software). Data are presented as mean ± standard error of the mean. Comparisons between multiple experimental groups were conducted using analysis of variance (ANOVA) after Box-Cox transformation to ensure normal distribution. Tukey post hoc analysis was then used to determine statistically significant differences between experimental groups, with a p-value < 0.05 indicating significance.

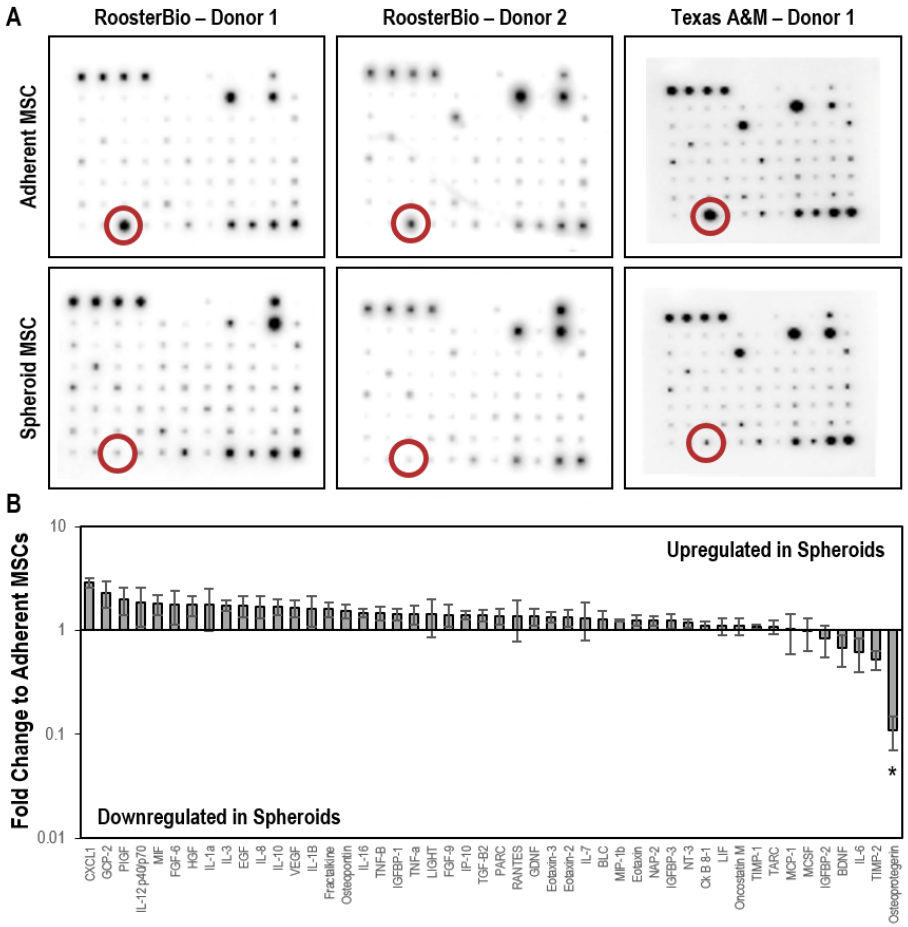

Figure 4.1. Cytokine array analysis of adherent and spheroid MSC paracrine factors reveals differential expression of OPG. (A) Conditioned medium from adherent and spheroid MSCs from three different donors displayed similar levels of cytokine expression with the exception of OPG (denoted by red circles). (B) The average OPG expression across all donors was the only cytokine significantly different in adherent and spheroid MSC medium, as determined by densitometry analysis of cytokine spots. * indicates p < 0.05 between adherent and spheroid MSC medium.

4.3 RESULTS

4.3.1 Osteoprotegerin is downregulated upon aggregation of MSCs

To examine the differences in paracrine factor expression between MSCs cultured as adherent monolayers and spheroids, an antibody array with 80 cytokine targets was used to broadly assess MSC cytokine expression. Conditioned medium from MSCs from 3 different donors cultured as adherent monolayers and as spheroids was collected and analyzed on the cytokine arrays (**Figure 4.1A**). Qualitatively, MSC cytokine expression was similar between adherent and spheroid cultures between all three donors. After densitometry quantification of spot intensity which is proportional to protein concentration, three cytokines were found to differ greater than 2-fold between adherent and spheroid conditioned medium (2.9-fold increase in CXCL-1, 2.3-fold increase in GCP-2, and 9.2-fold decrease in OPG; **Figure 4.1B**). However, osteoprotegerin (OPG) was the only cytokine found to exhibit statistically significant different expression in spheroid culture compared to adherent culture ($p = 0.004$). Furthermore, OPG was the most highly expressed cytokine in adherent conditioned medium but almost undetectable in spheroid conditioned medium. Because of the striking difference in OPG expression between adherent and spheroid cultures, we focused on understanding the functional effects of OPG in MSC conditioned medium and the mechanisms that regulate its differential expression in adherent and spheroid cultures.

To confirm and more precisely quantify the difference in OPG expression between adherent and spheroid MSC cultures, qRT-PCR and ELISAs were used to quantify gene and protein expression of OPG, respectively. A 16-fold decrease in OPG gene expression

($p < 0.001$) was found in spheroid MSC cultures compared to adherent cultures 24 hours after plating and aggregation (**Figure 4.2A**). Since OPG acts as a soluble decoy receptor for Receptor Activator of NF-κB Ligand (RANKL) and expression of these two proteins are inversely correlated, we also examined expression of RANKL. As expected, RANKL gene expression was increased 40-fold in MSC spheroid cultures ($p < 0.001$). At the protein level, aggregation of MSCs resulted in a 200-fold decrease in the OPG concentration in MSC spheroid conditioned medium compared to adherent medium (**Figure 4.2B**). However, no soluble RANKL protein could be detected within the conditioned medium, suggesting that RANKL remains membrane bound. Finally, the temporal kinetics of OPG expression was evaluated in MSC cultures to assess whether OPG expression can be recovered in aggregated MSCs after dissociation to single cells and subsequent plating as adherent monolayers (**Figure 4.2C**). Very low levels of OPG were secreted by MSC spheroids in suspension culture and OPG was only detectable after 3 days of medium conditioning. However, no statistical difference was observed in OPG expression of MSCs plated directly from adherent culture or MSCs dissociated from spheroids and plated as adherent monolayers, suggesting that loss of OPG expression after aggregation is reversible. Furthermore, MSC spheroids that were directly plated as aggregates initially had reduced OPG expression compared to adherent MSCs but began to recover OPG expression as cells began to spread out from MSC aggregates. Taken together, MSC expression of OPG is highly dependent on the physical environment (i.e. 2D or 3D) in which the cells are cultured.

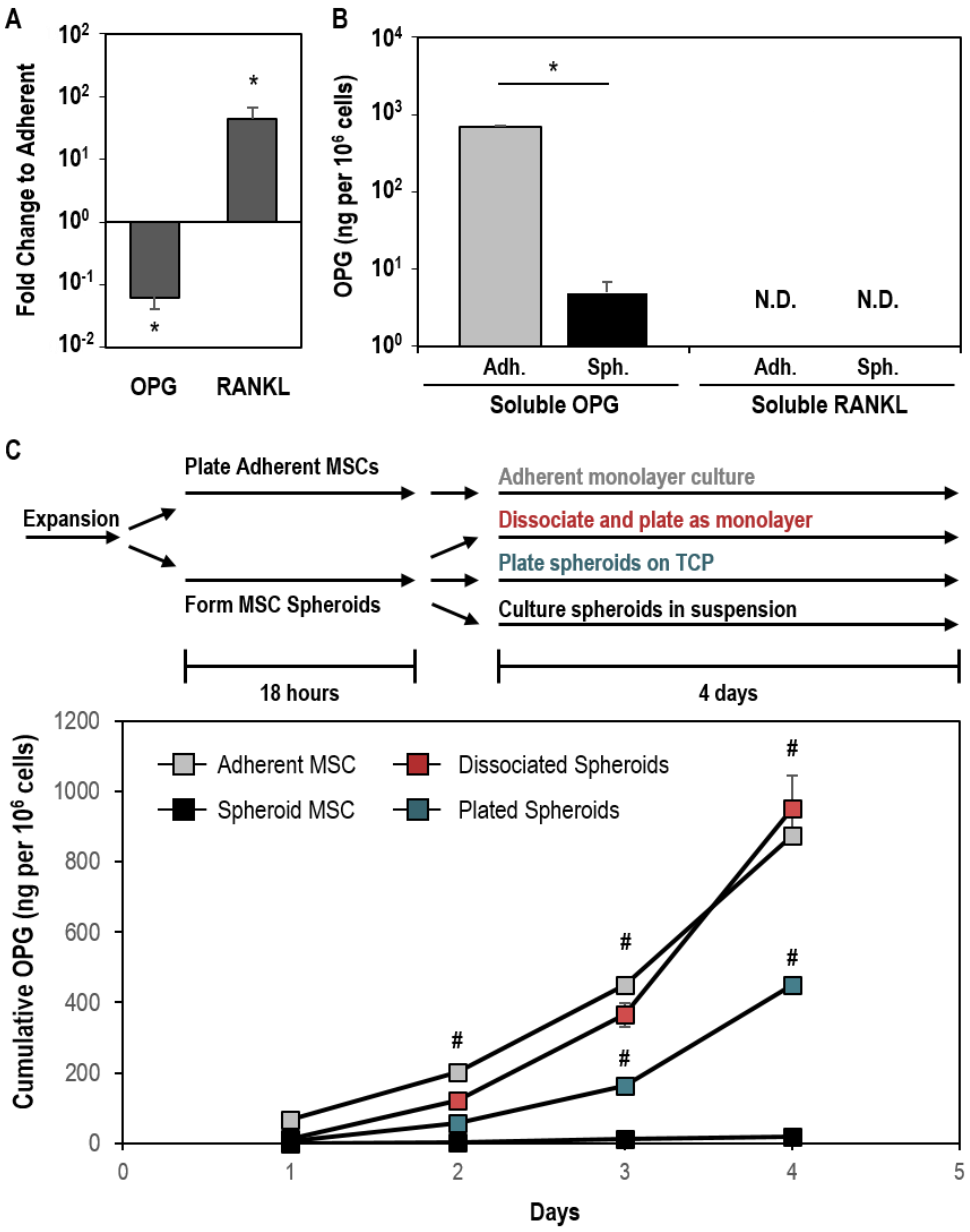

Figure 4.2. MSCs reversibly lose OPG expression upon aggregation. (A) MSC spheroids have significantly decreased OPG gene expression but increased RANKL gene expression after 18 hours of aggregation. (B) Similarly, a 200-fold increase in OPG protein could be detected by ELISA in adherent conditioned medium compared to spheroid conditioned medium, while no soluble RANKL could be detected in the culture medium of adherent or spheroid cultures. (C) The amount of OPG secreted by MSCs plated directly as adherent monolayers or plated from dissociated spheroids was not significantly different over 4 days of culture, demonstrating the reversibility of MSC OPG expression. * indicates $p < 0.05$ compared to adherent and spheroid cultures. # indicates $p < 0.05$ compared to spheroid culture at the same time point.

4.3.2 Osteoprotegerin is not responsible for difference in immunomodulatory activity between adherent and spheroid MSCs

Since spheroid MSCs do not express high levels of OPG and require a greater number of cells to suppress T-cell proliferation, we sought to determine if MSC expression of OPG was involved in inhibition of T-cell proliferation and activation. To perturb OPG inhibition of RANK/RANKL signaling in co-cultures with adherent MSCs, a range of concentrations of an OPG-blocking antibody (0.1-2.5 µg/mL; IC_{50} = 0.15-0.3 µg/mL for neutralization of 100 ng/mL OPG according to manufacturer) was added to MSC-PBMC co-cultures (1:3 MSC:PBMC ratio). However, supplementation of the OPG-blocking antibody into culture did not inhibit the ability of adherent MSCs to suppress T-cell proliferation at any of the concentrations tested (**Figure 4.3A;** ~20% $Ki67^+$ T-cells at each concentration of Ab). Additionally, T-cell IFN-γ expression was not significantly different between adherent MSC co-cultures with any concentration of blocking antibody (**Figure 4.3B**). Supplementation of a range of concentrations of recombinant OPG (20-500 ng/mL) into medium of MS-PBMC co-cultures (1:3 MSC:PBMC ratio) also did not restore the ability of MSCs to suppress T-cell proliferation at this ratio of MSCs-to-PBMCs (**Figure 4.3C;** ~65% $Ki67^+$ T-cells at each concentration of supplemented OPG). Likewise, no difference in T-cell expression of IFN-γ was observed in MSC spheroid co-cultures supplemented with any concentration of OPG (**Figure 4.3D**). Altogether, despite a significant difference in the expression of OPG by adherent and spheroid MSC cultures, OPG does not appear to play a significant role in MSC suppression of T-cell proliferation in CD3/CD28 activated PBMC co-cultures.

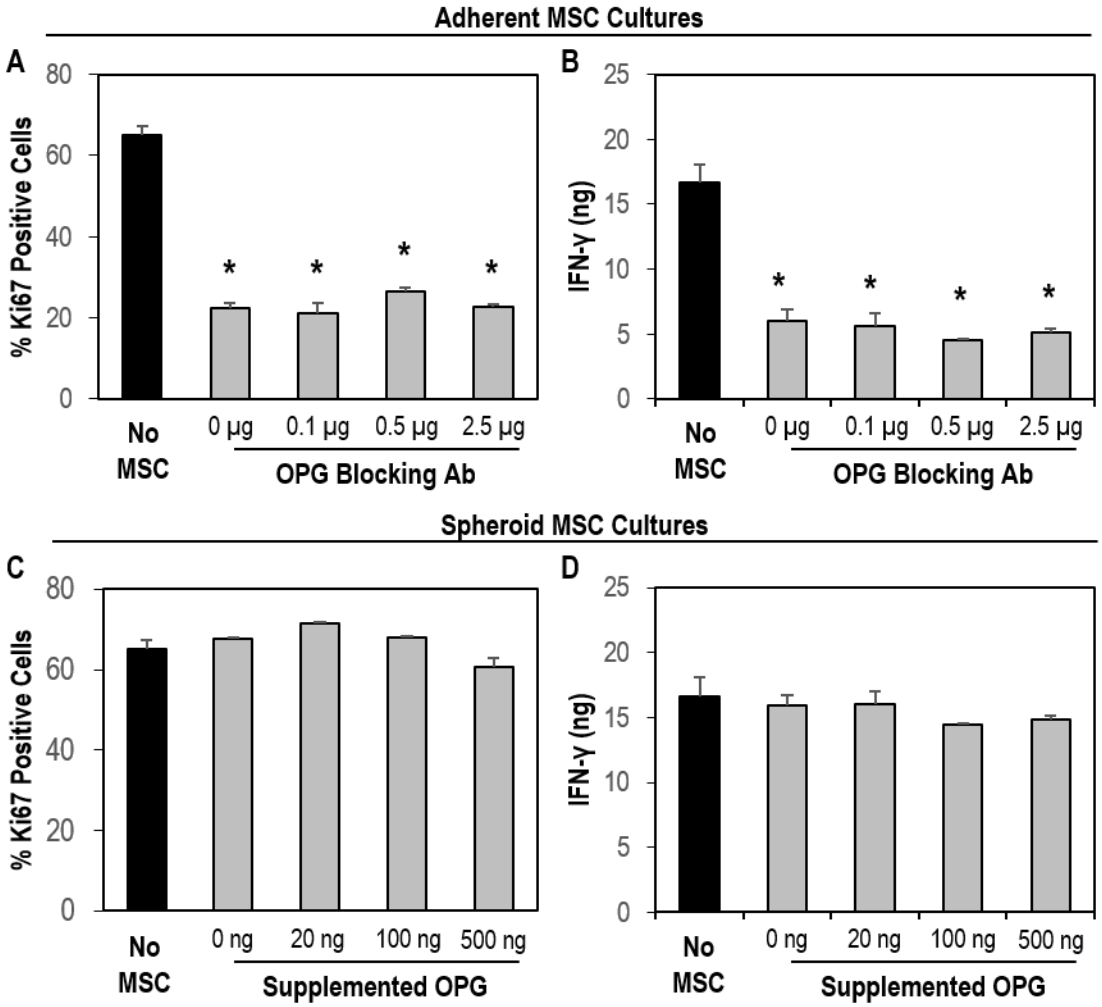

Figure 4.3. OPG does not play a role in MSC suppression of T-cell proliferation and activation in PBMC co-cultures. (A) Addition of an OPG-blocking antibody into co-cultures of PBMCs and adherent MSCs (1:3 MSC-to-PBMC ratio) did not significantly impair MSC suppression of T-cell proliferation. (B) Furthermore, MSC suppression of T-cell IFN-γ expression was not significantly impacted by addition of the OPG blocking antibody. (C) Supplementation of recombinant soluble OPG to co-cultures of PBMCs with spheroid MSCs (1:3 MSC-to-PBMC ratio) also did not recover the ability of MSCs to suppress T-cell proliferation at this MSC-to-PBMC ratio. (D) Similarly, IFN-γ expression was not significantly different with supplementation of OPG into MSC co-cultures. * indicates $p < 0.05$ compared to No MSC group.

4.3.3 Adherent and spheroid MSC paracrine factors differentially regulate osteoclast-precursor differentiation

Since RANKL signaling is critical for the differentiation and maturation of osteoclasts from osteoclast-precursors and OPG inhibits this process, we next examined the effect of MSC paracrine factors from adherent and spheroid cultures on osteoclast differentiation. The adherent fraction of PBMCs was cultured in the presence of RANKL and M-CSF in either base medium, adherent MSC conditioned medium, or spheroid MSC conditioned medium to stimulate osteoclast differentiation. After 15 days of culture, cells were analyzed by morphology and colorimetric staining for the expression of the osteoclast marker TRAP. After a week of culture, large multinucleated cells could be observed within cultures containing little or no OPG (spheroid MSC conditioned medium and base medium, respectively) (**Figure 4.4B**). However, these large multinucleated cells were not observed in adherent MSC conditioned medium containing approximately 100 ng/mL OPG. Furthermore, a significantly greater number of multinucleated cells was found within cultures with spheroid MSC conditioned medium compared to those in basal medium (**Figure 4.4C**; 8-fold increase in multinucleated cells, $p = 0.002$). Similarly, striking differences in TRAP staining were observed between spheroid MSC conditioned medium and adherent MSC conditioned medium (**Figure 4.4D**). Both basal medium and spheroid MSC conditioned medium induced $TRAP^+$ cells (~15 and ~260 $TRAP^+$ cells per well, respectively) whereas few $TRAP^+$ cells could be observed in cultures in adherent MSC medium (**Figure 4.4E**). Thus, spheroid MSC conditioned medium is permissive for or enhances osteoclast differentiation whereas adherent MSC conditioned medium is inhibitory for osteoclast differentiation.

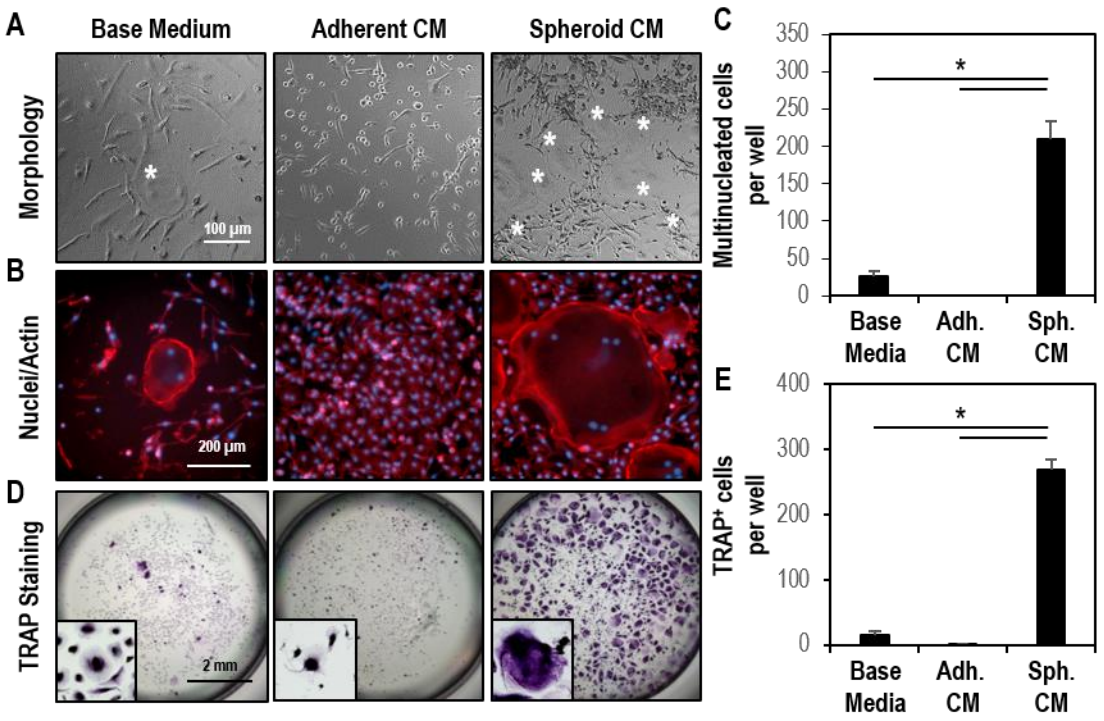

Figure 4.4. Adherent MSCs suppress whereas spheroid MSCs enhance osteoclast differentiation. (A) Large cells, morphologically resembling osteoclasts, could be seen in basal medium and MSC spheroid conditioned medium supplemented with M-CSF and RANKL after 15 days of culture. * indicates osteoclast-like cells. Scale bar = 100 µm (B) Furthermore, these osteoclast-like cells were found to be multinucleated after staining of nuclei and actin filaments. Scale bar = 200 µm (C) A significantly greater number of multinucleated cells were found in cultures with spheroid conditioned medium compared to basal medium while no multinucleated cells were observed in cultures with adherent conditioned medium (D) Finally, the large multinucleated cells in basal and spheroid conditioned medium stained positively for TRAP. Scale bar = 2 mm (E) Again, a significantly greater number of TRAP+ cells was observed in spheroid conditioned medium compared to basal medium or adherent conditioned medium. * indicates $p < 0.05$ between groups denoted by bar.

In order to evaluate functional activity of osteoclasts differentiated in the presence of adherent or spheroid MSC conditioned medium, the adherent fraction of PBMCs was cultured on fluoresceinated calcium phosphate coated plates for 15 days. Over the course

of differentiation, medium samples were taken to evaluate fluorescence intensity in order to determine resorption activity of differentiated osteoclasts. An increase in fluorescence intensity over baseline in spent media from osteoclast differentiation cultures could first be detected after 11 days in cultures in spheroid conditioned medium and basal medium, and continued to increase over the 15 days of culture (**Figure 4.5A**). Furthermore, the fluorescence intensity of culture medium was 1.6-, and 1.5- greater in cultures with MSC spheroid conditioned medium compared to basal medium on days 13 and 15, indicating more resorption activity of osteoclasts differentiated in the presence of MSC spheroid paracrine factors ($p = 0.01$ and 0.002, respectively). Finally, fluorescence intensity did not increase over baseline in cultures with adherent MSC conditioned medium indicating the lack of functioning osteoclasts in these cultures. Similarly, resorption pits were evident in cultures in basal medium and spheroid MSC conditioned medium after 15 days of culture whereas no resorption pits were observed in cultures with adherent MSC conditioned medium (**Figure 4.5B**). Furthermore, differentiation of osteoclasts in spheroid MSC conditioned medium or basal medium resulted in significantly greater resorption pit area compared to culture in adherent MSC conditioned media (**Figure 4.5C;** 35% and 20% resorption pit area, respectively, compared to 0% in adherent MSC conditioned medium). Altogether, M-CSF- and RANKL-induced osteoclast differentiation and maturation was enhanced in spheroid MSC conditioned medium whereas culture in adherent MSC conditioned medium inhibited osteoclast differentiation and maturation.

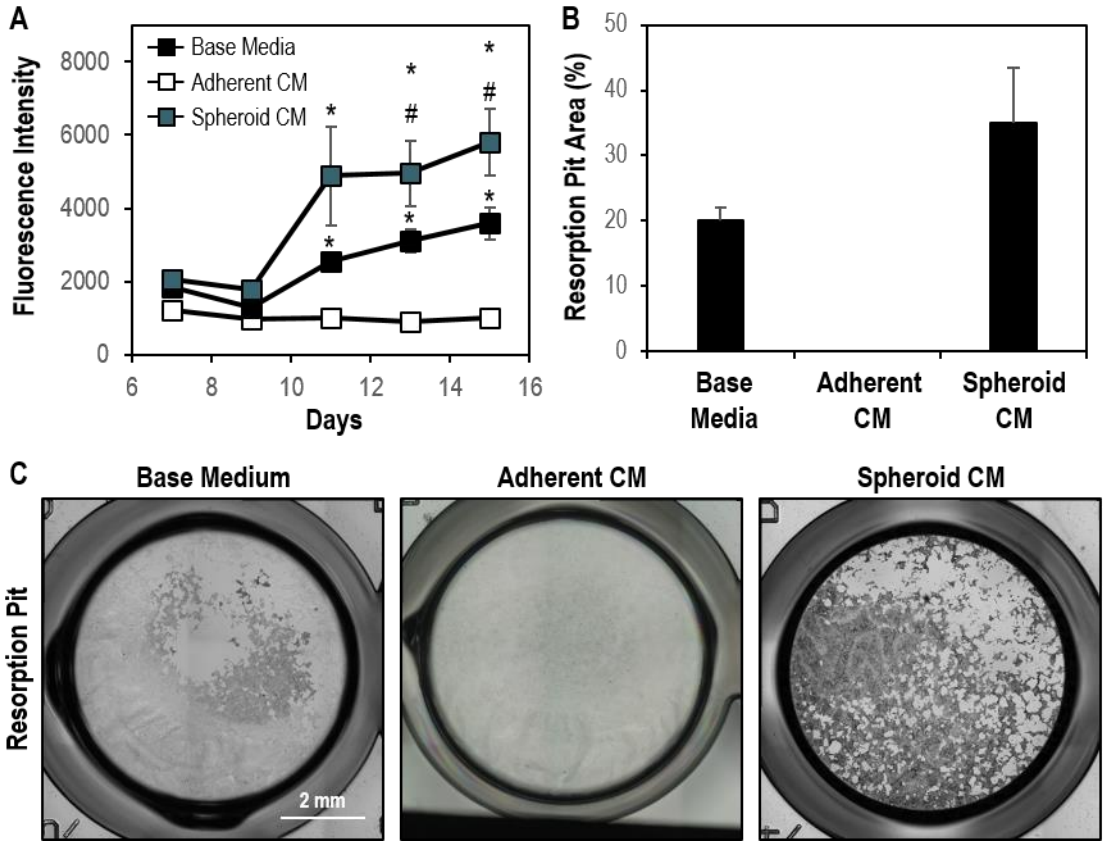

Figure 4.5. MSC spheroids promote osteoclast differentiation and resorption activity. (A) A greater amount of calcium phosphate resorption was observed in cultures differentiated in spheroid conditioned medium compared to basal medium, as indicated by an increase in fluorescein in culture medium released from calcium phosphate coatings by mature osteoclasts. (B) Resorption pits in the calcium phosphate coating could be observed from cells differentiated in basal medium or spheroid conditioned medium whereas no pits were observed in adherent conditioned medium cultures. (C) However, no significant difference was observed in resorption pit area between basal and spheroid conditioned medium. * indicates $p < 0.05$ compared to adherent conditioned medium at the same time point. # indicates $p < 0.05$ compared to basal medium at the same time point.

4.3.4 Differential expression of OPG mediates osteoclast-precursor response to MSC paracrine factors

Since OPG expression is drastically decreased in MSC spheroid medium, we sought to determine if restoration of OPG levels in MSC conditioned medium inhibited the ability of MSC spheroid conditioned medium to enhance osteoclast differentiation. Supplementation of OPG at an equivalent level found in adherent conditioned medium (~100ng/mL soluble OPG) effectively eliminated the capability of osteoprogenitor populations to differentiate to $TRAP^+$ osteoclasts in both basal medium and spheroid MSC conditioned medium (**Figure 4.6A**). Differentiation of osteoclasts in spheroid MSC conditioned media again induced approximately 120 TRAP+ cells per well (**Figure 4.6B**). However, when OPG was supplemented into spheroid MSC conditioned medium little to no TRAP+ cells per well were observed, similarly to the number observed when osteoclasts are differentiated in adherent MSC conditioned medium. While other MSC-expressed soluble factors may be involved in supporting osteoclast differentiation, these results suggest that aggregation switches MSCs from an osteoclast-inhibitory cell population to an osteoclast supporting population specifically by downregulating OPG expression and secretion.

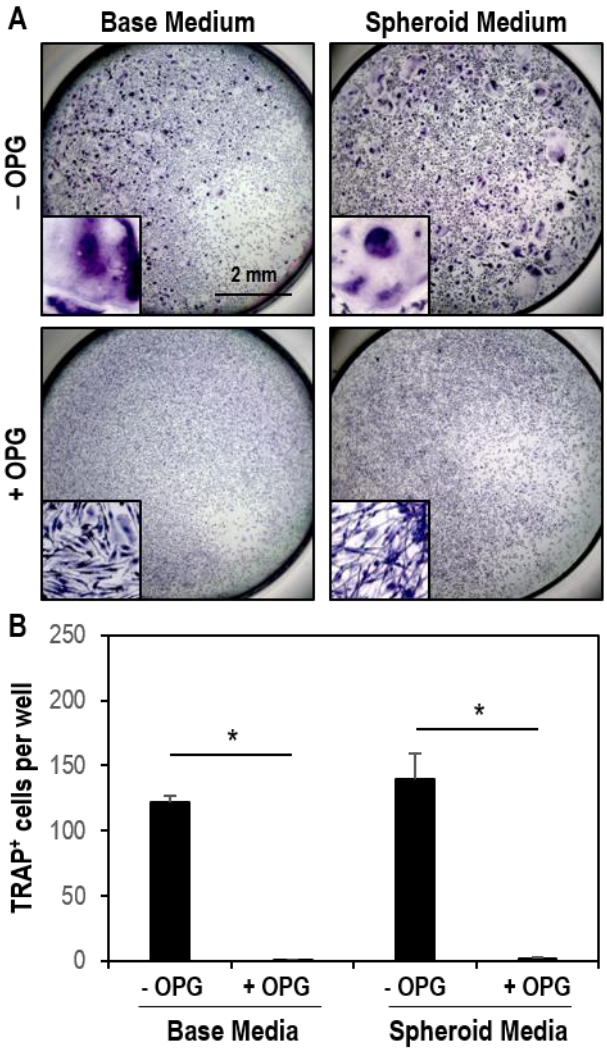

Figure 4.6. OPG inhibits osteoclasto-genesis in MSC spheroid conditioned medium. (A) Supplementation of 100 ng/mL of recombinant OPG into basal or MSC spheroid conditioned medium supplemented with M-CSF and RANKL inhibited osteoclast differentiation as determined by TRAP staining. Scale bar = 2 mm. (B) Quantification of the number of TRAP+ cells per well demonstrated that supplementation of OPG into the culture medium inhibited the differentiation of osteoclasts (184-fold decrease in $TRAP^+$ cells in basal medium and 84-fold decrease in spheroid conditioned medium). * indicates $p < 0.05$ between groups denoted by bar.

4.3.5 Increased β-Catenin Localization at the Cell Membrane in Spheroid Cultures

Due to the striking functional effects the presence or absence of OPG plays in the paracrine activity of MSCs, we began to investigate the mechanisms involved in regulating OPG expression in adherent and spheroid MSC cultures. Because MSC expression of OPG can be rapidly modulated within 24 hours (see Figure 4.2), we focused our efforts on the initial

signaling events that mediate aggregation of MSCs, in particular cadherin mediated β-catenin signaling. Additionally, β-catenin dependent signaling has been shown to be a critical mediator of OPG expression [235]. Therefore, we hypothesized that aggregation of MSCs induces increased cell-cell contacts and sequestration of β-catenin at the cell membrane, resulting in decreased transcription of β-catenin regulated genes, such as OPG. To investigate β-catenin signaling, MSCs were plated as adherent monolayers or aggregated into spheroids and stained for β-catenin 18 hours after plating and aggregate formation. In adherent cultures, the majority of β-catenin staining was diffuse throughout the cell, especially in cells with no contact with neighboring cells (**Figure 4.7A**). However, strong bands of localized β-catenin could be observed at the boundary between two contacting adjacent cells. In contrast, β-catenin was highly localized to the entire cell membrane in MSC spheroids and can be observed as a web-like pattern in 3D imaging of the aggregates (**Figure 4.7B**). Together, these results demonstrate a difference in β-catenin localization between adherent and spheroid MSC cultures, which may significantly influence downstream signaling in MSCs. However, whether sequestration of β-catenin at the membrane in spheroids is causative of decreased OPG expression still remains to be determined.

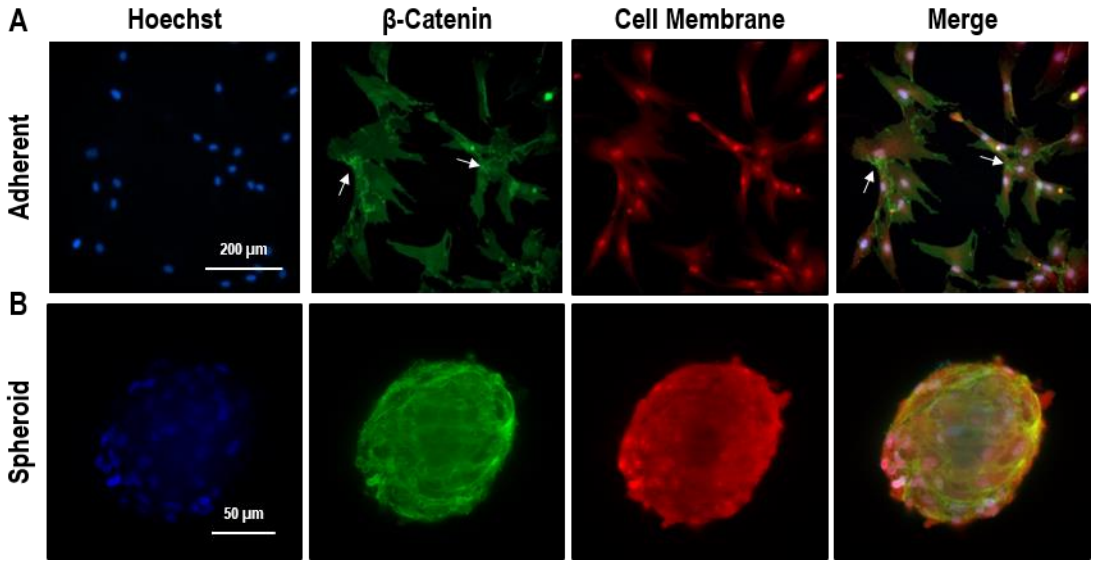

Figure 4.7. β-catenin is localized to the cell membrane in MSC spheroids. (A) In adherent MSC cultures, β-catenin staining was observed to be diffuse throughout the cell and was only strongly localized at the boundary of two adjacent and contacting cells (white arrows). (B) In contrast, β-catenin was observed to be localized to the entire cell membrane of MSCs in spheroid cultures likely due to contact with surrounding cells in all three dimensions.

4.4 DISCUSSION

In this study, we began to investigate the role MSC culture format (i.e. adherent vs. spheroid culture) plays on expression of the secreted soluble factor OPG and the functional role this difference plays in modulating immune responses and regulating osteoclast differentiation. The fact that MSCs can abundantly express OPG is not entirely unsurprising, given the role the stromal fraction of bone marrow plays in maintaining bone homeostasis *in vivo* through the expression of OPG [236]. However, few studies have rigorously investigated OPG expression by MSCs. Expression of OPG is commonly used as an indicator of osteogenic differentiation of MSCs, however, our results indicate that undifferentiated MSCs can rapidly and reversibly turn on or off (<24 hours) the expression

of OPG, depending on their environmental context. Therefore, expression of OPG is not necessarily dependent on differentiation. In this chapter we demonstrate that MSCs lose expression of OPG rapidly following aggregation. Furthermore, dissociation of aggregates to adherent monolayers restores OPG expression to levels comparable to adherent cultures of MSCs within 24 hours, demonstrating the ability of MSCs to rapidly regulate OPG expression in response to culture format. Altogether, MSCs dynamically express OPG, a critical factor in maintenance of bone tissue, in a manner that is highly regulated by the MSC environment. Furthermore, the dynamic expression of OPG highlights the plasticity of MSC paracrine activity that has the potential to be fine-tuned by engineering strategies, such as through aggregation, based on therapeutic need.

Since little work has investigated the functional role OPG expression plays in MSC paracrine activity, we sought to investigate its effects on modulating both T-cells and osteoclasts *in vitro*. Expression of OPG has not previously been linked to the immunomodulatory function of MSCs. Only one group has previously examined MSC expression of OPG in the context of inhibiting lymphocyte proliferation. The authors found that inhibiting OPG with a neutralizing antibody did not reduce the ability of MSCs to suppress proliferation and CD25 expression of PHA-stimulated lymphocytes in co-cultures [237]. However, since we found a striking difference in OPG expression and the ability to suppress T-cell proliferation between adherent and spheroid MSCs, we sought to interrogate this pathway directly in the CD3/CD28 activated PBMC co-culture assay. Consistent with the previously published work, inhibition of OPG in adherent MSC cultures did not reduce the ability of MSCs to suppress T-cell proliferation or activation.

Furthermore, supplementation of OPG within MSC spheroid co-cultures did not restore the suppression of T-cell proliferation to the extent observed in adherent MSC cultures. Together, these results indicate that MSC OPG expression does not play a significant role in MSC-mediated suppression of T-cell proliferation *in vitro*. Interestingly, IFN-γ inhibits RANK/RANKL signaling by promoting proteasomal degradation of tumor necrosis factor receptor-associated factor 6 (TRAF6), which is necessary for activating p38, JNK, and canonical NF-κB pathways downstream of RANK [238]. Since high levels of IFN-γ are detected within PBMC co-cultures (>5 ng/mL), the presence or absence of OPG may not have a large functional effect as downstream RANK signaling may already be inhibited by IFN-γ expression. Alternatively, future work focusing on MSC modulation of macrophage or dendritic cell populations in environments without a strong immune response (i.e. high levels of IFN-γ or other effector T-cell cytokines) may be beneficial for determining if MSC-expressed OPG plays a role in MSC anti-inflammatory function due to the similarity between macrophages, dendritic cells, and osteoclasts, which are all derived from a common progenitor.

Consistent with previously published reports, paracrine factors from adherent monolayer cultures of MSCs inhibited M-CSF- and RANKL-induced differentiation of osteoclasts from the adherent fraction of PBMCs. The inhibition of osteoclast differentiation by adherent MSCs has been attributed to both OPG expression [232] and CD200 expression [239]. However, as conditioned medium was used in this study, CD200 is unlikely to be involved in this system, as it requires direct cell-cell contact for signaling. Furthermore, it is unsurprising that osteoclasts differentiated in spheroid MSC conditioned medium

supplemented with soluble M-CSF and RANKL, which does not contain significant amounts of OPG. However, differentiation in spheroid conditioned medium increased the number of $TRAP^+$ and multinucleated cells and increased resorption of calcium phosphate coatings compared to osteoclasts differentiated in basal medium. Furthermore, addition of recombinant soluble OPG into MSC spheroid conditioned medium completely ablated the ability of spheroid conditioned medium to promote differentiation of osteoclasts. These results suggest that, in the absence of OPG, MSC paracrine factors stimulate and enhance osteoclastogenesis. Furthermore, osteoclastogeneiss may be enhanced in the presence of paracrine factors from MSC spheroids, since MSC aggregates upregulate expression of IL-6 (*See Chapter 3*) and IL-1 [175], which are both known osteoclastogenic cytokines [240]. Additionally, increased expression of PGE_2 by MSC spheroids could further suppress OPG expression and induce RANKL thereby aiding osteoclastogenesis [241]. Altogether, MSCs can highly express a critical factor in maintenance of bone homeostasis, which may be a critical consideration in strategies aimed at using paracrine-based MSC therapies to aid in bone healing and regeneration.

To determine the mechanisms governing OPG expression in adherent and spheroid MSCs, we began to explore β-catenin signaling within MSCs. Canonical Wnt signaling and downstream translocation of β-catenin to the nucleus has been shown to be critical for osteoblast expression of OPG [242]. Overexpression of β-catenin in osteoblasts resulted in high bone mass, while deletion of β-catenin expression in osteoblasts resulted in osteopenia [242]. Furthermore, the authors found that changes in bone mass were a result of dysregulated osteoclast bone resorption and that OPG is a direct target of β-catenin [242,

243]. Similarly, conditional deletion of APC in osteoblasts, a necessary component of the GSK-3 complex which marks β-catenin for degradation, results in constitutive activation of β-catenin, increased serum OPG levels, an absence of osteoclasts, and increased bone deposition [244]. Furthermore, deletion of β-catenin in osteoblasts results in decreased OPG levels and osteoporosis. While these studies focused on osteoblasts, they suggest that β-catenin dependent signaling may also be regulating OPG expression in MSCs. *In vitro,* β-catenin localization was found to be highly dependent on culture format. Diffuse staining of β-catenin was observed in adherent monolayer cultures except for at the boundary between two neighboring cells. In contrast, due to the aggregate structure of tightly packed cells with little to no surrounding matrix, β-catenin staining could be found localized to the entire cell membrane, potentially sequestering the majority of β-catenin and inhibiting downstream transcription. However, further studies will be necessary to confirm whether β-catenin signaling is mediating OPG expression in adherent and spheroid MSC cultures. Ultimately, a better characterization of signaling pathways regulated by aggregation may provide insight into the mechanisms governing the enhanced immunomodulatory, angiogenic, and trophic paracrine activity of MSC spheroids.

4.5 CONCLUSIONS

Overall, the results of this study demonstrate that aggregation of MSCs into spheroids regulates the composition of paracrine factors secreted by MSCs, in particular the RANKL decoy receptor OPG. Expression of OPG was found to be reversible after dissociation of spheroids, highlighting the critical importance of the MSC microenvironment on regulating MSC paracrine factor expression. Additionally, the differential expression of OPG by

adherent and spheroid MSCs resulted in functional differences in osteoclast differentiation in the presence of MSC paracrine factors. While adherent MSCs inhibit osteoclast differentiation by expressing OPG, MSC spheroids promote osteoclast differentiation through soluble paracrine factors while downregulating OPG expression. However, decreased OPG expression by MSC spheroids was not linked to the decreased ability to suppress T-cell proliferation compared to adherent MSCs in co-cultures with CD3/CD28 activated PBMCs. While the mechanisms mediating OPG expression in adherent and spheroid cultures is still unclear, the localization of β-catenin to the cell membrane in MSC spheroids suggests that cell-cell adhesions and the β-catenin pathway may be a critical mediator of MSC OPG expression and a compelling target for future studies determining mechanisms regulating MSC paracrine activity in response to aggregation.

CHAPTER 5

ENGINEERING 3D MSC/MICROPARTICLE CONSTRUCTS TO ENHANCE IMMUNOMODULATION

5.1 INTRODUCTION

Due to the dependency of MSC immunomodulation on the local cytokine milieu, the efficacy of MSC-based cellular therapies is highly dependent on the *in vivo* environment they are exposed to after injection. The environment may be highly variable based on the individual and disease being treated, the stage of inflammation, and the site of MSC transplantation. For example, high concentrations of inflammatory cytokines that often accompany acute inflammatory responses stimulate MSC immunomodulation[85]. However, the low levels of cytokines observed in chronic inflammation may not be sufficient to induce MSC immunomodulatory activity, thereby limiting the ability of MSCs to regulate inflammation of certain disease states and therefore contributing to variability in MSC treatment efficacy. Additionally, MSCs are typically infused intravenously and the majority of cells are entrapped within the capillary beds of the lung tissue, distant from sites of inflammation[245]. Entrapped MSCs are then rapidly cleared from the body within several days, limiting their residency time and effective window for immunomodulatory activity. Interestingly, the physical entrapment of MSCs in the lung causes the formation of aggregates of MSCs within the lung tissue, which results in upregulation of immunomodulatory factors such as PGE_2 and TSG-6, even in the absence of any cytokine priming[173, 174, 210]. While I.V. infused MSCs are capable of modulating immune responses in numerous disease models and human patients, presumably through systemic

effects of MSCs entrapped within the lung, the limited retention time and lack of exposure to local inflammatory cues may limit the overall immunomodulatory efficacy of transplanted MSCs.

To overcome these limitations, local transplantation of MSCs as pre-formed aggregates may improve retention of the cells at the site of interest, expose MSCs to the local inflammatory environment, and promote increased expression of immunomodulatory factors. Delivery of MSCs as aggregates is thought to preserve cell-cell and cell-matrix contacts within the aggregate structures, thereby preventing cell loss due to anoikis and resulting in better engraftment in host tissue[159, 169]. While systemic infusion of aggregates would not be possible due to the likelihood of occluding blood vessels, local transplantation through a larger bore needle is feasible and may be beneficial in concentrating MSC factors at sites of inflammation as well as exposing MSCs to the local inflammatory cytokine milieu. As a potentially complimentary strategy to enhance immunomodulation, MSCs are commonly pre-treated with inflammatory cytokines, such as IFN-γ, prior to intravenous infusion in order to augment their immunomodulatory activity during their minimal residence time after transplantation. IFN-γ pre-treated MSCs have exhibited improved resolution of inflammation in models of colitis[246] and graft-versus-host disease[247] compared to non-treated MSCs. Furthermore, pre-treatment of MSC aggregates with IFN-γ and TNF-α further increases the immunomodulatory activity of MSC spheroids[211]. However, despite the enhancement of MSC immunomodulation, the transient effects of pre-treatment of MSCs may limit the potential of MSC spheroids to

modulate immune responses for more than a few days in environments that do not expose the cells to high concentrations of IFN-γ, such as in chronic inflammatory states.

To address the transient effects of pre-treatment, we hypothesized that biomaterial-based presentation of cytokines within spheroidal MSC aggregates may provide a means of locally concentrating and sustaining presentation of bioactive IFN-γ to potentiate MSC immunomodulatory activity. Previous work from our group has demonstrated the use of microparticles to deliver growth factors and small molecules throughout stem cell aggregates[248–251]. Our first approach was to immobilize biotinylated IFN-γ to streptavidin-coated polystyrene microparticles in order to deliver IFN-γ within MSC spheroids. Additionally, microparticles consisting of cross-linked heparin have previously been fabricated and are capable of binding a large amount of heparin binding growth factors that remain bioactive when immobilized to the particles [252]. Since heparin has a high affinity for IFN-γ (K_D= 1-5 nM) [253, 254], can prevent proteolytic degradation of IFN-γ[255], and can enhance IFN-γ signaling[256], heparin microparticles were also used to deliver IFN-γ within MSC spheroids in these studies. The ability of microparticle delivered IFN-γ to induce sustained immunomodulatory activity was evaluated by measuring IDO expression of MSCs in response to microparticles and soluble pre-treatment and by assessing suppression of T-cell activation and proliferation in peripheral blood mononuclear cell (PBMC) co-cultures. Altogether, this strategy offers a translatable means of controlling MSC paracrine activity post-transplantation and therefore, improve the efficacy of MSC-based treatment strategies for inflammatory and immune diseases.

5.2 METHODS AND MATERIALS

5.2.1 Heparin microparticle synthesis

Heparin methacrylamide microparticles were fabricated as previously described[252]. Briefly, heparin methacrylamide was synthesized from heparin ammonium salt derived from porcine intestinal mucosa (17-19 kDa; Sigma-Aldrich, St. Louis, MO) and N-(3-aminopropyl) methacrylamide (APMAm; Polysciences, Warrington, PA) using 1-ethyl-3-(3-dimethylaminopropyl) carbodiimide (EDC; Thermo Scientific, Rockford, IL) and N-hydroxysulfosuccinimide (Sulfo-NHS; Thermo Scientific) [257]. Heparin ammonium salt (325 mg) was dissolved in distilled water (200 mL) with a 10-fold molar excess of EDC, sulfo-NHS, and APMAm in relation to the heparin carboxyl groups. The reaction was allowed to proceed for 5 hours at room temperature and pH 6.5, before being dialyzed against 2 L of water using 3.5 kDa molecular weight cutoff dialysis tubing (Spectrum Laboratories, Rancho Dominguez, CA) for 48 hours to remove excess reactants; dialysis water was exchanged ever 12 hours. The remaining heparin solution was then lyophilized for 4 days and stored at -20 ºC.

To fabricate heparin microparticles, a water-in-oil emulsion technique was used to generate small droplets of heparin solution that were subsequently stabilized by thermal cross-linking of the methacrylamide groups on the heparin species. 55.6 mg of lyophilized heparin methacrylamide was dissolved in 400 µL of phosphate buffered saline (PBS; Corning, Manassas, VA) supplemented with 18 mM of the free radical initiators ammonium persulfate (APS, Sigma Aldrich) and tetramethylethylenediamine (TEMED, Sigma Aldrich). The heparin solution was added dropwise to 60 mL of corn oil and 1 mL

of polysorbate-20 (Promega, Madison, WI). To form an emulsion, the entire solution was homogenized on ice at 3000 rpm for 5 min using a Polytron PT31000 homogenizer (Kinematica, Switzerland). After homogenization, free radical polymerization of the methacrylamide groups was initiated by submerging the emulsion in a hot water bath (55 ^{o}C) with gentle agitation under nitrogen purging for 30 minutes. The solution was then centrifuged at 3000 rpm for 10 minutes at 4 °C to obtain a pellet of microparticles. Microparticles were washed once in acetone followed by three water washes to remove residual oil and loosely cross-linked particles. The microparticles were then disinfected in a 70% ethanol solution for 30 minutes followed by additional washes with sterile water, lyophilized for two days, and stored at 4 $^{\circ}$C prior to use.

5.2.2 Heparin microparticle characterization

To determine the extent of IFN-γ binding to both streptavidin-coated polystyrene (3.0-3.4 μm diameter; SpheroTech, Lake Forest, IL) and heparin methacrylamide microparticles, approximately 1 x 10^6 particles were incubated at room temperature in 50 μL of PBS with 0.1% BSA and a range of IFN-γ (10-1000ng, R&D Systems, Minneapolis, MN) that is typically used to stimulate MSC IDO expression [258]. For all experiments with polystyrene particles, IFN-γ was first biotinylated using an EZ-Link Sulfo-NHS-Biotin biotinylation kit (ThermoFisher) according to the manufacturer's protocol. After 18 hours, the microparticles were centrifuged at 200x g for 5 minutes and the supernatant collected to determine the amount of free IFN-γ remaining in the solution. The amount of unbound IFN-γ was quantified using a human IFN-γ ELISA kit (R&D) and compared to an equivalent amount of IFN-γ incubated for 18 hours without microparticles in order to

generate a loading curve for IFN-γ binding to heparin microparticles. After the supernatant was collected to determine the amount of bound IFN-γ, microparticles were incubated in 1 mL of RPMI-1640 media with 10% FBS and incubated at 37°C for 7 days in a humidified 5% CO_2 incubator. 100 µL of the medium was sampled and replaced with an equivalent volume each day to determine the amount of IFN-γ released from the particles over time.

5.2.3 MSC expansion and culture

Human bone marrow-derived MSCs were obtained from RoosterBio Inc. (Frederick, MD). RoosterBio MSCs were demonstrated to undergo adipogenic and osteogenic differentiation and express the accepted panel of surface markers ($CD45^-$, $CD34^-$, $CD73^+$, $CD90^+$, $CD105^+$) by the manufacturer prior to use. Adipogenic and osteogenic differentiation potential was evaluated by Oil Red O and Alizarin Red staining respectively after 3 weeks of culture in the respective Life Technologies differentiation kits. Additionally, MSCs were 0% $CD45^+$, 0.1% $CD34^+$, 98.9% $CD73^+$, 99.5% $CD90^+$, and 95.9% $CD105^+$ as evaluated by flow cytometry. MSCs were expanded according to the manufacturer's protocols. Briefly, 1 x 10^7 cryopreserved MSCs were plated in twelve T225 flasks in 42 mL of RoosterBio High Performance Media and incubated at 37°C for 7 days in a humidified 5% CO_2 incubator. Media was exchanged after 4 days of culture. Cultures were passaged at 80% confluency by washing with 10 mL PBS followed by incubation with 10 mL of TrypLE at 37 ^oC. An equal volume of RoosterBio High Performance Media was added to quench TrypLE activity. Dissociated cells were then collected and centrifuged at 200x g. Cells were frozen in CryoStor CS5 cell cryopreservation media (STEMCELL Technologies, Vancouver, BC, Canada) prior to expansion for experiments. MSCs were

expanded for one or two passages from frozen stocks by plating $0.5x10^6$ cells in RoosterBio High Performance Media in 15 cm tissue culture treated dishes (manufacture details). Media was exchanged every three days and cells were passaged at 80% confluency. For all subsequent experiments, cell culture was conducted in RPMI-1640 medium (Corning Mediatech, Manassas, VA) supplemented with 10% FBS (Hyclone, Logan, UT), 1% L-Glutamine (Corning Mediatech), and 1% Penicillin/Streptomycin (Corning Mediatech).

5.2.4 IFN-γ loaded microparticle bioactivity

To evaluate the bioactivity of IFN-γ bound to polystyrene and heparin microparticles, adherent monolayer MSCs were cultured with microparticles loaded with 0 or 333 ng of IFN-γ per 1 x 10^6 particles. Particles were loaded with each IFN-γ concentration either 1, 2, 4, or 7 days prior to addition of particles to adherent MSC cultures to assess the activity of microparticle-bound IFN-γ over time. After 18 hours of loading, particles were washed to remove excess IFN-γ and incubated in RPMI-1640 medium supplemented with 10% FBS at 37°C until addition of particles to adherent MSC cultures. MSCs were plated in 24-well plates at a density of 50,000 cells/cm^2 and after 18 hours, ~200,000 particles were added to MSCs from each experimental group (IFN-γ loading concentration and incubation time). After 24 hours of culture, MSCs were lysed and RNA collected for quantitative real-time PCR (qRT-PCR) to measure IDO gene expression. RNA was extracted using an E.Z.N.A. Total RNA kit (OMEGA Bio-Tek, Norcross, GA) kit and cDNA was subsequently synthesized (300 ng RNA per sample) using an iScript cDNA synthesis kit (Bio-Rad, Hercules, CA). Forward and reverse primers for *IDO1* (Forward: AGCTTCGAGAAAGAGTTGAGAAG; Reverse: GTGATGCATCCCAGAACTAGAC)

and *18S* (Forward: CTTCCACAGGAGGCCTACAC; Reverse: CTTCGGCCCACACCCTTAAT) were designed using Primer-Blast (www.ncbi.nlm.nih.gov) and purchased from Invitrogen (Carlsbad, CA). *IDO1* gene expression was calculated with respect to untreated MSCs and normalized to *18S* expression using the ΔΔCT method.

5.2.5 MSC spheroid formation

Three dimensional spheroids were formed by forced aggregation of MSCs into an array of 400 x 400 μm inverse pyramidal agarose microwells as a high throughput method of generating homogenous cell aggregates. For all experiments, 500-cell spheroids were formed by adding $6x10^5$ cells to an agarose insert containing 1200 microwells and centrifuging at 200x g for 5 minutes. After 18 hours, MSCs self-assembled into spherical aggregates. In order to form spheroids with microparticles, a suspension of unloaded heparin microparticles or microparticles previously incubated with 33 or 333 ng IFN-γ per 1 x 10^6 MPs for 18 hours was mixed with the cell suspension at a 2:1 microparticle-to-MSC ratio and added to the microwells (**Figure 5.1**). The incorporation efficiency of heparin microparticles within MSCs spheroids was quantified by lysing spheroids after initial formation and counting the number of particles retrieved from the spheroids. Furthermore, MSC spheroids without particles were also formed, and a subset was pre-treated with IFN-γ at equivalent doses to IFN-γ microparticle groups (20 ng/mL or 200 ng/mL concentration, equivalent to 66 ng or 666 ng per 1 x 10^6 cell, respectively). After 18 hours of microwell aggregate formation, spheroids were either cultured alone to assess

IDO and immunomodulatory factor expression or with peripheral blood mononuclear cells (PBMCs) to assess the immunomodulatory activity of MSC spheroids.

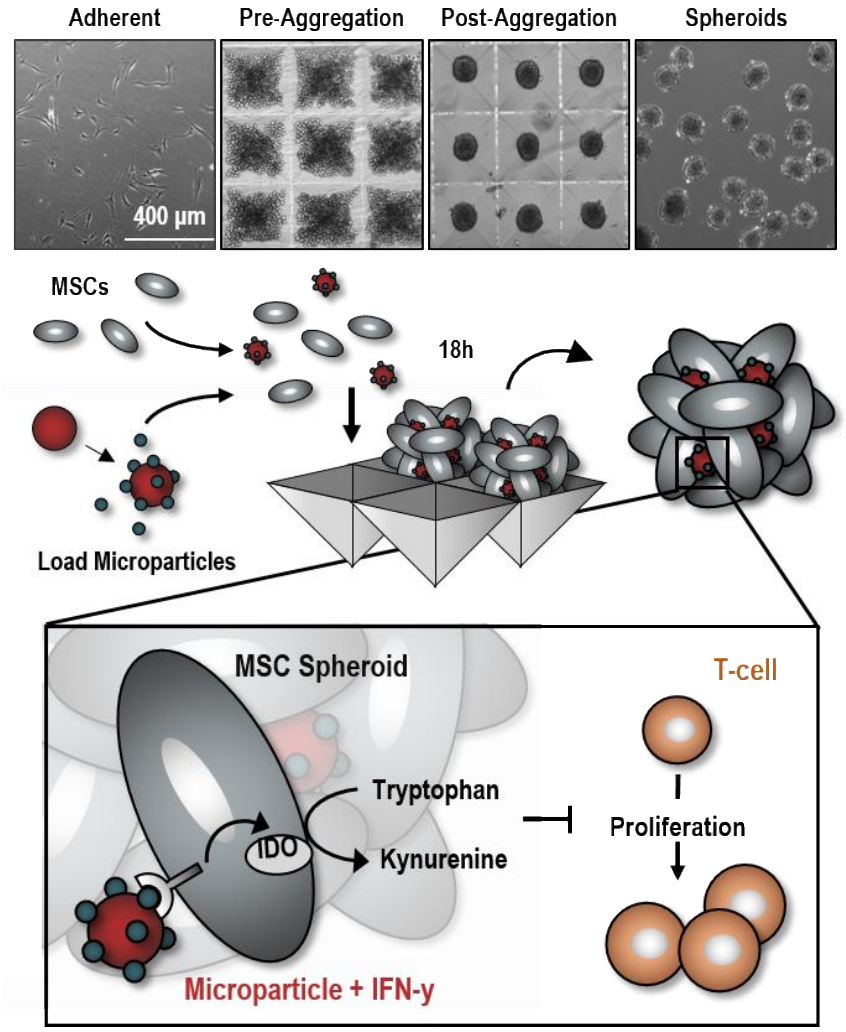

Figure 5.1. Microparticle delivery of IFN-γ within MSC spheroids. To form aggregates, MSCs were dissociated from adherent culture and mixed with IFN-γ loaded microparticles. Spheroids were subsequently formed via forced-aggregation of cells and particles within microwell arrays to entrap cytokine-loaded microparticles within the spheroidal construct in order to provide sustained local presentation of IFN-γ within the MSC aggregates.

5.2.6 Analysis of MSC immunomodulatory factor expression

To evaluate MSC IDO expression in response to IFN-γ pre-treatment or microparticle delivery, MSC spheroids were cultured for up to 7 days. At days 1, 2, 4, and 7, MSCs were collected for qRT-PCR analysis of *IDO1* gene expression relative to untreated MSC spheroids. Cell lysates of MSC spheroids were also collected at days 1 and 4 for Western blotting. Sample protein concentration was first determined using a BCA Protein Quantification kit (Pierce Biotechnology, Rockford, IL). SDS/PAGE loading buffer was then mixed with 25 µg of protein per sample and incubated at 95ºC for 5 min. Protein samples were subsequently loaded in 4-15% Mini-PROTEAN TGX gels (Bio-Rad Laboratories, Hercules, CA). Vertical electrophoresis was performed using the Mini-PROTEAN Tetra Cell (Bio-Rad) system with SDS/PAGE running buffer at 200V for 20 min with a 10-250 kDa protein ladder (Precision Plus Protein Kaleidoscope, Bio-Rad) as a molecular weight reference. Protein was then transferred to a nitrocellulose membrane (Bio-Rad) via semi-dry transfer (Trans-Blot SD, Bio-Rad) at 25V for 20 min. Membranes were blocked with infrared blocking medium (Rockland Immunochemicals, Pottstown, PA) for 1h followed by incubation with primary antibodies for IDO (rabbit anti-IDO IgG; Abcam, Cambridge, UK) and the loading control GAPDH (monoclonal goat anti-GAPDH; Abcam) overnight at 4ºC. Secondary IR antibodies (680 donkey anti-rabbit and donkey 800 anti-goat; Li-Cor Biosciences, Lincoln, NE) were used to detect IDO and GAPDH protein, respectively, and the blots were imaged using an Odyssey Infrared imager (LiCor Biosciences).

To evaluate spatial expression of IDO in response to IFN-γ pre-treatment or IFN-γ loaded microparticles, MSC spheroids were fixed in 10% formalin for 30 minutes for immunohistological analysis. After fixation, spheroids were washed three times with PBS, paraffin processed, embedded, and sectioned at 5 μm. Histological sections were de-paraffinized, incubated in a citrate-based Antigen Unmasking Solution (Vector Laboratories), and labeled with a primary antibody for human IDO (mouse anti-human IDO, Millipore) at a 1:200 dilution. Samples were subsequently incubated with horseradish peroxidase-conjugated anti-mouse IgG secondary antibody (ImmPRESS Reagent Kit, Vector Laboratories) followed by ImmPACT DAB Peroxidase Substrate (Vector Laboratories) to visualize IDO. Slides were counterstained with Alcian Blue (pH = 2.0) and Nuclear Fast Red to visualize sulfated glycosaminoglycans (in particular, heparin particles) and cell nuclei, respectively. An Axio Imager 2 upright microscope (Zeiss) was used to capture brightfield images of samples.

5.2.7 Peripheral blood mononuclear cell co-cultures

PBMCs were isolated from whole blood obtained with IRB approval from healthy volunteers via Ficoll (Sigma-Aldrich) density gradient separation. Isolated PBMCs were cultured at 400,000 cells per well in 24-well plates with MSCs spheroids at ratios of 1:3, 1:1, and 3:1 MSCs-to-PBMCs, based on ratios typically reported[78, 259, 260] and preliminary testing. At the start of co-culture, 0.2 μg/mL of anti-human CD3 and CD28 antibodies were added to the co-cultures to induce T-cell proliferation and activation. To evaluate microparticle delivery of IFN-γ within MSC spheroids, four experimental groups were evaluated: 1) MSC spheroids without additional treatment, 2) spheroids pre-treated

with 200 ng/mL (666 ng per 1 x 10^6 cells) of soluble IFN-γ, 3) spheroids containing unloaded heparin microparticles, and 4) spheroids containing heparin microparticles (2:1 MP:MSC ratio) loaded with 333 ng IFN-γ per 1 x 10^6 particles. Where indicated, 1-methyl$_{DL}$-tryptophan (1-MT, diluted in 0.1 N NaOH; Sigma-Aldrich), an inhibitor of IDO activity, or an equivalent volume of a vehicle control (0.1 N NaOH) was added to co-cultures at a final concentration of 5 mM 1-MT. In a subset of cultures, PBMCs were added to the upper well of a 0.4 μm pore polycarbonate transwell (Corning) and co-cultured with MSC spheroids pre-treated with 200 ng/mL IFN-γ at a 3:1 MSC-to-PBMC ratio. MSC spheroids were added to PBMC co-cultures immediately after aggregate formation, except where indicated otherwise. To test the persistence of spheroid immunomodulatory activity in culture, spheroids were added to PBMC co-cultures 2 or 4 days after initial aggregate formation and IFN-γ pre-treatment. For all PBMC co-cultures, T-cell proliferation was assessed 4 days later by flow cytometry analysis of CD3 (FITC-conjugated mouse anti-CD3 IgG; BD Biosciences, East Rutherford, NJ) and Ki67 (PE-conjugated mouse anti-Ki67 IgG; BD Biosciences) double positive stained cells. T-cell activation was also assessed after 4 days by measuring the amount of IFN-γ in co-culture spent media supernatants by ELISA (R&D). Finally, expression of anti-inflammatory cytokines was assessed after 4 days by measuring the amount of IL-10 in co-culture spent media supernatants by ELISA (R&D).

Monocytes were isolated from PBMCs using an EasySep Human CD14$^+$ Positive Selection Kit (STEMCELL Technologies) and cultured at 400,000 cells per well in 24-well plates with MSC spheroids from each experimental group as in PBMC co-culture experiments at

a 3:1 MSC-to-monocyte ratio with no supplemented cytokines. After 4 days of co-culture, phenotype was evaluated by flow cytometry analysis of CD14 (FITC-conjugated mouse anti- CD14 IgG) and CD206 (APC-conjugated mouse anti-CD206 IgG) stained cells. Additionally, the amount of the anti-inflammatory cytokine, IL-10, in co-culture spent media supernatants was measured by ELISA (R&D).

5.2.8 Statistical Analysis

Statistical analyses were performed using GraphPad Prism 6 software (Graphpad Software, La Jolla, CA). Data are presented as mean ± standard error of the mean. Comparisons between multiple experimental groups were conducted using analysis of variance (ANOVA) after Box-Cox transformation to ensure normal distribution. Tukey post hoc analysis was then used to determine statistically significant differences between experimental groups, with a p-value < 0.05 indicating significance.

5.3 RESULTS

5.3.1 Biotinylated IFN-γ binds to streptavidin-coated microparticles but does not remain bioactive over time

To determine the capacity of IFN- immobilization on polystyrene particles, streptavidin-coated polystyrene particles were incubated in solutions of varying concentrations of biotinylated IFN-γ (10-1000 ng per 1 x 10^6 particles) for 18 hours. When incubated with 100 ng or less of IFN-γ, polystyrene particles depleted approximately 98% of the initial biotinylated IFN-γ from solution (**Figure 5.2A**). However, polystyrene particles only

bound ~91% of IFN-γ from solution containing 333 ng IFN-γ and only 47% from a solution containing 1000ng IFN-γ solution, suggesting a maximum binding capacity on the order of 500ng per 1 x 10^6 particles. To determine release of biotinylated IFN-γ, microparticles were resuspended in fresh cell culture medium containing 10% FBS and incubated for one week. While an initial burst release of approximately 5% of initially loaded IFN-γ was released form particles loaded with 100 or 1000 ng IFN-γ, no subsequent release of IFN-γ occurred over the following 6 days (**Figure 5.2B**). Finally, to evaluate the bioactivity of biotinylated IFN-γ immobilized on polystyrene particles, adherent MSCs were cultured directly with particles loaded with IFN-γ (100 ng per 1 x 10^6 particles). Particles were loaded with IFN-γ 7, 4, and 1 day prior to addition to MSC cultures to assess the bioactivity of particle-bound IFN-γ over time. Particles loaded with IFN-γ one day prior to MSC culture significantly upregulated MSC IDO expression compared to MSCs receiving no treatment or unloaded microparticles (~470-fold increase in IDO expression compared to no treatment MSCs, $p < 0.001$), similar to the response of MSCs to an equivalent dose of biotinylated IFN-γ delivered solubly (**Figure 5.2C**). However, particle-bound IFN-γ completely lost the ability to induce MSC IDO expression after 4 and 7 days of culture. Altogether, while biotinylated IFN-γ could be immobilized on streptavidin-coated polystyrene microparticles, bioactivity of particle-bound IFN-γ significantly decreased over time and therefore were not suitable for sustained delivery of IFN-γ within MSC spheroids.

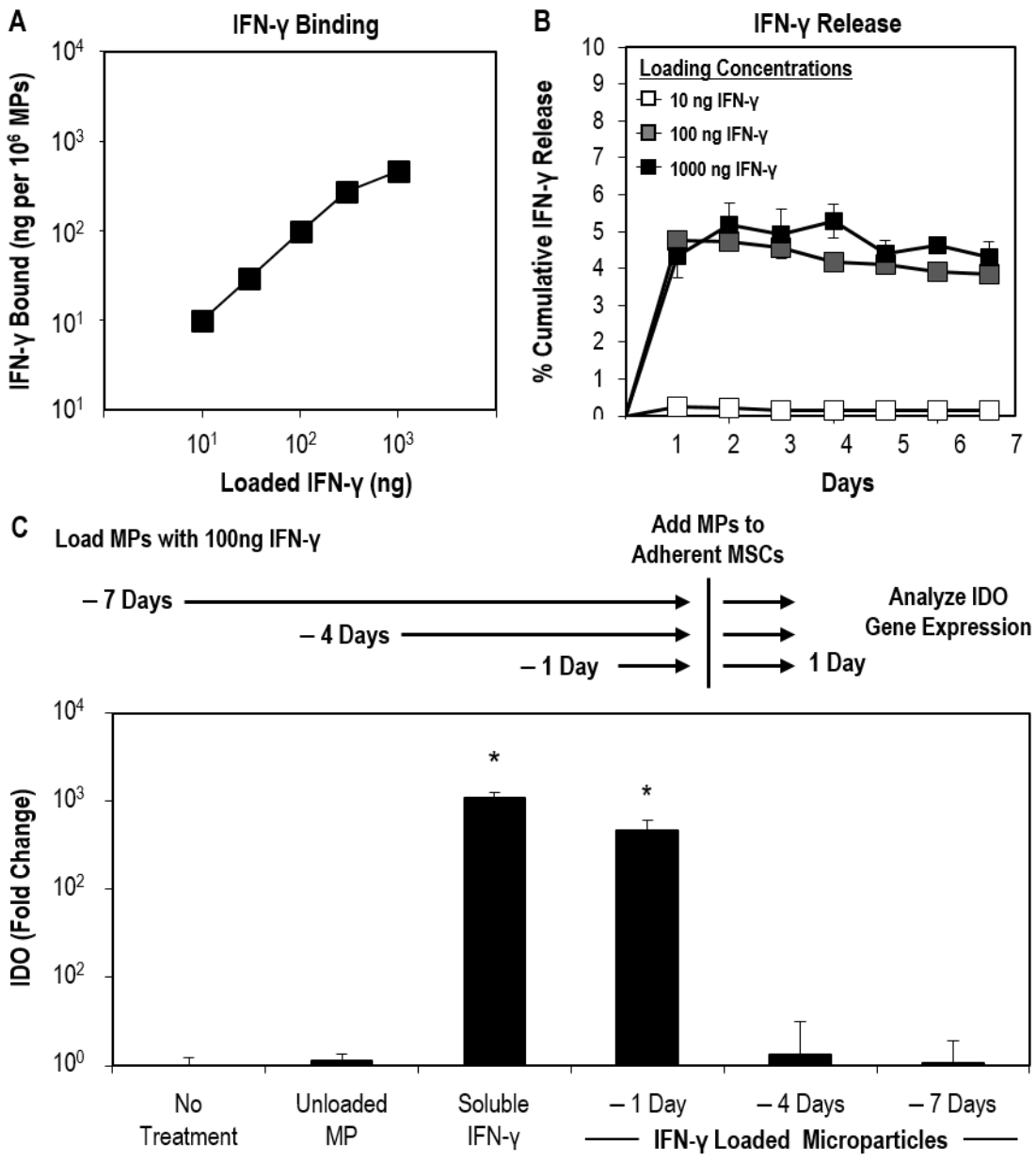

Figure 5.2. Streptavidin coated microparticles bind but do not maintain bioactivity of biotinylated IFN-γ. (A) Polystyrene microparticles bound ~98% of IFN-γ from solution over 10-100 ng per 1 x 10^6 particles but saturated at about 500 ng. (B) While an initial burst release of IFN-γ from the particles was observed, little IFN-γ was subsequently released from the particles over 7 days. (C) Particle-bound IFN-γ, while initially capable of inducing MSC IDO expression, did not remain bioactive over 7 days. * indicates $p < 0.05$ compared to no treatment group.

5.3.2 IFN-γ binds to heparin microparticles and remains bioactive over one week of culture

To establish an alternative microparticle vehicle for delivery of IFN-γ within MSC spheroids, the interaction between heparin microparticles and IFN-γ was investigated. Heparin particles have previously been characterized to have a large binding capacity for the growth factor BMP-2 (~300 µg per mg of MPs[252]). When heparin particles were incubated in solutions of varying concentrations of IFN-γ (10-1000 ng per 1 x 10^6 particles; equivalent to 0.2-20 µg per mg of MPs), more than 97% of the initial IFN-γ was depleted from solution after 18 hours for each concentration tested (**Figure 5.3A**). However, the maximum binding capacity of the microparticles for IFN-γ was not reached over the range of concentrations tested and the highest concentration of IFN-γ tested (approximately 20 µg IFN-γ per mg of MPs) was significantly lower than the maximal binding capacity of heparin microparticles for BMP-2 (300 µg BMP-2 per mg of MPs). Therefore, if desired, even greater amounts of IFN-γ could likely be loaded onto the particles.

After loading particles with different concentrations of IFN-γ, microparticles were resuspended in fresh cell culture medium containing 10% FBS and incubated for 1 week to examine release of IFN-γ from the particles. At each loading concentration, the majority of IFN-γ released from the particles occurred within the first 24 hours, suggesting an initial burst release of loosely bound IFN-γ from the particles (**Figure 5.3B**). The amount of IFN-γ released during this 24 hour period was dependent on the loading concentration, with approximately 1% of loaded IFN-γ at the lowest loading concentration and approximately 30% of loaded IFN-γ at the highest loading concentration. However, after the initial burst

release period, minimal IFN-γ was released from the particles over the next 6 days, suggesting that the majority of loaded IFN-γ remained bound to the heparin microparticles for at least one week of culture.

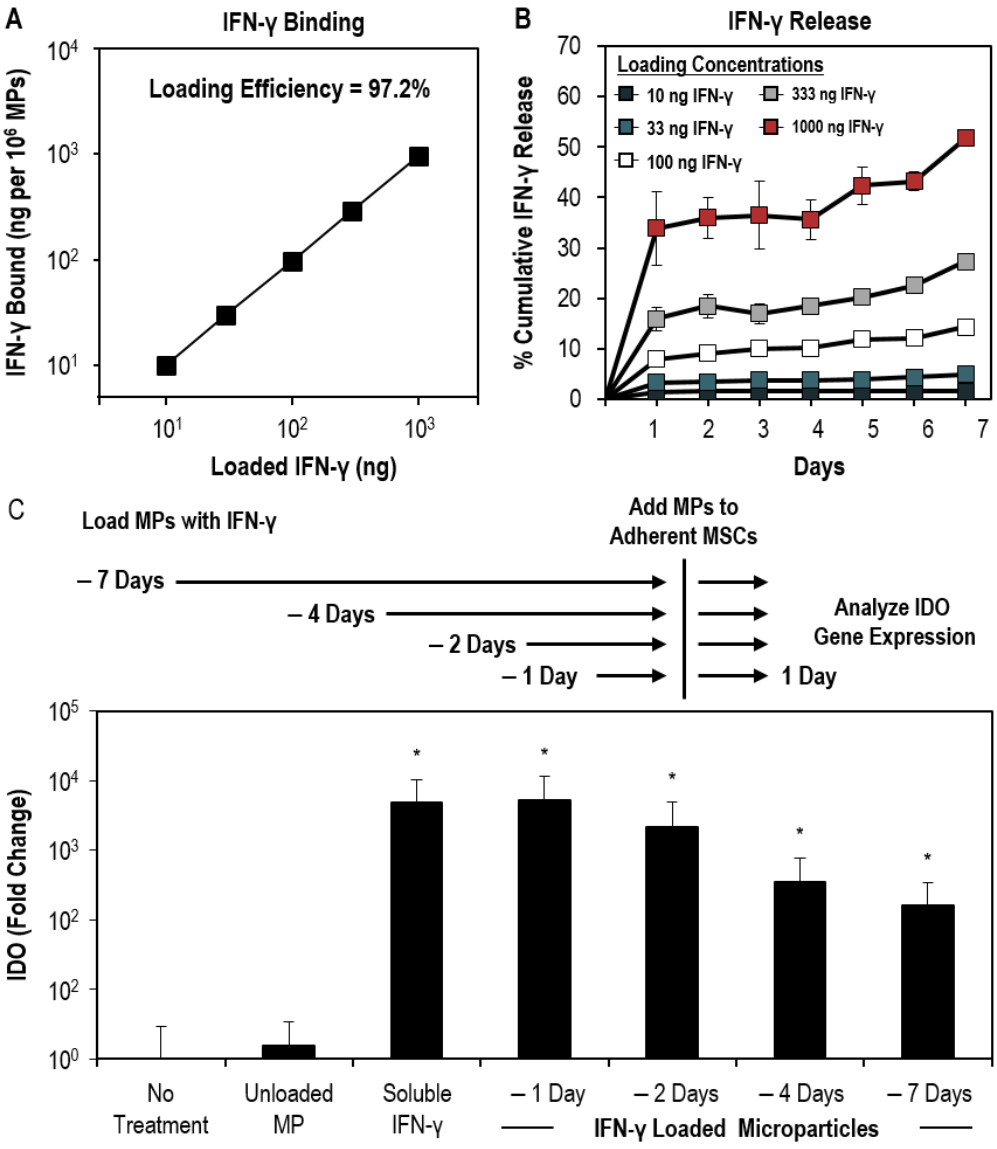

Figure 5.3. Heparin microparticles bind and present bioactive IFN-γ and incorporate stably within MSC aggregates. (A) Heparin microparticles bound >97% of IFN-γ from solution over the ranges tested. (B) While an initial burst release of IFN-γ from the particles was observed, little IFN-γ was subsequently released from the particles over 7 days. (C) Particle-bound IFN-γ remained bioactive and capable of inducing MSC expression of IDO over 7 days. * indicates $p < 0.05$ compared to no treatment.

The bioactivity of IFN-γ bound to heparin microparticles was evaluated by culturing adherent MSCs in direct contact with microparticles loaded with IFN-γ (333 ng per 1 x 10^6 MPs). Microparticles were loaded with IFN-γ 1, 2, 4, and 7 days prior to addition to MSC cultures to examine whether the bioactivity of microparticle-bound IFN-γ was retained over time. The ability of particle-bound IFN-γ to induce IDO expression in MSCs was compared to treatment with unloaded microparticles or an equivalent dose of soluble IFN-γ. As expected, treatment of adherent MSCs with IFN-γ induced IDO expression (>10^3-fold increase in IDO gene expression, $p < 0.001$) while the addition of unloaded microparticles did not significantly increase MSC IDO expression (**Figure 5.3C**). When an equivalent dose of IFN-γ was delivered via microparticles loaded 1 day prior to culture, IDO expression was induced in adherent MSCs to the same extent as soluble treatment, demonstrating that microparticle-bound IFN-γ remains bioactive. Furthermore, microparticles loaded with IFN-γ 2, 4, and 7 days prior to addition to MSCs maintained the ability to significantly induce MSC IDO expression (2000-, 350-, and 150-fold increase in IDO expression compared to untreated MSCs, respectively; $p < 0.001$), although microparticles loaded with IFN-γ 4 and 7 days prior to addition to MSCs induced IDO at a somewhat lower magnitude compared to freshly loaded microparticles (15- and 30-fold decrease in IDO expression, respectively; $p < 0.001$). Since, minimal IFN-γ is released from heparin microparticles following the first 24 hours, these results suggest that IFN-γ loaded onto microparticles retains its bioactivity and ability to elicit a MSC response while bound to heparin for at least one week of culture.

5.3.3 IFN-γ loaded microparticles induce sustained immunomodulatory factor expression

To evaluate incorporation of heparin microparticles within aggregates, fluorescently labeled, unloaded microparticles were incorporated within MSC aggregates at several different ratios of microparticles-to-MSCs (1:1, 2:1, 4:1 MP:MSC) and cultured for up to 7 days to evaluate the incorporation efficiency of particles within aggregates and retention of particles within the multicellular constructs. Fluorescently labeled microparticles were readily incorporated within MSC spheroids after initial formation and remained stably incorporated within spheroids for at least 1 week of culture (**Figure 5.4A**). Approximately 85% of the particles initially added during aggregate formation were incorporated within spheroids for all three ratios tested (**Figure 5.4B**). Additionally, only ~1.5% of these particles were found to escape from the spheroids into the culture medium over 1 week of culture. By determining the incorporation efficiency of microparticles within MSC spheroids (~85%) and persistence of particles within spheroids over the course of 7 days, we were able to adjust the number of particles added at the time of formation for subsequent experiments to ensure equivalent doses of IFN-γ presented via particles compared to soluble pre-treatment with IFN-γ.

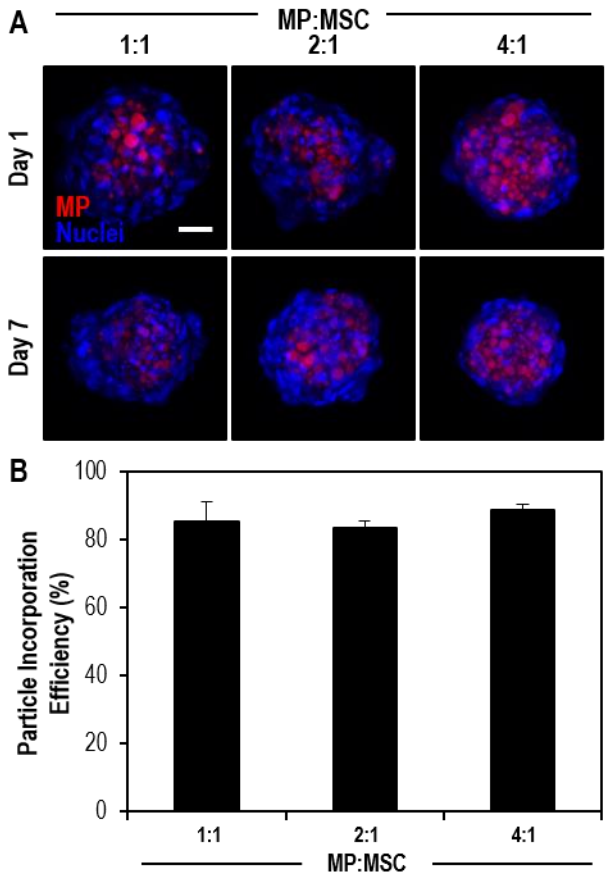

Figure 5.4. Heparin microparticles incorporate stably within MSC aggregates. (A) Fluorescently labeled microparticles were incorporated within MSC aggregates at various doses and remained stably incorporated for at least 7 days of culture. Maximal intensity projection, scale bar = 50 μm. (B) Approximately 85% of microparticles added during aggregate formation were incorporated within MSC spheroids over the range of microparticle-to-cell ratios tested, allowing for precise control of microparticle and loaded cytokine dose.

To investigate whether sustained delivery of IFN-γ directly within the MSC spheroidal microenvironment could enhance MSC immunomodulatory factor expression, heparin particles were loaded with two doses of IFN-γ (33 ng and 333 ng IFN-γ per 1 x 10^6 MPs) or without any cytokine and incorporated into MSC spheroids. The expression of IDO by MSC spheroids with microparticles or pre-treated with IFN-γ was then measured over one week of culture. Little change in IDO gene expression was observed in MSC spheroids

without IFN-γ pre-treatment or with unloaded microparticles over 1 week (**Figure 5.5A**). Both IFN-γ pre-treatment and incorporation of IFN-γ loaded microparticles initially induced IDO gene expression within the first day (approximately 10^4-fold, $p < 0.001$). However, IDO expression rapidly decreased over time when MSC spheroids were pre-treated with soluble IFN-γ. In contrast, MSC spheroids with IFN-γ loaded microparticles maintained an elevated level of IDO gene expression over an entire week of culture. Similarly, protein expression of IDO was detected initially on day 1 where MSC spheroids were exposed to IFN-γ by pre-treatment or via microparticles (**Figure 5.5B**). By day 4, only spheroids exposed to the sustained presentation of microparticle-bound IFN-γ continued to express elevated levels of IDO. Furthermore, the sustained delivery of IFN-γ on heparin microparticles was significantly greater than the IDO expression of MSC spheroids stimulated with soluble IFN-γ for 7 days (**Figure 5.6**). Finally, no IFN-γ was detected in the spent cell culture medium by ELISA indicating that little to no microparticle-bound IFN-γ escaped from the spheroids (<0.1% of IFN-γ initially loaded onto particles based on the lower detection limit of ELISA).

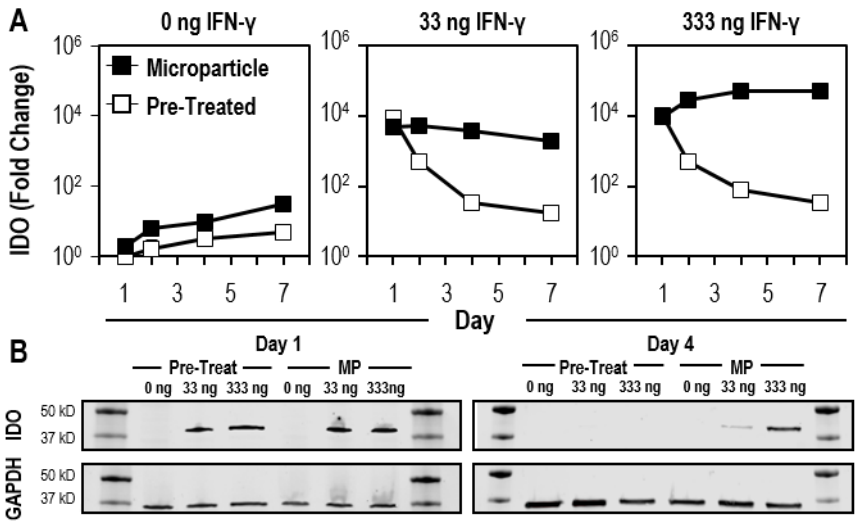

Figure 5.5. IFN-γ loaded heparin microparticles induce sustained IDO expression. (A) IDO gene expression rapidly decreased after initial pre-treatment of MSC spheroids with IFN-γ whereas IDO gene expression was sustained over 7 days when IFN-γ was delivered by microparticles within MSC spheroids. ***** indicates $p < 0.05$ compared between pre-treatment and microparticle treatment on the same day of culture. (B) Similarly, IDO protein expression was induced by IFN-γ but was only expressed by MSC spheroids after 4 days when IFN-γ was delivered by microparticles.

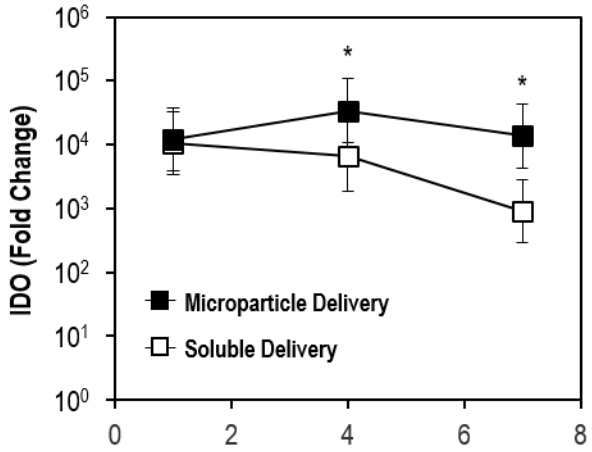

Figure 5.6. MSC IDO expression is greater when IFN-γ is delivered via microparticles than solubly. MSC IDO expression was significantly greater after 4 and 7 days of culture in response to 333 ng IFN-γ delivered on heparin microparticles compared to an equivalent dose delivered solubly in the culture medium for all 7 days of culture. * indicates $p < 0.05$ compared to the soluble IFN-γ delivery at the same day of culture.

To evaluate spatial distribution of IDO expression within MSC spheroids in response to IFN-γ pre-treatment or IFN-γ loaded microparticles, immunohistochemistry was used to examine the localization of IDO to the spheroid exterior or to heparin microparticles (**Figure 5.7**). In MSC spheroids without any treatment, no IDO expression could be observed after one or four days of culture, consistent with qRT-PCR and Western blot analysis (**Figure 5.7A,B**). When pre-treated with IFN-γ, IDO expression could be observed throughout the spheroid one day after stimulation, suggesting IFN-γ is able to penetrate into the spheroid and does not solely stimulate cells on the exterior of the aggregate (**Figure 5.7C**). However, four days after pre-treatment, little positive IDO staining could be observed in pre-treated spheroids (**Figure 5.7D**). Slight DAB staining was observed to be localized to heparin microparticles in spheroids incorporated with unloaded particles. However, DAB staining appeared to be localized only to particles, based on Alcian blue staining and morphology (**Figure 5.7E**, inset), and not to cells, suggesting a potential interaction between DAB and the particles. Finally, in MSC spheroids incorporated with IFN-γ microparticles, positive IDO staining and microparticles could be observed throughout the spheroids after one day of culture (**Figure 5.7G**). Furthermore, the intensity of IDO staining was greater after four days of culture, indicating that IDO production continued to be stimulated throughout the spheroid over four days, consistent with what was observed by qRT-PCR and Western blot analysis (**Figure 5.7H**).

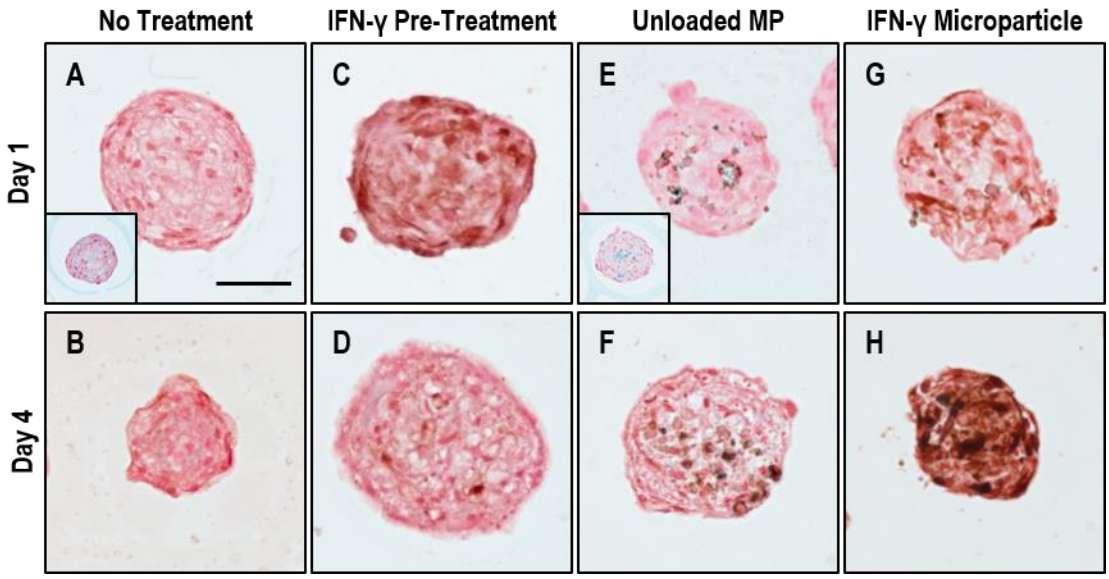

Figure 5.7. Delivery of IFN-γ on microparticles stimulates IDO throughout MSC spheroids. Representative images of MSC spheroids stained for IDO expression (DAB, brown) and counterstained for heparin particles (Alcian Blue, blue) and nuclei (Nuclear Fast Red, red). MSC spheroids were evaluated after one and four days of culture in (A, B) no treatment, (C, D) IFN-γ pre-treatment, (E, F) unloaded microparticles, and (G, H) IFN-γ loaded microparticles cultures to evaluate spatial localization of IDO expression. Scale bar = 50 μm.

5.3.4 IFN-γ loaded microparticles enhance MSC suppression of T-cell activation and proliferation

Since microparticle delivery of IFN-γ promoted sustained MSC expression of IDO, we next sought to determine if the enhanced IDO expression resulted in increased suppression of T-cell proliferation and activation. At the highest ratio of MSCs to PBMCs (3:1 MSC:PBMC), suppression of T-cell proliferation, as measured by decreased Ki67 expression, was observed in all MSC co-culture groups compared to the activated PBMCs alone (**Figure 5.8A**). However, MSC spheroids pre-treated with IFN-γ or incorporated with IFN-γ loaded microparticles induced greater suppression of T-cell proliferation compared to untreated MSC spheroids. Furthermore, only MSCs treated with IFN-γ (either through

pre-treatment or microparticles) were capable of suppressing T-cell proliferation at a 1:1 MSC:PBMC ratio. Additionally, the sustained microparticle delivery of IFN-γ within spheroids significantly enhanced suppression of T-cell proliferation at both a 3:1 and 1:1 ratio of MSCs:PBMCs compared to spheroids pre-treated with IFN-γ (**Figure 5.8B**). At a 3:1 MSC:PBMC ratio, only 15 ± 1% of T-cells were Ki67+ in co-culture with MSCs with IFN-γ loaded microparticles compared to 23 ± 2% in co-cultures with pre-treated MSC spheroids ($p = 0.029$). No suppression of T-cell proliferation was observed when MSCs were co-cultured at a 1:3 MSC:PBMC ratio in any of the IFN-γ treatment groups. Finally, a similar response was observed in expression of IFN-γ and IL-10 in co-cultures. As no IFN-γ or IL-10 could be detected in cultures of only MSC spheroids with or without IFN-γ loaded microparticles, the IFN-γ and IL-10 detected in MSC-PBMC co-cultures is expressed by cells from the PBMC fraction. The greatest suppression of IFN-γ secretion was observed in co-cultures with pre-treated MSC spheroids and MSC spheroids with IFN-γ loaded microparticles (**Figure 5.8C**). Similarly, IL-10 expression was increased in co-cultures with MSC spheroids at 3:1 and 1:1 MSC:PBMC ratios and was greatest in MSC spheroids pre-treated with IFN-γ or incorporated with IFN-γ loaded microparticles (Figure 5.8D).

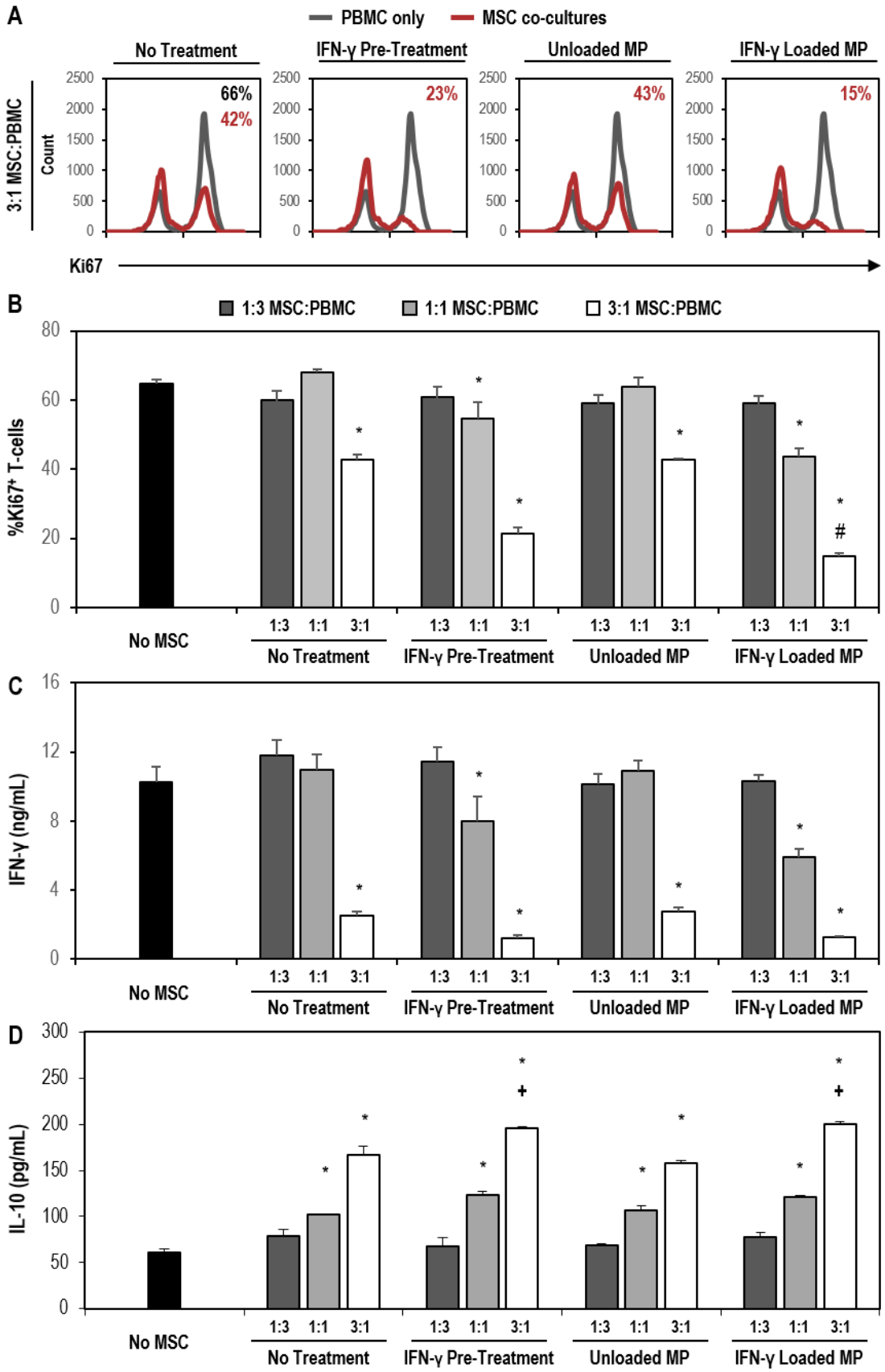

Figure 5.8. Microparticle delivery of IFN-γ enhances MSC spheroid suppression of T-cell activation and proliferation. (A) Representative histograms of $Ki67^+$ T-cells in co-culture with MSC spheroids at 1:3, 1:1, and 3:1 MSC:PBMC ratios demonstrate a dose dependent response of T-cell proliferation (B) Co-culture of activated PBMCs with IFN-γ loaded microparticle treated MSC spheroids resulted in the greatest suppression of T-cell proliferation at a 3:1 MSC:PBMC ratio. Only MSCs treated with IFN-γ (via pre-treatment or microparticle) suppressed T-cell proliferation at a 1:1 MSC:PBMC ratio. (C) Additionally, MSC spheroids suppressed expression of the effector cytokine IFN-γ and the greatest suppression was observed in co-cultures with MSCs treated with IFN-γ. (D) Similarly, IL-10 expression was increased in co-cultures with MSC spheroids and was greatest when MSCs were treated with IFN-γ via pre-treatment or microparticle delivery. * indicates $p < 0.05$ compared to No MSC cultures. # indicates $p < 0.05$ compared to IFN-γ pre-treated MSC spheroids at the same MSC:PBMC ratio. + indicates $p < 0.05$ compared to No Treatment and Unloaded Microparticle MSC spheroid co-cultures.

5.3.5 Microparticle induced suppression of T-cell activation and proliferation is dependent on induction of MSC IDO expression and aided by induction of M2-like monocytes

To determine if the IDO expression in response to IFN-γ loaded microparticles was responsible for the enhanced ability of MSCs to suppress T-cells, pre-treated and microparticle treated MSC spheroids were cultured with activated PBMCs in the presence of an IDO inhibitor, 1-methyl$_{DL}$-tryptophan (1-MT). Supplementation of 1-MT into co-cultures significantly impaired the ability of IFN-γ pre-treated spheroids and spheroids with IFN-γ loaded microparticles to suppress T-cell proliferation (**Figure 5.9A**). In PBMC co-cultures with IFN-γ pre-treated spheroids, 61 ± 2% of T-cells were $Ki67^+$ when 1-MT was added to the culture compared to 31±2% $Ki67^+$ T-cells in co-cultures with the vehicle control ($p < 0.001$). Similarly, 57 ± 2% of T-cells were $Ki67^+$ in co-cultures with MSC spheroids with IFN-γ loaded microparticles and 1-MT compared to 24 ± 1% $Ki67^+$ T-cells

in co-cultures treated with the vehicle control ($p < 0.001$). However, even with supplementation of 5 µM 1-MT into co-cultures, both pre-treated and microparticle treated spheroids were capable of slightly suppressing T-cell proliferation compared to activated PBMCs alone (77 ± 2% $Ki67^+$, $p < 0.001$, respectively). MSC suppression of T-cell IFN-γ expression was completely inhibited by treatment with 1-MT in both co-cultures with IFN-γ pre-treated MSC spheroids and spheroids with IFN-γ loaded microparticles (**Figure 5.9C**). However, PBMC expression of IL-10 in response to MSC spheroids was only partially inhibited by 1-MT (Figure 5.9D; 133 and 132 pg/mL of IL-10 in pre-treated and microparticle groups compared to 83 pg/mL of IL-10 in No MSC- 1-MT control, $p = 0.003$ and 0.004, respectively). Although additional immunomodulatory factors may contribute to the residual suppressive effects observed of MSC spheroids treated with 1-MT, IDO inhibition significantly impairs the ability of MSCs to suppress T-cell proliferation, as expected based on previous studies[78, 261].

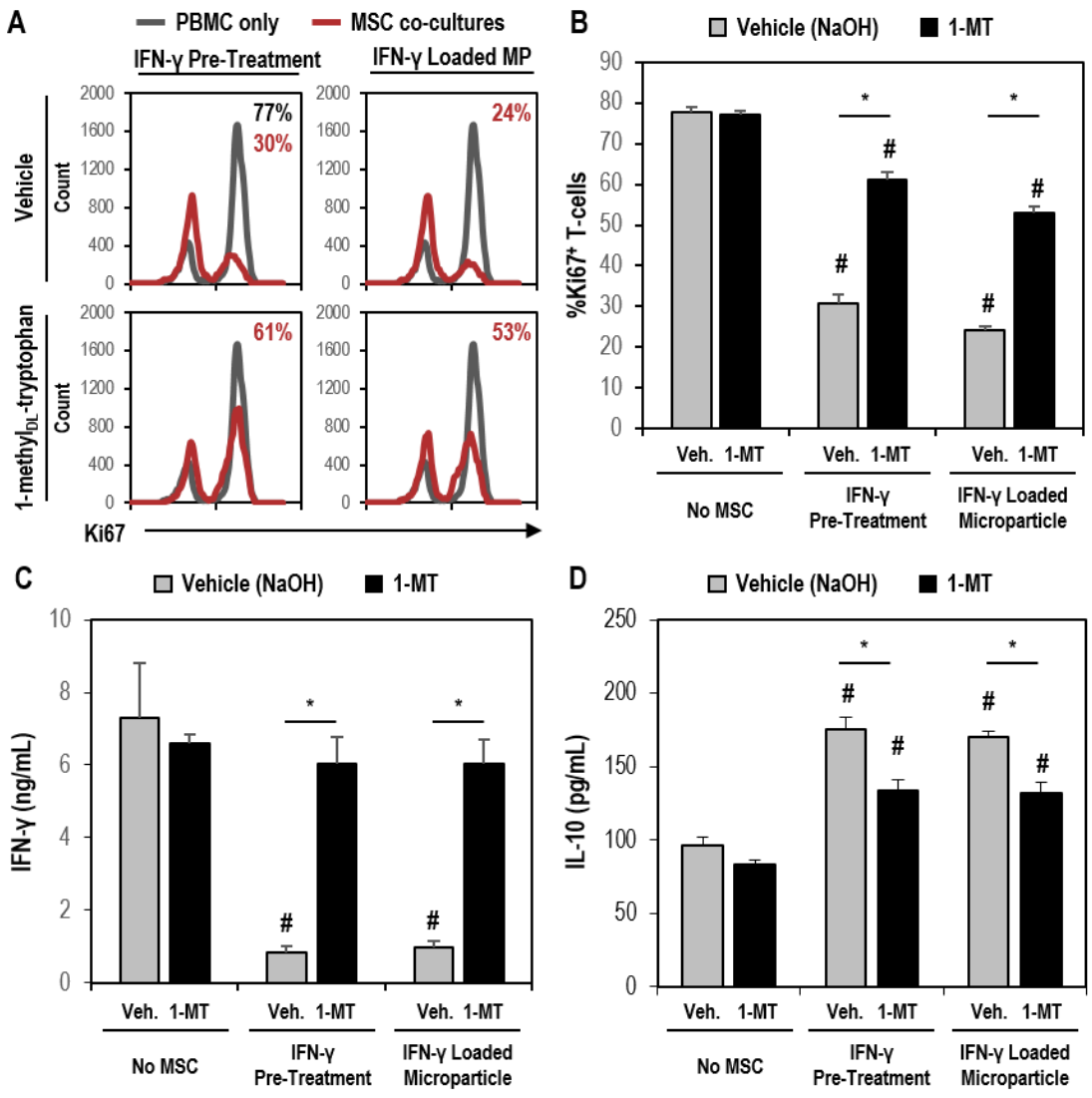

Figure 5.9. Increased suppression of T-cells by microparticle delivery of IFN-γ is dependent on induction of IDO expression. (A) Representative histograms of Ki67^{+} T-cells in co-culture with IFN-γ pre-treated or IFN-γ loaded microparticle treated MSC spheroids with or without the IDO inhibitor 1-MT. (B) Addition of 1-MT to MSC-PBMC co-culture (3:1 MSC:PBMC ratio) significantly inhibited the ability of IFN-γ primed MSCs to inhibit T-cell proliferation in both pre-treated and microparticle treated spheroids. Similarly, inhibition of IDO activity with 1-MT (C) increased T-cell expression of IFN-γ and (D) reduced the induction of IL-10 expression in PBMC co-cultures. * indicates $p < 0.05$ compared to groups denoted by bar. # indicates $p < 0.05$ compared to No MSC cultures.

In addition to IDO activity, MSC suppression of T-cell proliferation and activation in PBMC co-culture assays *in vitro* is also dependent on MSC induction of IL-10 expressing M2-like monocytes within these co-cultures.[78, 259, 260] Therefore, we investigated whether MSC spheroids containing IFN-γ loaded microparticles could also induce $CD206^+$ M2-like monocytes in direct co-cultures with monocytes isolated from PBMCs (**Figure 5.10A**). We did not observe a significant increase in the number of $CD206^+$ monocytes in co-cultures with non-treated MSC spheroids. Additionally, a modest increase in $CD206^+$ monocytes co-cultures was observed with MSC spheroids containing unloaded microparticles. However, MSCs spheroids pre-treated with IFN-γ and MSC spheroids with IFN-γ loaded microparticles induced the highest percentages of $CD206^+$ monocytes compared to the naïve monocyte population (**Figure 5.10B**, 17% and 18% $CD206^+$ monocytes in pre-treated and microparticle treated spheroid co-cultures respectively, $p < 0.001$ compared to naïve monocytes). Furthermore, the concentration of the immunoregulatory cytokine IL-10 in spent media supernatants was greatest in co-cultures with spheroids containing IFN-γ loaded microparticles (**Figure 5.10C**), suggesting that the induction of IL-10 expression by M2-like monocytes may be aiding the suppression of T-cells observed in co-cultures with spheroids containing IFN-γ loaded microparticles.

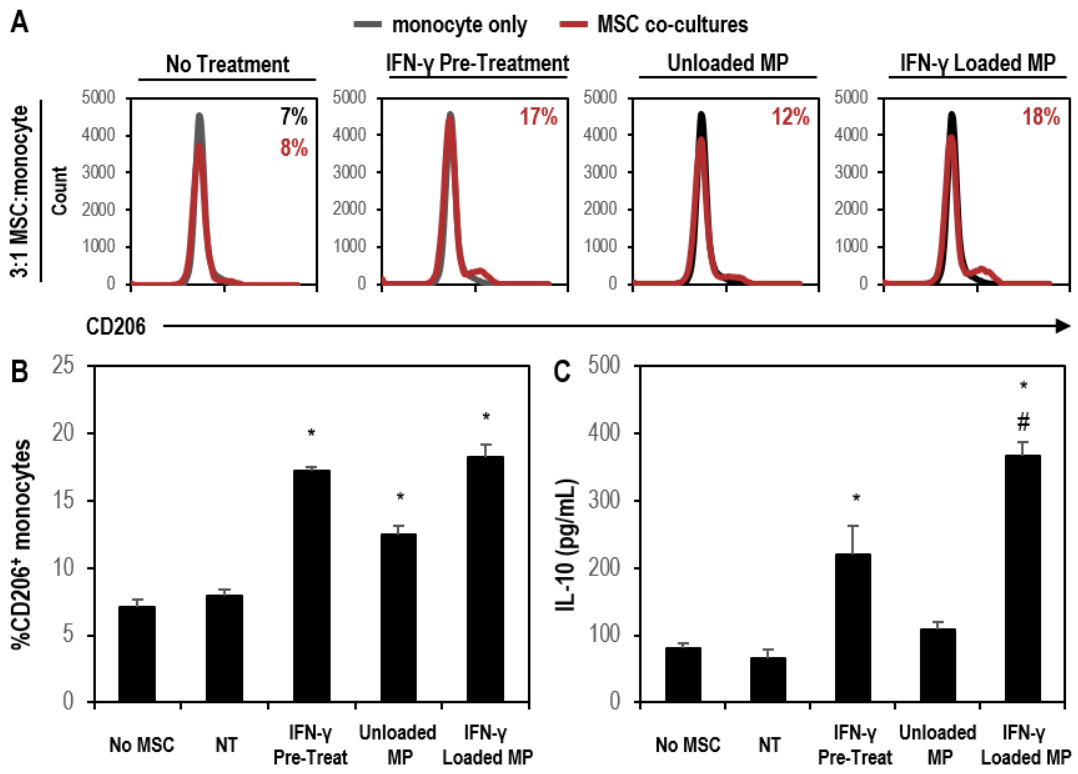

Figure 5.10. Microparticle delivery of IFN-γ increases MSC spheroid polarization of monocytes to anti-inflammatory phenotype. (A) Representative histograms of $CD206^+$ monocytes in co-culture with MSC spheroids. (B) Anti-inflammatory M2-like monocytes were induced by co-culture with IFN-γ pre-treated MSCs and IFN-γ loaded microparticle treated MSCs. (C) IL-10 production, an anti-inflammatory cytokine produced by alternatively activated macrophages, was greatest in co-cultures with IFN-γ loaded microparticle treated MSCs. Induction of M2-like monocytes may aid in the suppression of T-cell proliferation and activation in PBMC co-cultures. * indicates $p < 0.05$ compared to No MSC group. # indicates $p < 0.05$ compared to IFN-γ pre-treated MSC spheroid group.

5.3.6 Microparticle delivery of IFN-γ within MSC spheroids sustains immunomodulatory activity compared to soluble pre-treated MSCs

Since MSC spheroids with IFN-γ loaded microparticles expressed elevated levels of IDO for at least 7 days while IDO activity of pre-treated MSC spheroids decreased rapidly over 4 days, we investigated whether MSC spheroids containing IFN-γ loaded microparticles

continued to modulate T-cell responses even 4 days after formation. Therefore, MSC spheroids were pre-treated or formed with IFN-γ loaded microparticles and added to co-cultures with activated PBMCs after 0, 2, or 4 days following initial aggregate formation and pre-treatment. Consistently, both spheroids pre-treated with IFN-γ and spheroids with IFN-γ loaded microparticles suppressed T-cell proliferation when added to co-cultures immediately after spheroid formation (**Figure 5.11A**). However, when spheroids were added 2 days after formation and IFN-γ pre-treatment, the ability of pre-treated spheroids to suppress T-cell proliferation was significantly reduced ($p = 0.035$ pre-treated spheroid days 0-4 vs. pre-treated spheroid days 2-6). Conversely, no difference in T cell suppression ability was observed between spheroids added immediately after formation or 2 days after formation, in those spheroids containing IFN-γ loaded microparticles ($p = 0.978$ spheroids with IFN-γ loaded particles days 0-4 vs. spheroids with IFN-γ loaded particles days 2-4). Moreover, the ability of spheroids pre-treated with IFN-γ to suppress T-cell proliferation was further decreased when spheroids were added four days after initial formation and pre-treatment. The extent of T-cell suppression observed in pre-treated spheroids after four days was comparable to levels observed previously when non-treated MSC spheroids were co-cultured with activated PBMCs, suggesting that the effects of pre-treatment were completely abolished within four days. However, MSCs with IFN-γ loaded microparticles retained the ability to suppress T-cell proliferation even when added to PBMC co-cultures four days after initial formation (**Figure 5.11B**). Altogether, MSC spheroids incorporated with IFN-γ microparticles exhibit a sustained ability to suppress T-cell proliferation over at least one week of culture, whereas the immunosuppressive ability of MSC spheroids pre-treated with IFN-γ rapidly decreased over time.

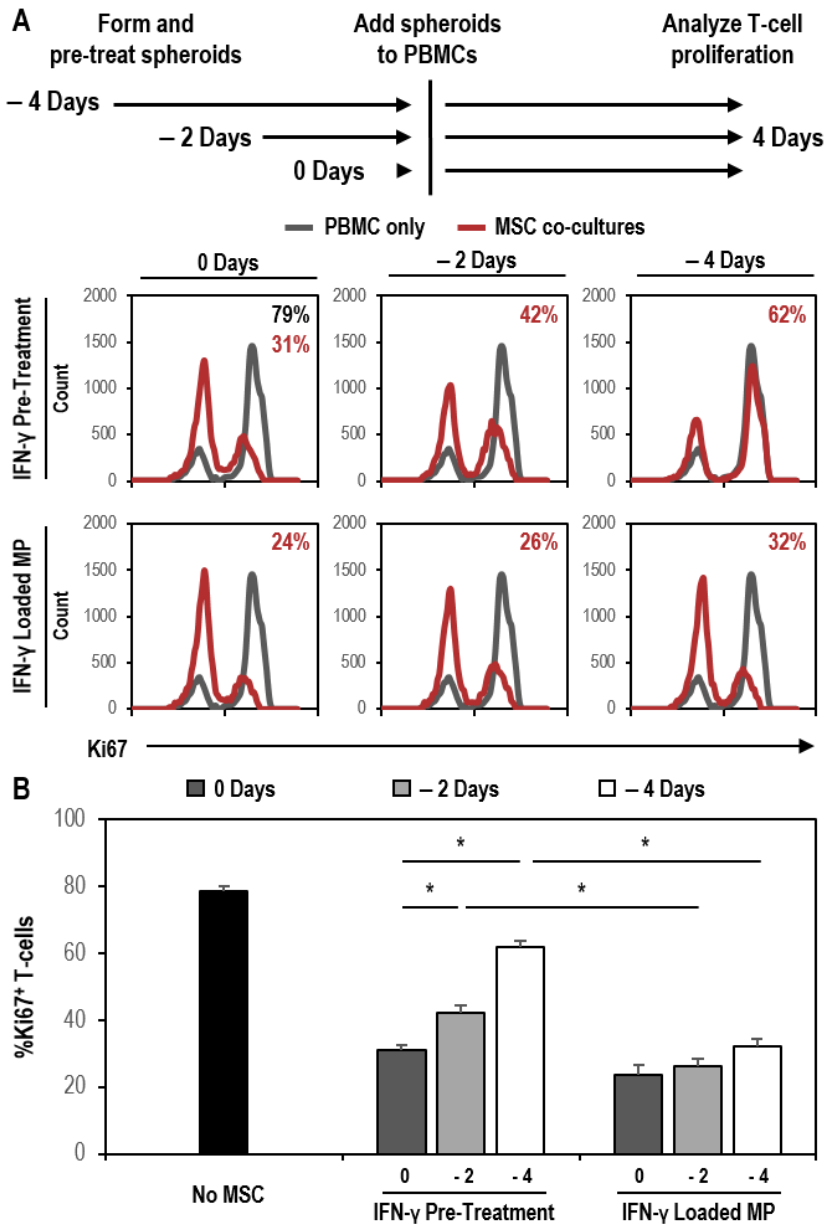

Figure 5.11. Microparticle delivery of IFN-γ enhances MSC suppression of T-cells for over one week. (A) Representative histograms of Ki67+ T-cells in co-culture with MSC spheroids treated with IFN-γ or IFN-γ loaded microparticles 0, 2, and 4 days prior to addition to PBMC co-culture. (B) IFN-γ loaded microparticles sustained the enhanced MSC suppression of T-cell proliferation in response to IFN-γ for up to 8 days, whereas the effects of pre-treating MSC spheroids with IFN-γ were transient and resulted in decreased ability to suppress T-cell proliferation over time. * indicates $p < 0.05$ compared to groups denoted by bars. # indicates $p < 0.05$ compared to No MSC group.

5.4 DISCUSSION

In this study, we designed and evaluated a strategy for locally presenting IFN-γ within MSC constructs in order to potentiate sustained MSC immunomodulatory activity. To do so, we took advantage of a microparticle-based approach previously developed to spatially and temporally control presentation of growth factors within stem cell aggregates[248–251]. Heparin-based microparticles were chosen to deliver IFN-γ in order to exploit the high native affinity of IFN-γ for heparin and the ability of heparin to maintain protein bioactivity since immobilization of IFN-γ on polystyrene particles did not maintain IFN-γ bioactivity. These heparin particles have previously been demonstrated to stably bind positively charged heparin-binding growth factors including BMP-2, vascular endothelial growth factor (VEGF), and fibroblast growth factor 2 (FGF-2) [252]. Consistent with previous studies, heparin microparticles bound large amounts of IFN-γ (>20 μg per mg MPs) and very little IFN-γ was released from the particles after the initial burst release period during the first 24 hours post-loading. Despite low IFN-γ release, IFN-γ loaded particles were still capable of inducing MSC IDO expression even after 7 days of incubation at physiologic conditions prior to addition to MSCs. These results are consistent with previous studies investigating the interaction between cell-derived heparan sulfate and IFN-γ signaling. Heparan sulfate present within plasma membranes can augment IFN-γ signaling by stably presenting IFN-γ at the cell surface in close proximity to cell membrane receptors[256]. In contrast, supplementation of soluble heparin into culture medium can suppress the activity of IFN-γ, likely due to sequestration of IFN-γ in solution that inhibits its interaction with cell surface receptors. Altogether, these results suggest that the ability of IFN-γ loaded microparticles to induce MSC IDO expression is dependent on direct

contact between particle-bound IFN-γ and MSCs and does not require the release of soluble IFN-γ from the particles. Furthermore, these results also corroborate results found in previous studies demonstrating that physical separation of cells and growth factor loaded heparin microparticles via transwell significantly reduces the activity of particle-bound growth factors[252]. Additionally, since heparin-bound IFN-γ bioactivity is mediated primarily through solid phase presentation of IFN-γ and not soluble release, there is little risk of exogenous IFN-γ escaping MSC spheroids and exacerbating an inflammatory response *in vivo*. Overall, these results demonstrate that heparin microparticles are an effective carrier for locally restricting sustained delivery of bioactive cytokines within MSCs spheroids.

Pre-treatment of MSCs with inflammatory cytokines is frequently used to enhance the immunomodulatory activity of the cells by activating expression of IDO and other immunomodulatory factors prior to infusion. However, we have demonstrated herein that sustained presentation of IFN-γ to MSCs enhances and extends the duration of immunomodulatory activity by MSCs. Using a heparin microparticle-based strategy, expression of IDO by MSCs was sustained throughout the spheroid structure for at least one week. Furthermore, microparticle delivery of IFN-γ within MSC spheroids increased MSC suppression of T-cell proliferation and activation compared to pre-treated spheroids. By locally concentrating IFN-γ within the MSC spheroid through particle-mediated delivery, MSCs may be exposed to an effectively higher dose of cytokine relative to an equal soluble amount, thereby resulting in enhanced immunomodulatory activity. More strikingly, incorporation of IFN-γ loaded microparticles within MSC spheroids

significantly extends the duration of MSC immunomodulation. While the immunomodulatory activity of pre-treated MSC spheroids was significantly reduced after 2 days, MSC spheroids with IFN-γ loaded microparticles continued to effectively suppress T-cells through one week of culture. Not surprisingly based on the targeted strategy we employed, immunosuppressive effects of MSCs were mediated by IDO expression since the IDO inhibitor 1-MT reduced the ability of MSCs to suppress T-cell proliferation. While IDO expression is necessary for MSC immunomodulation, additional MSC secreted factors or direct cell contact mediated mechanisms may also play an important role in the suppression of T-cell proliferation. In addition to direct modulation of T-cells by MSCs, MSC induction of M2-like monocytes within PBMC co-cultures also aids in the suppression of T-cells *in vitro* [78]. Therefore, the increased induction of M2-like monocytes by MSC spheroids loaded with IFN-γ microparticles could also augment the increased immunosuppressive activity of 3D MSC constructs.

Despite the extensive use of biomaterials with specific biophysical and biochemical properties and ability to deliver biochemical stimuli to direct differentiation of MSCs, similar approaches have largely been unexplored for directing the immunomodulatory paracrine activity and broader trophic effects of MSCs. Numerous studies have demonstrated that MSC paracrine factor secretion is modulated in response to environmental cues in addition to the local cytokine milieu including matrix composition, mechanics, and topography [262, 263], as well as oxygen tension [264]. Furthermore, environmental stimuli are highly amenable to manipulation via biomaterials to specifically define the microenvironment of stem cells and direct their function [265]. To date, only

one biomaterial-based approach has been used to increase MSC expression of IDO in order to enhance suppression of T-cell proliferation and activation. Delivery of glucocorticoids within MSCs via poly-lactic-co-glycolic acid (PLGA) nanoparticles internalized by MSCs enhanced the upregulation of IDO in response to IFN-γ and resulted in increased suppression of CD3/CD28-activated PBMCs [266]. However, IDO expression by MSCs was still dependent on the presence of soluble IFN-γ and the glucocorticoid budesonide was unable to stimulate IDO alone. Therefore, sustained presentation of IFN-γ and glucocorticoids may offer complementary approaches for enhancing MSC immunomodulatory activity. Ultimately, engineering the local environment of transplanted MSCs through biomaterial-based approaches provides an additional level of control over the efficacy of MSC therapies to promote maximal activity post-transplantation.

Overall, the approach described in this study provides a novel means of enhancing MSC immunomodulatory activity by locally concentrating and sustaining presentation of immunomodulatory stimuli, and represents a method of potentiating MSC immunomodulation after local injection *in vivo*. Since MSCs are highly dependent on local inflammatory signals to stimulate their immunomodulatory activity, spatially controlled presentation of inflammatory cues within MSC aggregates provides a means of stimulating these cells even when environmental inflammatory signals may not be present, such as in systemic delivery strategies, states of chronic inflammation, or when used in combination with traditional anti-inflammatory drugs. For example, although MSCs have been effective in treating GvHD when infused at the height of inflammation, they are much less effective if delivered prior to the onset of inflammation[33, 267]. Similarly, MSCs are less effective

at treating experimental autoimmune encephalomyelitis (EAE) when administered during disease remission[134, 268]. In clinical studies, MSC-based therapies have been most effective in treating immunosuppressant-refractory acute inflammatory diseases [269, 270]. At low concentrations of strong inflammatory signals (i.e. IFN-γ or TNF-α) present during chronic inflammatory states, MSCs upregulate chemokines that recruit lymphocytes [85, 271]. However, low cytokine concentrations are not sufficient to induce substantial expression of IDO by MSCs to suppress lymphocyte activation and therefore can actually augment inflammation. Such studies highlight the critical importance of attaining minimal threshold concentrations of inflammatory stimuli in order to effectively stimulate MSC immunomodulation. By presenting a sustained, high concentration of a cytokine, such as IFN-γ, through incorporation of microparticles within MSC aggregates, the use of MSCs for *in vivo* immunomodulatory applications could be greatly expanded; for example, MSCs could potentially be transplanted concurrently with graft tissue to effectively suppress an immune response prior to the development of GvHD and severe inflammation. Furthermore, based on evidence that MSCs administered together with steroids or cyclosporine to immunosuppressant-responsive patients exhibit no clinical effect[272, 273], it is speculated that the lack of immunosuppression may be due to the decreased availability of inflammatory cytokines needed to stimulate MSC immunomodulation[274]. Hence, in such a situation, locally sustained presentation of IFN-γ to MSCs may improve outcomes in patients receiving both MSCs and traditional immunosuppressants by stimulating IDO expression despite the lack of systemic cytokines present in the host environment. Altogether, sustained presentation of IFN-γ within MSC aggregates may provide a clinically relevant approach for inducing and enhancing MSC

immunomodulatory activity in disease states previously deemed to be unresponsive to MSC-based therapies.

5.5 CONCLUSIONS

The results of this study demonstrate that heparin microparticle delivery of IFN-γ within spheroidal MSC aggregates presents bioactive IFN-γ locally within the MSC microenvironment that in turn induces a sustained MSC suppression of CD3/CD28-activated T-cells *in vitro*. The enhanced T-cell suppression by MSC spheroids containing IFN-γ loaded microparticles is mediated, in part, through upregulation of IDO expression and induction of M2-like monocytes. Overall, this approach could aid in overcoming the limitations of transient pre-treatment strategies by continuously presenting bioactive IFN-γ within the MSC microenvironment and thereby maximizing the immunomodulatory potential of transplanted MSCs. Furthermore, this approach provides a means of inducing potent MSC immunomodulation irrespective of unknown and/or ill-defined environmental inflammatory milieu, such as in chronic inflammation or when administered with immunosuppressants. Altogether, biomaterial-based engineering of the MSC microenvironment provides a means of controlling the function of transplanted cells to specifically direct their therapeutic activity and may improve the efficacy of MSC-based therapies aimed at treating a number of inflammatory and immune diseases.

CHAPTER 6

FUTURE CONSIDERATIONS

Taken together, the data presented in this dissertation establishes a novel approach for utilizing aggregation techniques and biomaterial technologies to engineer the local MSC microenvironment in order to enhance the intrinsic immunomodulatory capabilities of these cells. In Chapter 3, aggregation of MSCs was found to increase the secretion of PGE_2, TGF-β1, and IL-6 and that stimulation with the cytokines IFN-γ and TNF-α could further enhance spheroid expression of immunomodulatory factors and induce expression of the key immunosuppressive factor IDO. Furthermore, MSCs spheroids were capable suppressing inflammatory responses of macrophages and inhibiting T-cell proliferation and activation *in vitro*. In Chapter 4, the secretome of MSCs was more broadly examined; while, the overall composition of MSC-expressed paracrine factors was strikingly similar, the expression of OPG was found to be highly regulated between adherent and spheroid MSCs and this difference critically regulates the differentiation of osteoclasts in the presence of MSC paracrine factors. Finally, in Chapter 5, sustained delivery of IFN-γ within the MSC spheroidal microenvironment was found to enhance and sustain MSC suppression of T-cell activation and proliferation through inducing sustained expression of IDO. Altogether, the findings of this work motivate further studies to better characterize the modulation of MSC paracrine activity in response to aggregation and to evaluate the efficacy of engineered MSC constructs as a therapeutic agent for treating disease in animal models of inflammatory and immune diseases.

6.1 Non-biased screening approaches to evaluate changes in MSC secretome

While many studies have demonstrated increased paracrine activity of MSCs after aggregation, no studies to date have systematically determined the exact changes in the composition of paracrine factors expressed by MSCs or the mechanisms and signaling pathways mediating these changes in the secretome in response to aggregation. Typically, assays targeting individual proteins or transcripts are used to determine expression of paracrine factors known to play a role in MSC paracrine activity, such as through ELISA or qRT-PCR analysis. Other studies have used relatively small protein or PCR arrays to examine expression of a larger number of paracrine factors. However, these are still biased approaches, in that specific protein or transcript targets must be chosen *a priori* and are still limited by the number of analytes measured. Therefore, unbiased screening approaches to evaluate the secretome or transcriptome of MSCs may be beneficial in fully characterizing the cocktail of factors expressed by MSCs and evaluate how the composition of this cocktail changes in response to aggregation, cytokine treatment, or other approaches aimed at manipulating the secretome of MSCs. Furthermore, identification of changes in key components of signaling pathways or in expression patterns of gene groups regulated through common pathways may provide insight into the upstream pathways mediating paracrine factor signaling in MSC spheroids. Finally, these approaches may be useful in identifying novel immunoregulatory factors expressed by MSCs, especially in IFN-γ treated cells, as immunomodulatory mechanisms have largely been focused on a set of approximately 10 factors. Furthermore, broadly identifying differentially regulated genes in response to IFN-γ would represent a more holistic approach to determine how IFN-γ switches MSCs to an immunomodulatory state.

Transcriptome analysis and RNA sequencing (RNA-seq) technology, in particular, is rapidly becoming a powerful tool for quantifying the entire profile of RNA expressed by cells, either at a population or single cell level. However, there has been limited application of this technology to studying the MSC transcriptome, especially in terms of cytokine priming of MSCs to stimulate immunomodulatory function. The majority of published experiments examining the transcriptome of MSCs have primarily focused on the transcriptional differences of MSCs isolated from different tissue sources as well as other stromal or fibroblast populations. These studies have largely been focused on understanding the functional differences (differentiation potential) between MSC-like cells from various tissue sources and identifying unique markers of MSC populations. The focus of transcriptome studies on cell source and differentiation potential of MSCs has likely been due to the focus of MSC research on the application of these cells for the repair of skeletal tissues. However, as MSC research transitions to become more focused on the trophic and paracrine ability of MSCs, transcriptome analysis of MSCs in response to environmental parameters could provide valuable information that is missing within the current body of literature. For example, genome-wide array comparison of human bone marrow-MSCs to human hematopoietic and embryonic stem cells and fibroblasts demonstrated a unique transcriptional profile of MSCs, 4,700 genes were differentially regulated between MSCs and HSCs, 3,172 genes between MSCs and hESCs, and 1,991 genes between MSCs and fibroblasts [275]. Similarly, comparison of MSC-like populations from different sources, such as bone marrow, umbilical cord, and even pluripotent stem cells, reveals significant source dependent differences in gene expression,

however, the number of differentially expressed genes between MSCs of different origins tend to be fewer than the number of differentially expressed genes between other stem cell populations or fibroblasts [276, 277]. Additionally, heterogeneity amongst MSC preparations and lineage priming has been frequently studied using RNA-seq technology. A recent RNA-seq experiment examining heterogeneity within MSCs populations supported the concept of lineage priming amongst MSCs, in that individual cells are primed for differentiation to a specific lineage [9], similarly to previously published studies [278]. However, this study also examined expression of a set of 12 immunomodulatory factors was evaluated in 16 unprimed mouse MSCs, however, expression of these 16 factors was fairly homogenous with the exception of IL-6, which almost solely contributed to the variability in the primary principal component. However, the functional relevancy of variation in IL-6 was not investigated. Furthermore, categories related to immune response regulation were not found in ontological analysis of the entire data set, suggesting little variation in immunomodulatory function between cells within their cell preparations. Altogether, while these studies demonstrate a unique, yet heterogeneous, transcriptome of MSCs from different tissues sources, evaluating the transcriptome of MSCs in response to environmental parameters, such as culture format or cytokine treatment, may provide further insight into the immunomodulatory mechanisms of MSCs.

6.2 Animal models for evaluating engineered MSC construct immunomodulation

Animal models of disease are critically important to evaluate the safety and efficacy of potential therapeutic treatments before proceeding to clinical studies with human patients. In this dissertation, we have proposed a novel therapeutic strategy for enhancing and

sustaining MSC immunomodulatory activity by incorporation of IFN-γ laden microparticles within transplantable 3D aggregates. Therefore, animal models of inflammatory and immune diseases would be a vital tool for evaluating if sustained delivery of IFN-γ within MSC spheroids enhances MSC immunomodulation *in vivo*. The efficacy of human MSC immunomodulatory activity has frequently been investigated in mouse models of DTH, graft-versus-host disease, inflammatory bowel diseases, multiple sclerosis, and other models of inflammatory and immune diseases [41]. However, one of the major challenges of examining the immunomodulatory capabilities of human MSCs in animal models is the species mismatch. Since immunocompromised animals lack a complete, functioning immune system, these models are not completely appropriate for investigating MSC immunomodulation. However, human MSCs will ultimately be rejected by the immune system in immunocompetent animals, although rejection tends to be delayed due to the immunosuppressive ability of MSCs [101]. Furthermore, differences in critical mechanisms used by MSCs to regulate immune responses (i.e. IDO expression in human MSCs and production of nitric oxide through iNOS expression in rodent MSCs) also provide a challenge for interpreting results and evaluating mechanisms used by MSCs to modulate immune responses in animal models [279]. Finally, licensing of MSCs by inflammatory cytokines, particularly IFN-γ, is reduced when transplanted in mice since IFN-γ is not well conserved across species and mouse-derived IFN-γ does not cross-react with the human IFN-γ receptor. Altogether, significant challenges limit the ability to accurately assess human MSC immunomodulation in animal models.

Despite the limitations of testing human MSC immunomodulation in animal models, several different approaches have been attempted to address these challenges. To address the species differences, mice with humanized immune systems have been proposed and used for testing human MSC immunomodulation *in vivo*. Generation of humanized mice is typically accomplished by transplantation of hematopoietic stem and progenitor cells into immunocompromised mice, such as NSG (Nod.Cg-*Prkdc*^{scid}*Il2rg*^{tm1Wjl}) mice [280]. Additionally, improved models have recently been created that improve development of innate immune cells, a population that is largely defective in NOG/NSG mice. These transgenic mice were created from a Rag2$^{-/-}$Il2rg$^{-/-}$ background and human genes for cytokines important for myeloid cell development (M-CSF, IL-3, GM-CSF, TPO, and SIRPα) were knocked-in to the endogenous mouse loci. These humanized mice, referred to as MISTRG mice, develop functional myeloid cell populations and better recapitulate the percentage of myeloid cells found in humans [281]. Several groups have used these humanized mouse models to study MSC interactions with the components of the human immune system in models of GvHD, type 1 diabetes, and wound healing which may better elucidate how transplanted human MSCs behave in human patients [282–286]. An alternative approach to humanized mice is to use IDO humanized mouse MSCs that are deficient in iNOS expression (Nos2$^{-/-}$) but express human IDO under the iNOS promoter, allowing for syngeneic cell treatment [287]. IDO humanized mouse MSCs were shown to be responsive to mouse-derived IFN-γ, which induces transcription of human IDO, and were capable of inhibiting T-cell proliferation in an IDO-dependent manner. However, humanized mouse models also have their limitations. The models are technically challenging due to the necessity of engraftment of transplanted human hematopoietic

progenitor cells. Additionally, current humanized mouse models do not precisely recapitulate the naturally occurring percentages of myeloid and lymphoid cell populations. Despite these limitations, humanized mouse models offer a promising alternative approach for examining the response of the immune system to human MSCs while decreasing the complications of xenogeneic transplantation of cells and the inability of human MSCs to respond to the mouse cytokine milieu.

Since inflammatory bowel diseases (IBD) are a major target for MSC-based therapies clinically, animal models of IBD are frequently used for examining MSC immunomodulation. Inflammatory bowel diseases represent a significant health burden with over 1 million Americans affected, resulting in over $6 billion in treatment costs in the United States [288]. Crohn's Disease (CD) and Ulcerative Colitis (UC), the two major forms of IBD, are characterized by chronic, uncontrolled inflammation of the intestinal mucosa and arise due to a combination of environmental factors, individual immune responses, and genetics. In both CD and UC, intestinal microbiota antigens are thought to trigger an excessive host immune response [289]; while the exact causes and mechanisms of IBDs remain unclear, increased production of inflammatory cytokines in the gut play a central role in the pathogenesis of these diseases. In CD, elevated levels of the cytokines IFN-γ, TNF-α, and IL-17 in the gut have been attributed to pro-inflammatory T-helper 1 and 17 (Th1, Th17) responses. In contrast, UC is characterized by a non-conventional Th2 immune response [289]. However, common drug treatments, such as corticosteroids and anti-TNF therapies, for CD and UC are often ineffective and the failure of these treatment regimens frequently result in the need for multiple intestinal resection [290]. Thus, novel

therapies are needed to combat progression of these diseases and MSC-based therapies are a potential alternative treatment due to the innate capacity of MSCs to regulate multiple immune cell populations and signaling pathways.

Mouse models of IBD are an important tool in studying the pathogenesis of IBD. While there are differences between these mouse models and the human manifestation of the disease, important immunological processes of human mucosal inflammation can be recapitulated [291]. Mouse models of IBD fall into 3 general categories: 1) chemical-induced colitis through damage to the intestinal mucosal barrier, 2) spontaneous colitis in mice with genetic knockouts of immunoregulatory factors, and 3) adoptive transfer of T-cells in immunocompromised mice [292]. Chemically induced models are commonly used for evaluating MSC immunomodulation due to their ease of use and because they can recapitulate many key aspects of human disease. Furthermore, as adoptive T-cell models lack a completely functioning immune system due to use of immunocompromised mice, these models may be more appropriate for specifically investigating MSC effects on T-cell populations. Additionally, in genetic knockout models, knockout of critical immunoregulatory factors, such as IL-10, may limit the ability of MSCs to suppress inflammation as MSCs induce endogenous immune cell populations to anti-inflammatory phenotypes expressing immunoregulatory factors, like IL-10, to aid in suppressing inflammation.

The two most common chemically-induced colitis models for evaluating MSC immunomodulation include trinitrobenzene sulfonate (TNBS) and dextran sulfate sodium

(DSS) induced colitis. In TNBS-induced colitis, TNBS is delivered in ethanol directly within the colon through an enema. The ethanol disrupts the mucosal barrier while the TNBS haptenizes colonic microbiota proteins, causing the proteins to become immunogenic, thereby triggering a host immune response in the intestinal mucosa [293]. Both acute and chronic TNBS-induced colitis models have been used to explore different aspects of innate and adaptive immune responses in mouse colitis. In the acute model, mice display increased myeloperoxidase (MPO) activity and an increased IL-12, IL-17, IFN-γ, and MIP-1α cytokine and chemokine profile, suggesting a predominant macrophage-derived cytokine profile, increased neutrophil response, and Th1/Th17 polarized $CD4^+$ T-cells [294]. In contrast, chronic TNBS-induced colitis displays significantly greater IL-12 and IL-17 and decreased MPO activity compared to the acute model, suggesting a heightened T-cell (Th1/Th17) response as the disease progresses to a chronic inflammatory state. Alternatively, in DSS-induced colitis, DSS is dissolved in the drinking water of mice and is toxic to gut epithelial cells resulting in significant damage to the mucosal barrier [295]. However, as C.B-17^{scid} and $Rag1^{-/-}$ mice also develop intestinal inflammation in response to DSS, the adaptive immune response does not seem to play a significant role in the acute phase of inflammation and is therefore useful for studying the contribution of innate immune mechanisms of colitis. However, repeated administration of DSS results in the development of chronic inflammation, which involves the activation of $CD4^+$ T-cells and is therefore dependent on adaptive immune responses. Therefore, the differential immune response in acute and chronic TNBS-induced and DSS-induced colitis enables the evaluation of MSC immunomodulation of separate components of the mucosal

inflammatory response and serves as a means for studying immunomodulatory characteristics of engineered MSC constructs.

Through preliminary studies, we have begun working on developing these models and determining the baseline immunomodulatory activity of single cell suspensions of MSCs (see Appendix A). Ultimately, these animal models could be used to address several questions, including: 1) does transplantation of pre-formed aggregates improve cell retention compared to single cell suspensions, 2) does transplantation of pre-formed aggregates increase immunomodulatory activity compared to single cell suspensions, and 3) does sustained delivery of IFN-γ within MSC aggregates further enhance the immunomodulatory activity of these cells? As spheroids are too large to safely be delivered intravenously, due to the likelihood of occlusion of blood vessels, another route of administration would be necessary for these studies. Intraperitoneal (I.P.) injection has also been commonly used with MSC treatments of chemically induced colitis and pre-formed spheroids could be injected into the peritoneal space with a wider-bore needle. Interestingly, I.P. injection of single cells suspensions of MSCs actually results in the formation of aggregates within the peritoneal cavity [175, 176]. However, as aggregation is thought to improve the viability and retention of transplanted MSCs, we may still expect greater therapeutic benefit from injection of pre-formed spheroids compared to single cell suspensions. Alternatively, intraluminal injection of MSC spheroids directly within the colon has also been used to treat colitis in a DSS model and may serve as a more local delivery site for MSC immunomodulation [176]. To further address the retention of cells, MSCs transduced to express luciferase under the ubiquitin promoter can be used with

bioluminescent imaging to evaluate retention of MSCs post-transplantation in order to determine whether aggregation improves cell retention post-transplantation [296, 297]. Altogether, chemically-induced colitis models provide a clinically relevant test bed for evaluating the retention and immunomodulatory activity of engineered MSC constructs *in vivo*.

6.3 Conclusions

The results of this dissertation provide a basis for future exploration of the effects of environmental parameters on MSC paracrine activity and engineering approaches to take advantage of environmental regulation of MSCs to enhance their therapeutic potential. Future studies evaluating the transcriptome of MSCs in response to aggregation and cytokine treatment could provide valuable information into the mechanisms used by MSCs to regulate immune responses. Furthermore, evaluation of engineered constructs in animal models could inform how this approach could ultimately be applied to MSC-based therapies to improve treatment efficacy. The microparticle-based approach presented here represents a novel application of biomaterials to manipulate the presentation of individual cytokines within the local environment of MSCs to promote immunomodulatory activity. Furthermore, while we have investigated presentation of IFN-γ within MSC spheroids, this approach could be expanded to examine the presentation of other or multiple cytokines simultaneously to precisely tune the immunomodulatory response of MSCs. Additionally, targeting other functional aspects of MSC paracrine activity, such as the angiogenic factors secreted by MSCs, could additionally open up new areas of research aimed at regulating MSC paracrine activity by manipulating environmental factors. Ultimately, biomaterial-

based engineering of the MSC microenvironment provides a means of controlling the function of transplanted cells to specifically direct their therapeutic activity and may improve the efficacy of MSC-based therapies.

APPENDIX A

MOUSE MODELS OF CHEMICALLY-INDUCED COLITIS FOR EVALUATING MSC IMMUNOMODULATION

A.1 INTRODUCTION

Animal models of inflammatory and immune diseases are critically important for evaluating MSC immunomodulation and would be a vital tool for evaluating if sustained delivery of IFN-γ within MSC spheroids enhances MSC immunomodulation *in vivo*. Since inflammatory bowel diseases (IBD) are a major target for MSC-based therapies clinically, animal models of IBD are frequently used for examining MSC immunomodulation. Therefore, the objectives of these studies were to evaluate if MSCs reduce inflammation in acute models of TNBS- and DSS-induced colitis in order to establish a working model and a baseline response of MSCs for future studies evaluating engineered MSC constructs.

A.2 MATERIALS AND METHODS

A.2.1 TNBS-Induced Colitis Model

MSCs were purchased from Texas A&M Institute for Regenerative Medicine and expanded according to the manufacturer's protocol, as described in Chapter 3. Acute TNBS induced colitis was induced in BALB/c mice (Jackson Labs) according to previously reported protocols [125, 298]. 100 μL of TNBS (Sigma Aldrich) diluted in 50% ethanol (30 mg/mL) was intrarectally injected. Control mice received an equal volume of 50% ethanol alone. After TNBS instillation, mice were injected intraperitoneally with a PBS

sham injection or $1x10^6$ MSCs either as a single cell suspension or as 500-cell spheroids (n= 8 per group). Animals were monitored daily for diarrhea, body weight, and survival. After 3 days, mice were euthanized, and colons were extracted for histological evaluation as well as cytokine and protein extraction. Colons were divided longitudinally for histological analysis and protein extraction. Colon samples were fixed and 5 µm paraffin embedded sections were stained with hematoxylin and eosin (H&E). Colon inflammation and damage was assessed as previously described on a scale of 0-4 [299]. Briefly, 0: no signs of inflammation; 1: very low level of inflammation; 2: low level of leukocyte infiltration; 3: high level of leukocyte infiltration, high vascular density, thickening of the colon wall; 4: transmural infiltrations, goblet cell loss, high vascular density, colon wall thickening.

A.2.2 DSS-Induced Colitis Model

MSCs were purchased from RoosterBio and expanded according to the manufacturer's protocol, as described in Chapters 3, 4, and 5. 8-week-old male C57Bl/6 mice (~25g, Jackson Labs) were used for the dextran sodium sulfate (DSS) induced experimental colitis model (n=3 for each experimental group). On Day 0, drinking water was switched to a 3% DSS (w/v, MP Biomedicals) in autoclaved water solution to induce colitis. Two days after switching drinking water to a 3% DSS solution, mice were injected intraperitoneally (I.P.) using a 26G needle (450 µm diameter to allow free passage of cells and MSC spheroids) with MSCs from each MSC experimental group or PBS as a vehicle control. For this initial pilot study, dissociated MSC monolayers were injected I.P. at either $0.2x10^6$ or $1x10^6$ million MSCs per mouse to evaluate dosing of MSCs. Mice were weighed daily

to monitor the progression of the disease. After 6 days of DSS treatment, drinking water was switched back to standard drinking water without DSS to allow for recovery. After 10 days, animals were euthanized. After weight measurement, the colon was removed and its length was measured. After colon length measurement, the colon was dissected into 3 segments: 0.5 cm segments at the proximal and distal ends were flash frozen in liquid nitrogen for cytokine analysis while the remainder was fixed in 10% neutral buffered formalin for histological analysis. Colon samples were embedded in paraffin and 5µm sections were stained with hematoxylin and eosin (H&E). Colon inflammation and damage was assessed as previously described on a scale of 0-4 [299]. Briefly, 0: no signs of inflammation; 1: very low level of inflammation; 2: low level of leukocyte infiltration; 3: high level of leukocyte infiltration, high vascular density, thickening of the colon wall; 4: transmural infiltrations, goblet cell loss, high vascular density, colon wall thickening.

A.3 RESULTS

A.3.1 TNBS-Induced Colitis

Intrarectal instillation of TNBS (3 mg in 50% ethanol) resulted in significant weight loss over 3 days compared to control mice injected with ethanol only (**Figure A.1A**). Mice receiving an injection of a single cell suspension of $1x10^6$ MSCs or a sham injection that displayed significantly greater weight loss compared to control mice receiving no TNBS. However, mice receiving an injection of $1x10^6$ MSCs as spheroids had less weight loss than those treated with a PBS sham injection or single MSC suspension and this weight loss was not statistically significant compared to control mice receiving no TNBS. Histological analysis of colon inflammation revealed indications of inflammation in mice

treated with TNBS, although only mice treated with a single cell suspension of MSCs had significantly higher histological scores than the "No TNBS" treatment group (**Figure A.1B**). Overall, the histological scores were not as high as expected for mice receiving TNBS and indicated that severe acute colitis was not efficiently induced in these mice. Therefore, a higher dose of TNBS or a greater percentage ethanol carrier solution may be necessary to increase absorption of TNBS into the colon epithelium and further damage the mucosal barrier integrity. Interestingly, injection of single cell MSCs resulted in increased histological indications of inflammation whereas MSC spheroids protected against body weight loss. However, overall there was a large amount of variability in weight loss and histological scores in mice and inflammation was not consistently seen in each individual animal. Additionally, Texas A&M cells, which were later shown to not have T-cell suppressive capabilities *in vitro* (See Chapter 3, Figure 3.10), were used for these experiments, further complicating interpretation of these results. Future studies tuning the dose of ethanol and TNBS may therefore be necessary to ensure consistent induction of inflammation. Furthermore, analysis of cytokine levels in tissue may also provide further insight into the inflammatory state after induction of colitis and MSC treatment. Finally, delivery of MSCs that have demonstrated the ability to suppress T-cell proliferation *in vitro* should be used as a quality control for immunomodulation activity prior to use in animal models.

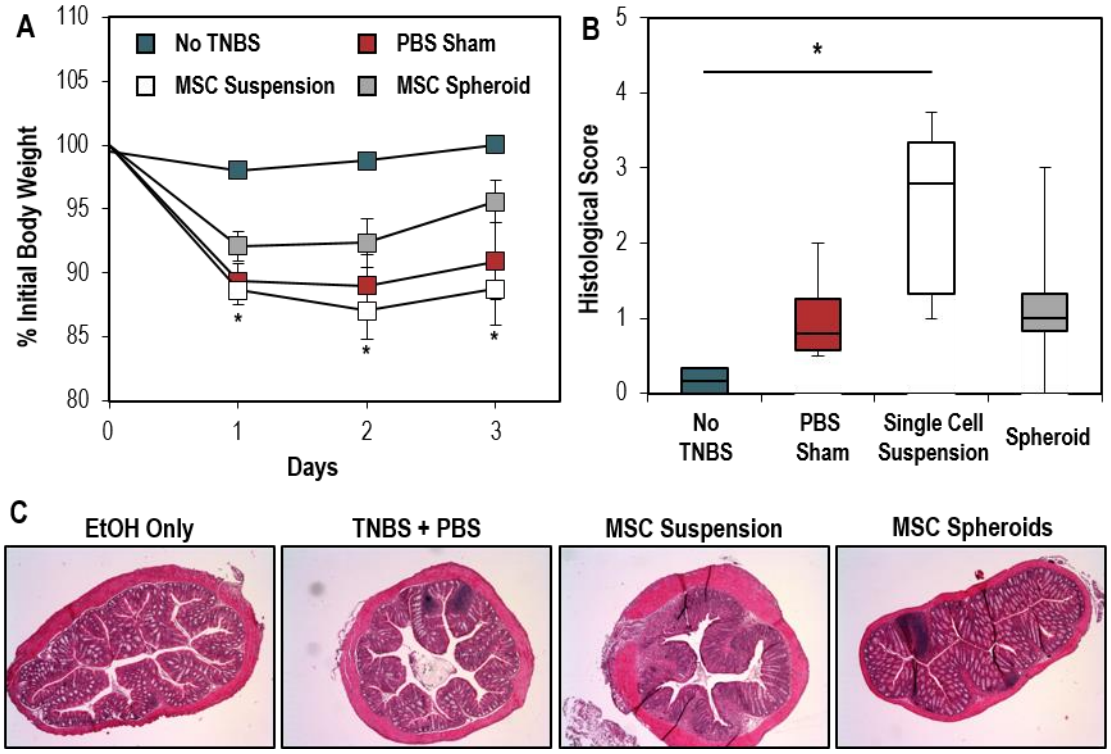

Figure A.1: Validation of TNBS-Induced Colitis Model. (A) Measurement of mouse weight loss over time demonstrated weight loss in mice receiving TNBS and either a PBS sham injection or an injection of single cell suspension of 10^6 MSCs compared to control mice that did not receive TNBS. (B) Histological scoring of H&E stained mouse colon sections demonstrated increased histological indications of inflammation in mice receiving TNBS and treated with a single cell suspension of MSCs compared to mice that did not receive TNBS. (C) Representative cross-sectional images of H&E stained colons of mice from each experimental group. * indicates $p < 0.5$ compared to "No TNBS" experimental group at the same time point.

A.3.2 DSS-Induced Colitis

As expected, supplementation of 3% DSS in the drinking water of mice resulted in significant loss of body weight over time. Significant loss of weight was observed in mice receiving a PBS I.P. sham injection five days after switching to DSS drinking water (**Figure A.2A**). Furthermore, weight loss of mice receiving a PBS sham injection plateaued

at approximately 83% of initial body weight, with no significant recovery seen after 10 days. Mice receiving injection of $0.2x10^6$ or $1x10^6$ MSCs showed a similar weight loss trajectory over the first eight days. However, by day nine, mice receiving the lower dose of MSCs ($0.2x10^6$ cells) had significantly lower weight loss compared to the PBS sham injection. Furthermore, by day 10, both mice receiving a low or high dose of MSCs had significantly greater weight loss compared to the PBS sham injection. The lengths of colons, and indication of disease severity, from mice receiving I.P. injections were significantly shorter in length compared to control mice receiving no DSS (**Figure A.2B**). Finally, colon sections stained with H&E revealed significant signs of inflammation, including infiltration of leukocytes, colon wall thickening, and destruction of crypt structure in mice receiving DSS, regardless of sham or MSC treatment group (**Figure A.2C**). Thus, the results of this study demonstrate a working model of DSS-induced colitis. While injected MSCs appeared to exacerbate indications of disease, the number of replicates was relatively low for these pilot experiments (n=2 for low dose MSC group and n=3 for high dose MSC group). Additionally, previous studies have indicated that MSCs that do not receive IFN-γ priming may actually aid in the immune response by secretion of chemokines that can recruit leukocytes to sites of inflammation without concurrent expression of immunosuppressive factors, such as IDO. In this study, MSCs were not pre-treated with IFN-γ prior to injection, therefore, the cells may not have been sufficiently stimulated by the *in vivo* environment to express IDO or other immunosuppressive factors.

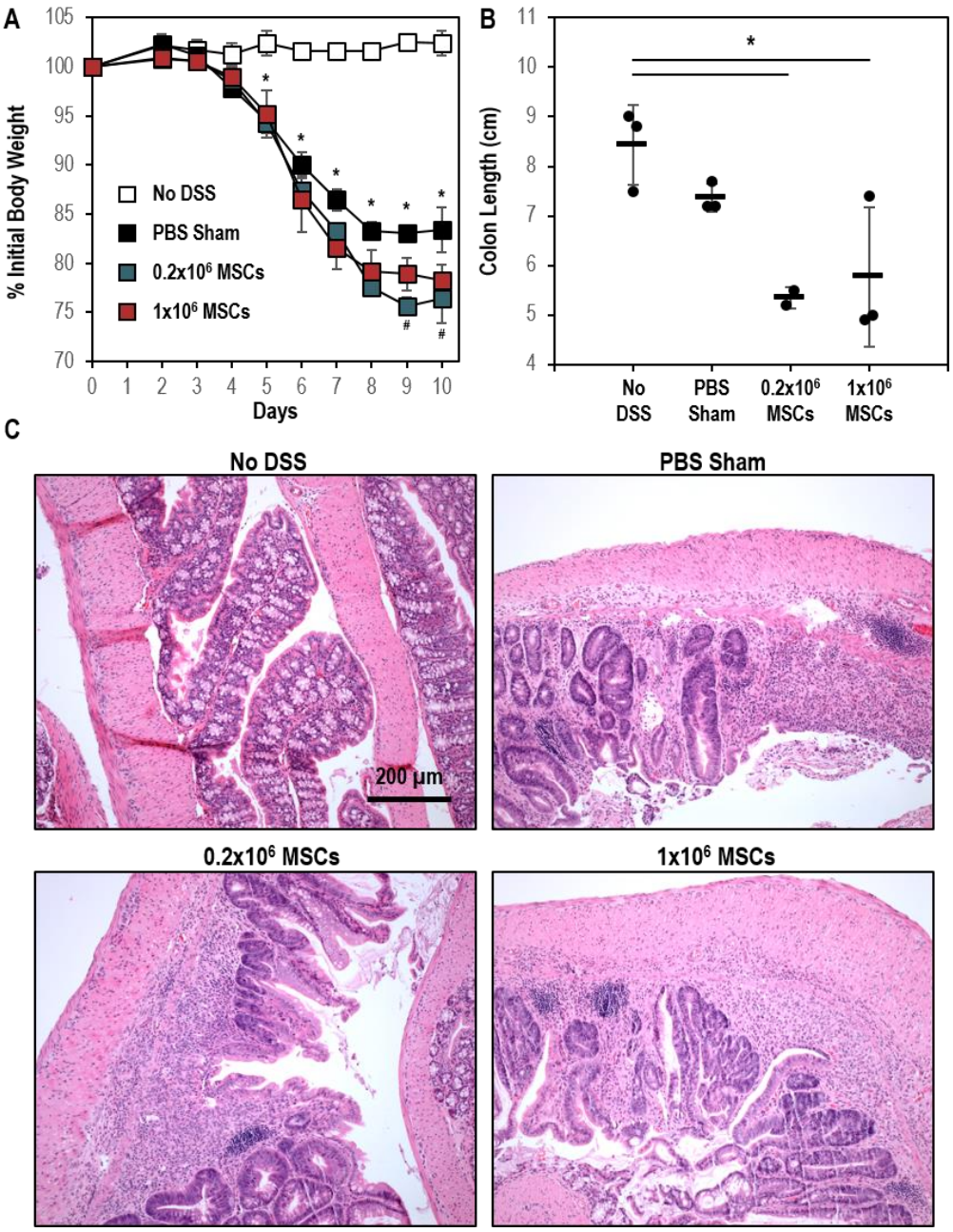

Figure A.2: Validation of DSS-Induced Colitis Model. (A) Measurement of mouse weight loss over time demonstrated severe weight loss in mice receiving a 3% DSS drinking water solution (regardless of sham or MSC treatment) compared to control mice receiving normal drinking water. (B) Mice injected I.P. with either $0.2x10^6$ or $1x10^6$ MSCs had significantly shorter colons after 10 days compared to mice receiving normal drinking water. (C) H&E stained colon tissue sections demonstrate severe signs of inflammation in mice receiving DSS drinking water, regardless of treatment group. * indicates $p < 0.05$ compared to "No DSS" group on the same day. # indicates $p < 0.05$ compared to "PBS Sham" group on the same day.

A.4 CONCLUSIONS

Altogether, while technical challenges still remain for delivery of immunomodulatory MSCs to suppress inflammation in these models, the results of these studies demonstrate working models of both TNBS- and DSS- induced colitis in mice that could be used in the future to evaluate engineered MSC construct immunomodulation.

REFERENCES

[1] Tavassoli M, Crosby WH. Transplantation of marrow to extramedullary sites. *Science*. 1968;161(3836):54-56.

[2] Friedenstein A, Chailakhjan R, Lalykina K. The development of fibroblast colonies in monolayer cultures of guinea-pig bone marrow and spleen cells. *Cell Tissue Kinet*. 1970;3(4):393-403.

[3] Caplain A. Mesenchymal Stem Cells. *J Orthop Res*. 1991;9(5):641-650.

[4] Pittenger MF, Mackay a M, Beck SC, et al. Multilineage potential of adult human mesenchymal stem cells. *Science*. 1999;284(5411):143-147.

[5] Zuk P a, Zhu M, Mizuno H, et al. Multilineage cells from human adipose tissue: implications for cell-based therapies. *Tissue Eng*. 2001;7(2):211-228.

[6] Erices A, Conget P, Minguell JJ. Mesenchymal progenitor cells in human umbilical cord blood. *Br J Haematol*. 2000;109(1):235-242.

[7] Dominici M, Le Blanc K, Mueller I, et al. Minimal criteria for defining multipotent mesenchymal stromal cells. The International Society for Cellular Therapy position statement. *Cytotherapy*. 2006;8(4):315-317.

[8] Tremain N, Korkko J, Ibberson D, Kopen GC, DiGirolamo C, Phinney DG. MicroSAGE Analysis of 2,353 Expressed Genes in a Single Cell-Derived Colony of Undifferentiated Human Mesenchymal Stem Cells Reveals mRNAs of Multiple Cell Lineages. *Stem Cells*. 2001;19(5):408-418.

[9] Freeman BT, Jung JP, Ogle BM. Single-Cell RNA-Seq of Bone Marrow-Derived Mesenchymal Stem Cells Reveals Unique Profiles of Lineage Priming. Covas DT,

ed. *PLoS One*. 2015;10(9):e0136199.

[10] Sacchetti B, Funari A, Michienzi S, et al. Self-renewing osteoprogenitors in bone marrow sinusoids can organize a hematopoietic microenvironment. *Cell*. 2007;131:324-336.

[11] Lorenz K, Sicker M, Schmelzer E, et al. Multilineage differentiation potential of human dermal skin-derived fibroblasts. *Exp Dermatol*. 2008;17(11):925-932.

[12] Majumdar MK, Banks V, Peluso DP, Morris E a. Isolation, characterization, and chondrogenic potential of human bone marrow-derived multipotential stromal cells. *J Cell Physiol*. 2000;185:98-106.

[13] Qian H, Le Blanc K, Sigvardsson M. Primary Mesenchymal Stem and Progenitor Cells from Bone Marrow Lack Expression of CD44 Protein. *J Biol Chem*. 2012;287(31):25795-25807.

[14] Gronthos S. Molecular and cellular characterisation of highly purified stromal stem cells derived from human bone marrow. *J Cell Sci*. 2003;116(9):1827-1835.

[15] Jones E, McGonagle D. Human bone marrow mesenchymal stem cells in vivo. *Rheumatology*. 2007;47(2):126-131.

[16] Méndez-Ferrer S, Michurina T V, Ferraro F, et al. Mesenchymal and haematopoietic stem cells form a unique bone marrow niche. *Nature*. 2010;466(7308):829-834.

[17] Tormin A, Li O, Brune JC, et al. CD146 expression on primary nonhematopoietic bone marrow stem cells is correlated with in situ localization. *Blood*. 2011;117(19):5067-5077.

[18] Lv F-J, Tuan RS, Cheung KMC, Leung VYL. Concise review: the surface markers

and identity of human mesenchymal stem cells. *Stem Cells*. 2014;32(6):1408-1419.

[19] Tang W, Zeve D, Suh JM, et al. White fat progenitor cells reside in the adipose vasculature. *Science*. 2008;322(5901):583-586.

[20] Dellavalle A, Sampaolesi M, Tonlorenzi R, et al. Pericytes of human skeletal muscle are myogenic precursors distinct from satellite cells. *Nat Cell Biol*. 2007;9(3):255-267.

[21] Caplan AI. MSCs: The Sentinel and Safe-Guards of Injury. *J Cell Physiol*. 2016;231(7):1413-1416.

[22] Crisan M, Yap S, Casteilla L, et al. A perivascular origin for mesenchymal stem cells in multiple human organs. *Cell Stem Cell*. 2008;3(3):301-313.

[23] Collett GDM, Canfield AE. Angiogenesis and pericytes in the initiation of ectopic calcification. *Circ Res*. 2005;96(9):930-938. doi:10.1161/01.RES.0000163634.51301.0d.

[24] Farrington-Rock C, Crofts NJ, Doherty MJ, Ashton BA, Griffin-Jones C, Canfield AE. Chondrogenic and adipogenic potential of microvascular pericytes. *Circulation*. 2004;110(15):2226-2232.

[25] Doherty MJ, Ashton BA, Walsh S, Beresford JN, Grant ME, Canfield AE. Vascular pericytes express osteogenic potential in vitro and in vivo. *J Bone Miner Res*. 1998;13(5):828-838.

[26] Shi S, Gronthos S. Perivascular niche of postnatal mesenchymal stem cells in human bone marrow and dental pulp. *J Bone Miner Res*. 2003;18(4):696-704.

[27] Sugiyama T, Kohara H, Noda M, Nagasawa T. Maintenance of the Hematopoietic Stem Cell Pool by CXCL12-CXCR4 Chemokine Signaling in Bone Marrow

Stromal Cell Niches. *Immunity*. 2006;25(December):977-988.

[28] Broxmeyer HE. Stromal cell-derived factor-1/CXCL12 directly enhances survival/antiapoptosis of myeloid progenitor cells through CXCR4 and Galphai proteins and enhances engraftment of competitive, repopulating stem cells. *J Leukoc Biol*. 2003;73(5):630-638.

[29] Zhou BO, Yue R, Murphy MM, Peyer JG, Morrison SJ. Leptin-Receptor-Expressing Mesenchymal Stromal Cells Represent the Main Source of Bone Formed by Adult Bone Marrow. *Cell Stem Cell*. 2014:1-15.

[30] Shi C, Jia T, Mendez-Ferrer S, et al. Bone marrow mesenchymal stem and progenitor cells induce monocyte emigration in response to circulating toll-like receptor ligands. *Immunity*. 2011;34(4):590-601.

[31] Chow A, Lucas D, Hidalgo A, et al. Bone marrow CD169+ macrophages promote the retention of hematopoietic stem and progenitor cells in the mesenchymal stem cell niche. *J Exp Med*. 2011;208(2):261-271.

[32] English K, Barry FP, Field-Corbett CP, Mahon BP. IFN-gamma and TNF-alpha differentially regulate immunomodulation by murine mesenchymal stem cells. *Immunol Lett*. 2007;110(2):91-100.

[33] Ren G, Zhang L, Zhao X, et al. Mesenchymal stem cell-mediated immunosuppression occurs via concerted action of chemokines and nitric oxide. *Cell Stem Cell*. 2008;2(2):141-150.

[34] Prasanna SJ, Gopalakrishnan D, Shankar SR, Vasandan AB. Pro-inflammatory cytokines, IFNgamma and TNFalpha, influence immune properties of human bone marrow and Wharton jelly mesenchymal stem cells differentially. *PLoS One*.

2010;5(2):e9016.

[35] Hegyi B, Kudlik G, Monostori E, Uher F. Activated T-cells and pro-inflammatory cytokines differentially regulate prostaglandin E2 secretion by mesenchymal stem cells. *Biochem Biophys Res Commun*. 2012;419(2):215-220.

[36] Sivanathan KN, Rojas-Canales DM, Hope CM, et al. Interleukin-17A-Induced Human Mesenchymal Stem Cells Are Superior Modulators of Immunological Function. *Stem Cells*. 2015;33(9):2850-2863.

[37] Opitz C a, Litzenburger UM, Lutz C, et al. Toll-like receptor engagement enhances the immunosuppressive properties of human bone marrow-derived mesenchymal stem cells by inducing indoleamine-2,3-dioxygenase-1 via interferon-beta and protein kinase R. *Stem Cells*. 2009;27(4):909-919.

[38] Waterman RS, Tomchuck SL, Henkle SL, Betancourt AM. A new mesenchymal stem cell (MSC) paradigm: polarization into a pro-inflammatory MSC1 or an Immunosuppressive MSC2 phenotype. *PLoS One*. 2010;5(4):e10088.

[39] Di Nicola M. Human bone marrow stromal cells suppress T-lymphocyte proliferation induced by cellular or nonspecific mitogenic stimuli. *Blood*. 2002;99(10):3838-3843.

[40] Bartholomew A, Sturgeon C, Siatskas M, et al. Mesenchymal stem cells suppress lymphocyte proliferation in vitro and prolong skin graft survival in vivo. *Hematology*. 2002;30:42-48.

[41] English K. Mechanisms of mesenchymal stromal cell immunomodulation. *Immunol Cell Biol*. 2013;91(1):19-26.

[42] Pérez-Simon JA, López-Villar O, Andreu EJ, et al. Mesenchymal stem cells

expanded in vitro with human serum for the treatment of acute and chronic graft-versus-host disease: results of a phase I/II clinical trial. *Haematologica*. 2011;96(7):1072-1076.

[43] Baron F, Lechanteur C, Willems E, et al. Cotransplantation of mesenchymal stem cells might prevent death from graft-versus-host disease (GVHD) without abrogating graft-versus-tumor effects after HLA-mismatched allogeneic transplantation following nonmyeloablative conditioning. *Biol Blood Marrow Transplant*. 2010;16(6):838-847.

[44] Zhou H, Guo M, Bian C, et al. Efficacy of bone marrow-derived mesenchymal stem cells in the treatment of sclerodermatous chronic graft-versus-host disease: clinical report. *Biol Blood Marrow Transplant*. 2010;16(3):403-412.

[45] Le Blanc K, Frassoni F, Ball L, et al. Mesenchymal stem cells for treatment of steroid-resistant, severe, acute graft-versus-host disease: a phase II study. *Lancet*. 2008;371:1579-1586.

[46] Connick P, Kolappan M, Crawley C, et al. Autologous mesenchymal stem cells for the treatment of secondary progressive multiple sclerosis: an open-label phase 2a proof-of-concept study. *Lancet Neurol*. 2012;11(2):150-156.

[47] Connick P, Kolappan M, Patani R, et al. The mesenchymal stem cells in multiple sclerosis (MSCIMS) trial protocol and baseline cohort characteristics: an open-label pre-test: post-test study with blinded outcome assessments. *Trials*. 2011;12:62.

[48] Llufriu S, Sepúlveda M, Blanco Y, et al. Randomized placebo-controlled phase II trial of autologous mesenchymal stem cells in multiple sclerosis. *PLoS One*.

2014;9(12):e113936.

[49] Karussis D, Karageorgiou C, Vaknin-Dembinsky A, et al. Safety and immunological effects of mesenchymal stem cell transplantation in patients with multiple sclerosis and amyotrophic lateral sclerosis. *Arch Neurol*. 2010;67:1187-1194.

[50] Duijvestein M, Vos ACW, Roelofs H, et al. Autologous bone marrow-derived mesenchymal stromal cell treatment for refractory luminal Crohn's disease: results of a phase I study. *Gut*. 2010;59:1662-1669.

[51] Ciccocioppo R, Bernardo ME, Sgarella A, et al. Autologous bone marrow-derived mesenchymal stromal cells in the treatment of fistulising Crohn's disease. *Gut*. 2011;60(6):788-798.

[52] Forbes GM, Sturm MJ, Leong RW, et al. A phase 2 study of allogeneic mesenchymal stromal cells for luminal Crohn's disease refractory to biologic therapy. *Clin Gastroenterol Hepatol*. 2014;12(1):64-71.

[53] Mayer L, Pandak WM, Melmed GY, et al. Safety and tolerability of human placenta-derived cells (PDA001) in treatment-resistant crohn's disease: a phase 1 study. *Inflamm Bowel Dis*. 19(4):754-760.

[54] Sun L, Akiyama K, Zhang H, et al. Mesenchymal stem cell transplantation reverses multiorgan dysfunction in systemic lupus erythematosus mice and humans. *Stem Cells*. 2009;27(6):1421-1432.

[55] Liang J, Zhang H, Hua B, et al. Allogenic mesenchymal stem cells transplantation in refractory systemic lupus erythematosus: a pilot clinical study. *Ann Rheum Dis*. 2010;69(8):1423-1429.

[56] Eggenhofer E, Benseler V, Kroemer A, et al. Mesenchymal stem cells are short-lived and do not migrate beyond the lungs after intravenous infusion. *Front Immunol*. 2012;3:297.

[57] Fischer UM, Harting MT, Jimenez F, et al. Pulmonary passage is a major obstacle for intravenous stem cell delivery: the pulmonary first-pass effect. *Stem Cells Dev*. 2009;18(5):683-692.

[58] Sharma RR, Pollock K, Hubel A, McKenna D. Mesenchymal stem or stromal cells: a review of clinical applications and manufacturing practices. *Transfusion*. 2014;54:1418-1437.

[59] Gao F, Chiu SM, Motan DAL, et al. Mesenchymal stem cells and immunomodulation: current status and future prospects. *Cell Death Dis*. 2016;7:e2062.

[60] Aggarwal S, Pittenger MF. Human mesenchymal stem cells modulate allogeneic immune cell responses. *Blood*. 2005;105(4):1815-1822.

[61] Zhao W, Wang Y, Wang D, et al. TGF-beta expression by allogeneic bone marrow stromal cells ameliorates diabetes in NOD mice through modulating the distribution of CD4+ T cell subsets. *Cell Immunol*. 2008;253(1-2):23-30.

[62] Djouad F, Charbonnier L-M, Bouffi C, et al. Mesenchymal stem cells inhibit the differentiation of dendritic cells through an interleukin-6-dependent mechanism. *Stem Cells*. 2007;25(8):2025-2032.

[63] Meisel R, Zibert A, Laryea M, Göbel U, Däubener W, Dilloo D. Human bone marrow stromal cells inhibit allogeneic T-cell responses by indoleamine 2,3-dioxygenase-mediated tryptophan degradation. *Blood*. 2004;103(12):4619-4621.

[64] Selmani Z, Naji A, Zidi I, et al. Human leukocyte antigen-G5 secretion by human mesenchymal stem cells is required to suppress T lymphocyte and natural killer function and to induce CD4+CD25highFOXP3+ regulatory T cells. *Stem Cells*. 2008;26(1):212-222.

[65] Bai L, Lennon DP, Caplan AI, et al. Hepatocyte growth factor mediates mesenchymal stem cell–induced recovery in multiple sclerosis models. *Nat Neurosci*. 2012;15(6):862-870.

[66] Mougiakakos D, Jitschin R, Johansson CC, Okita R, Kiessling R, Le Blanc K. The impact of inflammatory licensing on heme oxygenase-1-mediated induction of regulatory T cells by human mesenchymal stem cells. *Blood*. 2011;117(18):4826-4835.

[67] Ryan JM, Barry F, Murphy JM, Mahon BP. Interferon-gamma does not break, but promotes the immunosuppressive capacity of adult human mesenchymal stem cells. *Clin Exp Immunol*. 2007;149(2):353-363.

[68] Ge W, Jiang J, Arp J, Liu W, Garcia B, Wang H. Regulatory T-cell generation and kidney allograft tolerance induced by mesenchymal stem cells associated with indoleamine 2,3-dioxygenase expression. *Transplantation*. 2010;90(12):1312-1320.

[69] Yang S-H, Park M-J, Yoon I-H, et al. Soluble mediators from mesenchymal stem cells suppress T cell proliferation by inducing IL-10. *Exp Mol Med*. 2009;41(5):315-324.

[70] Németh K, Leelahavanichkul A, Yuen PST, et al. Bone marrow stromal cells attenuate sepsis via prostaglandin E(2)-dependent reprogramming of host

macrophages to increase their interleukin-10 production. *Nat Med*. 2009;15(1):42-49.

[71] Nauta AJ, Kruisselbrink AB, Lurvink E, Willemze R, Fibbe WE. Mesenchymal stem cells inhibit generation and function of both CD34+-derived and monocyte-derived dendritic cells. *J Immunol*. 2006;177(4):2080-2087.

[72] Jiang X-X, Zhang Y, Liu B, et al. Human mesenchymal stem cells inhibit differentiation and function of monocyte-derived dendritic cells. *Blood*. 2005;105(10):4120-4126.

[73] Schena F, Gambini C, Gregorio A, et al. Interferon-γ-dependent inhibition of B cell activation by bone marrow-derived mesenchymal stem cells in a murine model of systemic lupus erythematosus. *Arthritis Rheum*. 2010;62(9):2776-2786.

[74] Corcione A, Benvenuto F, Ferretti E, et al. Human mesenchymal stem cells modulate B-cell functions. *Blood*. 2006;107(1):367-372.

[75] Di Nicola M, Carlo-Stella C, Magni M, et al. Human bone marrow stromal cells suppress T-lymphocyte proliferation induced by cellular or nonspecific mitogenic stimuli. *Blood*. 2002;99(10):3838-3843.

[76] Burr SP, Dazzi F, Garden O a. Mesenchymal stromal cells and regulatory T cells: the Yin and Yang of peripheral tolerance? *Immunol Cell Biol*. 2013;91(1):12-18.

[77] Spaggiari GM, Capobianco A, Abdelrazik H, Becchetti F, Mingari MC, Moretta L. Mesenchymal stem cells inhibit natural killer-cell proliferation, cytotoxicity, and cytokine production: role of indoleamine 2,3-dioxygenase and prostaglandin E2. *Blood*. 2008;111(3):1327-1333.

[78] François M, Romieu-Mourez R, Li M, Galipeau J. Human MSC suppression

correlates with cytokine induction of indoleamine 2,3-dioxygenase and bystander M2 macrophage differentiation. *Mol Ther*. 2012;20(1):187-195.

[79] Maggini J, Mirkin G, Bognanni I, et al. Mouse bone marrow-derived mesenchymal stromal cells turn activated macrophages into a regulatory-like profile. *PLoS One*. 2010;5(2):e9252.

[80] Chiesa S, Morbelli S, Morando S, et al. Mesenchymal stem cells impair in vivo T-cell priming by dendritic cells. *Proc Natl Acad Sci U S A*. 2011;108(42):17384-17389.

[81] Duffy MM, Pindjakova J, Hanley S a, et al. Mesenchymal stem cell inhibition of T-helper 17 cell- differentiation is triggered by cell-cell contact and mediated by prostaglandin E2 via the EP4 receptor. *Eur J Immunol*. 2011;41(10):2840-2851.

[82] Croitoru-Lamoury J, Lamoury FMJ, Caristo M, et al. Interferon-γ regulates the proliferation and differentiation of mesenchymal stem cells via activation of indoleamine 2,3 dioxygenase (IDO). *PLoS One*. 2011;6(2):e14698.

[83] Krampera M, Cosmi L, Angeli R, et al. Role for interferon-gamma in the immunomodulatory activity of human bone marrow mesenchymal stem cells. *Stem Cells*. 2006;24(2):386-398.

[84] Krampera M, Galipeau J, Shi Y, Tarte K, Sensebe L. Immunological characterization of multipotent mesenchymal stromal cells--The International Society for Cellular Therapy (ISCT) working proposal. *Cytotherapy*. 2013;15(9):1054-1061.

[85] Li W, Ren G, Huang Y, et al. Mesenchymal stem cells: a double-edged sword in regulating immune responses. *Cell Death Differ*. 2012;19:1505-1513.

[86] Chan JL, Tang KC, Patel AP, et al. Antigen-presenting property of mesenchymal stem cells occurs during a narrow window at low levels of interferon-gamma. *Blood*. 2006;107(12):4817-4824.

[87] François M, Romieu-Mourez R, Stock-Martineau S, Boivin M-N, Bramson JL, Galipeau J. Mesenchymal stromal cells cross-present soluble exogenous antigens as part of their antigen-presenting cell properties. *Blood*. 2009;114(13):2632-2638.

[88] Wang Y, Chen X, Cao W, Shi Y. Plasticity of mesenchymal stem cells in immunomodulation: pathological and therapeutic implications. *Nat Immunol*. 2014;15(11):1009-1016.

[89] Mosser DM, Edwards JP. Exploring the full spectrum of macrophage activation. *Nat Rev Immunol*. 2008;8(12):958-969.

[90] Chen L, Tredget EE, Wu PYG, Wu Y, Wu Y. Paracrine factors of mesenchymal stem cells recruit macrophages and endothelial lineage cells and enhance wound healing. *PLoS One*. 2008;3(4).

[91] Kim J, Hematti P. Mesenchymal stem cell–educated macrophages: A novel type of alternatively activated macrophages. *Exp Hematol*. 2009;37(12):1445-1453.

[92] Abumaree MH, Al Jumah MA, Kalionis B, et al. Human Placental Mesenchymal Stem Cells (pMSCs) Play a Role as Immune Suppressive Cells by Shifting Macrophage Differentiation from Inflammatory M1 to Anti-inflammatory M2 Macrophages. *Stem Cell Rev Reports*. 2013;9(5):620-641.

[93] Gupta N, Su X, Popov B, Lee JW, Serikov V, Matthay MA. Intrapulmonary Delivery of Bone Marrow-Derived Mesenchymal Stem Cells Improves Survival and Attenuates Endotoxin-Induced Acute Lung Injury in Mice. *J Immunol*.

2007;179(3):1855-1863.

[94] Choi H, Lee RH, Bazhanov N, Oh JY, Prockop DJ. Anti-inflammatory protein TSG-6 secreted by activated MSCs attenuates zymosan-induced mouse peritonitis by decreasing TLR2/NF- B signaling in resident macrophages. *Blood*. 2011;118(2):330-338.

[95] Lanier LL. Up on the tightrope: natural killer cell activation and inhibition. *Nat Immunol*. 2008;9(5):495-502.

[96] Sotiropoulou PA, Perez SA, Gritzapis AD, Baxevanis CN, Papamichail M. Interactions Between Human Mesenchymal Stem Cells and Natural Killer Cells. *Stem Cells*. 2006;24(1):74-85.

[97] Sotiropoulou PA, Perez SA, Gritzapis AD, Baxevanis CN, Papamichail M. Interactions Between Human Mesenchymal Stem Cells and Natural Killer Cells. *Stem Cells*. 2006;24(1):74-85.

[98] Spaggiari GM. Mesenchymal stem cell-natural killer cell interactions: evidence that activated NK cells are capable of killing MSCs, whereas MSCs can inhibit IL-2-induced NK-cell proliferation. *Blood*. 2006;107(4):1484-1490.

[99] Spaggiari GM. Mesenchymal stem cell-natural killer cell interactions: evidence that activated NK cells are capable of killing MSCs, whereas MSCs can inhibit IL-2-induced NK-cell proliferation. *Blood*. 2006;107(4):1484-1490.

[100] Götherström C, Lundqvist A, Duprez IR, Childs R, Berg L, le Blanc K. Fetal and adult multipotent mesenchymal stromal cells are killed by different pathways. *Cytotherapy*. 2011;13(3):269-278.

[101] Ankrum JA, Ong JF, Karp JM. Mesenchymal stem cells: immune evasive, not

immune privileged. *Nat Biotechnol*. 2014;32(3):252-260.

[102] Zhang W, Ge W, Li C, et al. Effects of mesenchymal stem cells on differentiation, maturation, and function of human monocyte-derived dendritic cells. *Stem Cells Dev*. 2004;13(3):263-271.

[103] English K, Barry FP, Mahon BP. Murine mesenchymal stem cells suppress dendritic cell migration, maturation and antigen presentation. *Immunol Lett*. 2008;115(1):50-58.

[104] Li Y-P, Paczesny S, Lauret E, et al. Human Mesenchymal Stem Cells License Adult CD34+ Hemopoietic Progenitor Cells to Differentiate into Regulatory Dendritic Cells through Activation of the Notch Pathway. *J Immunol*. 2008;180(3):1598-1608.

[105] Zhang B, Liu R, Shi D, et al. Mesenchymal stem cells induce mature dendritic cells into a novel Jagged-2-dependent regulatory dendritic cell population. *Blood*. 2009;113(1):46-57.

[106] Liu X, Qu X, Chen Y, et al. Mesenchymal Stem/Stromal Cells Induce the Generation of Novel IL-10-Dependent Regulatory Dendritic Cells by SOCS3 Activation. *J Immunol*. 2012;189(3):1182-1192.

[107] Zhang B, Liu R, Shi D, et al. Mesenchymal stem cells induce mature dendritic cells into a novel Jagged-2-dependent regulatory dendritic cell population. *Blood*. 2009;113(1):46-57.

[108] Spaggiari GM, Abdelrazik H, Becchetti F, Moretta L. MSCs inhibit monocyte-derived DC maturation and function by selectively interfering with the generation of immature DCs: central role of MSC-derived prostaglandin E2. *Blood*.

2009;113(26):6576-6583.

[109] Li Y-P, Paczesny S, Lauret E, et al. Human Mesenchymal Stem Cells License Adult CD34+ Hemopoietic Progenitor Cells to Differentiate into Regulatory Dendritic Cells through Activation of the Notch Pathway. *J Immunol*. 2008;180(3):1598-1608.

[110] Zhang Y, Cai W, Huang Q, et al. Mesenchymal stem cells alleviate bacteria-induced liver injury in mice by inducing regulatory dendritic cells. *Hepatology*. 2014;59(2):671-682.

[111] Spaggiari GM, Abdelrazik H, Becchetti F, Moretta L. MSCs inhibit monocyte-derived DC maturation and function by selectively interfering with the generation of immature DCs: central role of MSC-derived prostaglandin E2. *Blood*. 2009;113(26):6576-6583.

[112] Ge W, Jiang J, Baroja ML, et al. Infusion of Mesenchymal Stem Cells and Rapamycin Synergize to Attenuate Alloimmune Responses and Promote Cardiac Allograft Tolerance. *Am J Transplant*. 2009;9(8):1760-1772.

[113] Wan YY, Flavell RA. How diverse--CD4 effector T cells and their functions. *J Mol Cell Biol*. 2009;1(1):20-36.

[114] Duffy MM, Ritter T, Ceredig R, Griffin MD. Mesenchymal stem cell effects on T-cell effector pathways. *Stem Cell Res Ther*. 2011;2(4):34.

[115] Glennie S, Soeiro I, Dyson PJ, Lam EW-F, Dazzi F. Bone marrow mesenchymal stem cells induce division arrest anergy of activated T cells. *Blood*. 2005;105(7):2821-2827.

[116] Munn DH, Sharma MD, Mellor AL. Ligation of B7-1/B7-2 by human CD4+ T

cells triggers indoleamine 2,3-dioxygenase activity in dendritic cells. *J Immunol*. 2004;172(7):4100-4110.

[117] Frumento G, Rotondo R, Tonetti M, Damonte G, Benatti U, Ferrara GB. Tryptophan-derived Catabolites Are Responsible for Inhibition of T and Natural Killer Cell Proliferation Induced by Indoleamine 2,3-Dioxygenase. *J Exp Med*. 2002;196(4):459-468.

[118] Munn DH, Sharma MD, Baban B, et al. GCN2 kinase in T cells mediates proliferative arrest and anergy induction in response to indoleamine 2,3-dioxygenase. *Immunity*. 2005;22:633-642.

[119] Najar M, Raicevic G, Boufker HI, et al. Mesenchymal stromal cells use PGE2 to modulate activation and proliferation of lymphocyte subsets: Combined comparison of adipose tissue, Wharton's Jelly and bone marrow sources. *Cell Immunol*. 2010;264(2):171-179.

[120] Nasef A, Chapel A, Mazurier C, et al. Identification of IL-10 and TGF-beta transcripts involved in the inhibition of T-lymphocyte proliferation during cell contact with human mesenchymal stem cells. *Gene Expr*. 2007;13(4-5):217-226.

[121] Batten P, Sarathchandra P, Antoniw JW, et al. Human mesenchymal stem cells induce T cell anergy and downregulate T cell allo-responses via the TH2 pathway: relevance to tissue engineering human heart valves. *Tissue Eng*. 2006;12(8):2263-2273.

[122] Fiorina P, Jurewicz M, Augello A, et al. Immunomodulatory function of bone marrow-derived mesenchymal stem cells in experimental autoimmune type 1 diabetes. *J Immunol*. 2009;183(2):993-1004.

[123] Bai L, Lennon DP, Eaton V, et al. Human bone marrow-derived mesenchymal stem cells induce Th2-polarized immune response and promote endogenous repair in animal models of multiple sclerosis. *Glia*. 2009;57(11):1192-1203.

[124] Lim J-H, Kim J-S, Yoon I-H, et al. Immunomodulation of Delayed-Type Hypersensitivity Responses by Mesenchymal Stem Cells Is Associated with Bystander T Cell Apoptosis in the Draining Lymph Node. *J Immunol*. 2010;185(7):4022-4029.

[125] González M a, Gonzalez-Rey E, Rico L, Büscher D, Delgado M. Adipose-derived mesenchymal stem cells alleviate experimental colitis by inhibiting inflammatory and autoimmune responses. *Gastroenterology*. 2009;136(3):978-989.

[126] Boumaza I, Srinivasan S, Witt WT, et al. Autologous bone marrow-derived rat mesenchymal stem cells promote PDX-1 and insulin expression in the islets, alter T cell cytokine pattern and preserve regulatory T cells in the periphery and induce sustained normoglycemia. *J Autoimmun*. 2009;32(1):33-42.

[127] Madec AM, Mallone R, Afonso G, et al. Mesenchymal stem cells protect NOD mice from diabetes by inducing regulatory T cells. *Diabetologia*. 2009;52(7):1391-1399.

[128] Goodwin M, Sueblinvong V, Eisenhauer P, et al. Bone marrow-derived mesenchymal stromal cells inhibit Th2-mediated allergic airways inflammation in mice. *Stem Cells*. 2011;29(7):1137-1148.

[129] Kavanagh H, Mahon BP. Allogeneic mesenchymal stem cells prevent allergic airway inflammation by inducing murine regulatory T cells. *Allergy*. 2011;66(4):523-531.

[130] Tatara R, Ozaki K, Kikuchi Y, et al. Mesenchymal stromal cells inhibit Th17 but not regulatory T-cell differentiation. *Cytotherapy*. 2011;13(6):686-694.

[131] Ghannam S, Pène J, Torcy-Moquet G, Jorgensen C, Yssel H. Mesenchymal stem cells inhibit human Th17 cell differentiation and function and induce a T regulatory cell phenotype. *J Immunol*. 2010;185(1):302-312.

[132] Wang J, Wang G, Sun B, et al. Interleukin-27 suppresses experimental autoimmune encephalomyelitis during bone marrow stromal cell treatment. *J Autoimmun*. 2008;30(4):222-229.

[133] Zappia E, Casazza S, Pedemonte E, et al. Mesenchymal stem cells ameliorate experimental autoimmune encephalomyelitis inducing T-cell anergy. *Blood*. 2005;106(5):1755-1761.

[134] Rafei M, Campeau PM, Aguilar-Mahecha A, et al. Mesenchymal Stromal Cells Ameliorate Experimental Autoimmune Encephalomyelitis by Inhibiting CD4 Th17 T Cells in a CC Chemokine Ligand 2-Dependent Manner. *J Immunol*. 2009;182:5994-6002.

[135] Bouffi C, Bony C, Courties G, Jorgensen C, Noël D, No<unicode>235</unicode>l D. IL-6-dependent PGE2 secretion by mesenchymal stem cells inhibits local inflammation in experimental arthritis. *PLoS One*. 2010;5(12):e14247.

[136] English K, Ryan JM, Tobin L, Murphy MJ, Barry FP, Mahon BP. Cell contact, prostaglandin E2 and transforming growth factor beta 1 play non-redundant roles in human mesenchymal stem cell induction of CD4+CD25Highforkhead box P3+ regulatory T cells. *Clin Exp Immunol*. 2009;156:149-160.

[137] Gonzalez-Rey E, Gonzalez M a, Varela N, et al. Human adipose-derived

mesenchymal stem cells reduce inflammatory and T cell responses and induce regulatory T cells in vitro in rheumatoid arthritis. *Ann Rheum Dis*. 2010;69(1):241-248.

[138] Fallarino F, Grohmann U, You S, et al. The combined effects of tryptophan starvation and tryptophan catabolites down-regulate T cell receptor zeta-chain and induce a regulatory phenotype in naive T cells. *J Immunol*. 2006;176(11):6752-6761.

[139] Curti A, Trabanelli S, Salvestrini V, Baccarani M, Lemoli RM. The role of indoleamine 2,3-dioxygenase in the induction of immune tolerance: focus on hematology. *Blood*. 2009;113(11):2394-2401.

[140] Kong Q-F, Sun B, Bai S-S, et al. Administration of bone marrow stromal cells ameliorates experimental autoimmune myasthenia gravis by altering the balance of Th1/Th2/Th17/Treg cell subsets through the secretion of TGF-beta. *J Neuroimmunol*. 2009;207(1-2):83-91.

[141] Tasso R, Ilengo C, Quarto R, Cancedda R, Caspi RR, Pennesi G. Mesenchymal stem cells induce functionally active T-regulatory lymphocytes in a paracrine fashion and ameliorate experimental autoimmune uveitis. *Invest Ophthalmol Vis Sci*. 2012;53(2):786-793.

[142] Akiyama K, Chen C, Wang D, et al. Mesenchymal-stem-cell-induced immunoregulation involves FAS-ligand-/FAS-mediated T cell apoptosis. *Cell Stem Cell*. 2012;10:544-555.

[143] Casiraghi F, Azzollini N, Cassis P, et al. Pretransplant infusion of mesenchymal stem cells prolongs the survival of a semiallogeneic heart transplant through the

generation of regulatory T cells. *J Immunol*. 2008;181(6):3933-3946.

[144] Wang Y, Zhang A, Ye Z, Xie H, Zheng S. Bone marrow-derived mesenchymal stem cells inhibit acute rejection of rat liver allografts in association with regulatory T-cell expansion. *Transplant Proc*. 2009;41(10):4352-4356.

[145] Zhang Q, Shi S, Liu Y, et al. Mesenchymal stem cells derived from human gingiva are capable of immunomodulatory functions and ameliorate inflammation-related tissue destruction in experimental colitis. *J Immunol*. 2009;183(12):7787-7798.

[146] Nemeth K, Keane-Myers A, Brown JM, et al. Bone marrow stromal cells use TGF-beta to suppress allergic responses in a mouse model of ragweed-induced asthma. *Proc Natl Acad Sci U S A*. 2010;107(12):5652-5657.

[147] Rasmusson I, Uhlin M, Le Blanc K, Levitsky V. Mesenchymal stem cells fail to trigger effector functions of cytotoxic T lymphocytes. *J Leukoc Biol*. 2007;82(4):887-893.

[148] Maccario R, Podestà M, Moretta A, et al. Interaction of human mesenchymal stem cells with cells involved in alloantigen-specific immune response favors the differentiation of CD4+ T-cell subsets expressing a regulatory/suppressive phenotype. *Haematologica*. 2005;90(4):516-525.

[149] Rasmusson I, Ringdén O, Sundberg B, Le Blanc K. Mesenchymal stem cells inhibit the formation of cytotoxic T lymphocytes, but not activated cytotoxic T lymphocytes or natural killer cells. *Transplantation*. 2003;76(8):1208-1213.

[150] Karlsson H, Samarasinghe S, Ball LM, et al. Mesenchymal stem cells exert differential effects on alloantigen and virus-specific T-cell responses. *Blood*. 2008;112(3):532-541.

[151] Sart S, Tsai A-C, Li Y, Ma T. Three-Dimensional Aggregates of Mesenchymal Stem Cells: Cellular Mechanisms, Biological Properties, and Applications. *Tissue Eng Part B Rev*. 2013;00(00):1-46.

[152] Cesarz Z, Tamama K. Spheroid Culture of Mesenchymal Stem Cells. *Stem Cells Int*. 2016;2016:9176357.

[153] Lin R-Z, Lin R-Z, Chang H-Y. Recent advances in three-dimensional multicellular spheroid culture for biomedical research. *Biotechnol J*. 2008;3(9-10):1172-1184.

[154] Kurosawa H. Methods for inducing embryoid body formation: in vitro differentiation system of embryonic stem cells. *J Biosci Bioeng*. 2007;103(5):389-398. doi:10.1263/jbb.103.389.

[155] Gonzalez-Rodriguez D, Guevorkian K, Douezan S, Brochard-Wyart F. Soft matter models of developing tissues and tumors. *Science*. 2012;338(6109):910-917.

[156] Pastrana E, Silva-Vargas V, Doetsch F. Eyes wide open: a critical review of sphere-formation as an assay for stem cells. *Cell Stem Cell*. 2011;8(5):486-498.

[157] Follin B, Juhl M, Cohen S, Perdersen AE, Kastrup J, Ekblond A. Increased Paracrine Immunomodulatory Potential of Mesenchymal Stromal Cells in Three-Dimensional Culture. *Tissue Eng Part B Rev*. 2016.

[158] Kim J, Ma T. Endogenous extracellular matrices enhance human mesenchymal stem cell aggregate formation and survival. *Biotechnol Prog*. 2013;29(2):441-451.

[159] Lee EJ, Park SJ, Kang SK, et al. Spherical bullet formation via E-cadherin promotes therapeutic potency of mesenchymal stem cells derived from human umbilical cord blood for myocardial infarction. *Mol Ther*. 2012;20(7):1424-1433.

[160] Dromard C, Bourin P, André M, De Barros S, Casteilla L, Planat-Benard V.

Human adipose derived stroma/stem cells grow in serum-free medium as floating spheres. *Exp Cell Res*. 2011;317(6):770-780.

[161] Kapur SK, Wang X, Shang H, et al. Human adipose stem cells maintain proliferative, synthetic and multipotential properties when suspension cultured as self-assembling spheroids. *Biofabrication*. 2012;4(2):025004.

[162] Wuchter P, Boda-Heggemann J, Straub BK, et al. Processus and recessus adhaerentes: giant adherens cell junction systems connect and attract human mesenchymal stem cells. *Cell Tissue Res*. 2007;328(3):499-514.

[163] Frith JE, Thomson B, Genever PG. Dynamic three-dimensional culture methods enhance mesenchymal stem cell properties and increase therapeutic potential. *Tissue Eng Part C Methods*. 2010;16(4):735-749.

[164] Baraniak PR, Cooke MT, Saeed R, Kinney M a, Fridley KM, McDevitt TC. Stiffening of human mesenchymal stem cell spheroid microenvironments induced by incorporation of gelatin microparticles. *J Mech Behav Biomed Mater*. 2012;11:63-71.

[165] Ichinose S, Tagami M, Muneta T, Sekiya I. Morphological examination during in vitro cartilage formation by human mesenchymal stem cells. *Cell Tissue Res*. 2005;322(2):217-226.

[166] Peng R, Yao X, Cao B, Tang J, Ding J. The effect of culture conditions on the adipogenic and osteogenic inductions of mesenchymal stem cells on micropatterned surfaces. *Biomaterials*. 2012;33(26):6008-6019.

[167] McBeath R, Pirone DM, Nelson CM, Bhadriraju K, Chen CS. Cell shape, cytoskeletal tension, and RhoA regulate stem cell lineage commitment. *Dev Cell*.

2004;6(4):483-495.

[168] Engler AJ, Sen S, Sweeney HL, Discher DE. Matrix elasticity directs stem cell lineage specification. *Cell*. 2006;126(4):677-689.

[169] Bhang SH, Cho S-W, La W-G, et al. Angiogenesis in ischemic tissue produced by spheroid grafting of human adipose-derived stromal cells. *Biomaterials*. 2011;32(11):2734-2747.

[170] Zhang Q, Nguyen AL, Shi S, et al. Three-dimensional spheroid culture of human gingiva-derived mesenchymal stem cells enhances mitigation of chemotherapy-induced oral mucositis. *Stem Cells Dev*. 2012;21(6):937-947.

[171] Santos JM, Camões SP, Filipe E, et al. Three-dimensional spheroid cell culture of umbilical cord tissue-derived mesenchymal stromal cells leads to enhanced paracrine induction of wound healing. *Stem Cell Res Ther*. 2015;6:90.

[172] Lee EJ, Choi E-K, Kang SK, et al. N-cadherin determines individual variations in the therapeutic efficacy of human umbilical cord blood-derived mesenchymal stem cells in a rat model of myocardial infarction. *Mol Ther*. 2012;20:155-167.

[173] Bartosh TJ, Ylöstalo JH, Mohammadipoor A, et al. Aggregation of human mesenchymal stromal cells (MSCs) into 3D spheroids enhances their antiinflammatory properties. *Proc Natl Acad Sci U S A*. 2010;107(31):13724-13729.

[174] Ylöstalo JH, Bartosh TJ, Coble K, Prockop DJ. Human mesenchymal stem/stromal cells cultured as spheroids are self-activated to produce prostaglandin E2 that directs stimulated macrophages into an anti-inflammatory phenotype. *Stem Cells*. 2012;30(10):2283-2296.

[175] Bartosh TJ, Ylöstalo JH, Bazhanov N, Kuhlman J, Prockop DJ. Dynamic compaction of human mesenchymal stem/precursor cells (MSC) into spheres self-activates caspase-dependent IL1 signaling to enhance secretion of modulators of inflammation and immunity (PGE2, TSG6 and STC1). *Stem Cells*. 2013;(254).

[176] Molendijk I, Barnhoorn MC, de Jonge-Muller ESM, et al. Intraluminal Injection of Mesenchymal Stromal Cells in Spheroids Attenuates Experimental Colitis. *J Crohns Colitis*. 2016.

[177] Johnstone B, Hering TM, Caplan AI, Goldberg VM, Yoo JU. In vitro chondrogenesis of bone marrow-derived mesenchymal progenitor cells. *Exp Cell Res*. 1998;238(1):265-272.

[178] Winter A, Breit S, Parsch D, et al. Cartilage-like gene expression in differentiated human stem cell spheroids: A comparison of bone marrow-derived and adipose tissue-derived stromal cells. *Arthritis Rheum*. 2003;48(2):418-429.

[179] Baraniak PR, McDevitt TC. Scaffold-free culture of mesenchymal stem cell spheroids in suspension preserves multilineage potential. *Cell Tissue Res*. 2011.

[180] Hsu S, Huang G, Lin S. Enhanced Chondrogenic Differentiation Potential of Human Gingival Fibroblasts by Spheroid Formation on Chitosan Membranes. *Tissue Eng Part A*. 2011;18.

[181] Yoon H, Bhang S, Shin J. Enhanced Cartilage Formation Via Three-Dimensional Cell Engineering of Human Adipose-Derived Stem Cells. *Tissue Eng Part A*. 2012;18:1-8.

[182] Sen A, Kallos MS, Behie LA. Effects of Hydrodynamics on Cultures of Mammalian Neural Stem Cell Aggregates in Suspension Bioreactors. *Ind Eng*

Chem Res. 2001;40(23):5350-5357.

[183] Kabiri M, Kul B, Lott WB, et al. 3D mesenchymal stem/stromal cell osteogenesis and autocrine signalling. *Biochem Biophys Res Commun*. 2012;419(2):142-147.

[184] Suzuki S, Muneta T, Tsuji K, et al. Properties and usefulness of aggregates of synovial mesenchymal stem cells as a source for cartilage regeneration. *Arthritis Res Ther*. 2012;14(3):R136.

[185] Wang C-C, Chen C-H, Hwang S-M, et al. Spherically Symmetric Mesenchymal Stromal Cell Bodies Inherent with Endogenous Extracellular Matrices for Cellular Cardiomyoplasty. *Stem Cells*. 2009;27(3):724-732.

[186] Amos PJ, Kapur SK, Stapor PC, et al. Human Adipose-Derived Stromal Cells Accelerate Diabetic Wound Healing: Impact of Cell Formulation and Delivery. *Tissue Eng Part A*. 2010;16(5):1595-1606.

[187] Li Y, Guo G, Li L, et al. Three-dimensional spheroid culture of human umbilical cord mesenchymal stem cells promotes cell yield and stemness maintenance. *Cell Tissue Res*. 2015;360(2):297-307.

[188] Isern J, Martín-Antonio B, Ghazanfari R, et al. Self-Renewing Human Bone Marrow Mesenspheres Promote Hematopoietic Stem Cell Expansion. *Cell Rep*. 2013:1-11.

[189] Pennock R, Bray E, Pryor P, et al. Human cell dedifferentiation in mesenchymal condensates through controlled autophagy. *Sci Rep*. 2015;5:13113.

[190] Kelm JM, Fussenegger M. Scaffold-free cell delivery for use in regenerative medicine. *Adv Drug Deliv Rev*. 2010;62(7-8):753-764.

[191] Ma D, Zhong C, Yao H, et al. Engineering Injectable Bone Using Bone Marrow

Stromal Cell Aggregates. *Stem Cells Dev*. 2011;20(6):989-999.

[192] Lee W-Y, Chang Y-H, Yeh Y-C, et al. The use of injectable spherically symmetric cell aggregates self-assembled in a thermo-responsive hydrogel for enhanced cell transplantation. *Biomaterials*. 2009;30(29):5505-5513.

[193] Roemeling-van Rhijn M, Mensah FKF, Korevaar SS, et al. Effects of Hypoxia on the Immunomodulatory Properties of Adipose Tissue-Derived Mesenchymal Stem cells. *Front Immunol*. 2013;4(July):203.

[194] Bassi EJ, Aita CAM, Câmara NOS. Immune regulatory properties of multipotent mesenchymal stromal cells: Where do we stand? *World J Stem Cells*. 2011;3(1):1-8.

[195] Yi T, Song SU. Immunomodulatory properties of mesenchymal stem cells and their therapeutic applications. *Arch Pharm Res*. 2012;35(2):213-221.

[196] Tolar J, Le Blanc K, Keating A, Blazar BR. Concise review: hitting the right spot with mesenchymal stromal cells. *Stem Cells*. 2010;28(8):1446-1455.

[197] Sekiya I, Larson BL, Smith JR, Pochampally R, Cui J-G, Prockop DJ. Expansion of human adult stem cells from bone marrow stroma: conditions that maximize the yields of early progenitors and evaluate their quality. *Stem Cells*. 2002;20(6):530-541.

[198] Ungrin MD, Joshi C, Nica A, Bauwens C, Zandstra PW. Reproducible, ultra high-throughput formation of multicellular organization from single cell suspension-derived human embryonic stem cell aggregates. *PLoS One*. 2008;3(2):e1565.

[199] François M, Copland IB, Yuan S, Romieu-Mourez R, Waller EK, Galipeau J. Cryopreserved mesenchymal stromal cells display impaired immunosuppressive

properties as a result of heat-shock response and impaired interferon-γ licensing. *Cytotherapy*. 2012;14(2):147-152.

[200] Moll G, Alm JJ, Davies LC, et al. Do Cryopreserved Mesenchymal Stromal Cells Display Impaired Immunomodulatory and Therapeutic Properties? *Stem Cells*. 2014;32(9):2430-2442.

[201] Chinnadurai R, Copland IB, Patel SR, Galipeau J. IDO-independent suppression of T cell effector function by IFN-γ-licensed human mesenchymal stromal cells. *J Immunol*. 2014;192:1491-1501.

[202] Jung S, Panchalingam KM, Rosenberg L, Behie L a. Ex vivo expansion of human mesenchymal stem cells in defined serum-free media. *Stem Cells Int*. 2012;2012:123030.

[203] Abdelrazik H, Spaggiari GM, Chiossone L, Moretta L. Mesenchymal stem cells expanded in human platelet lysate display a decreased inhibitory capacity on T- and NK-cell proliferation and function. *Eur J Immunol*. 2011;41(11):3281-3290.

[204] Flemming A, Schallmoser K, Strunk D, Stolk M, Volk H-D, Seifert M. Immunomodulative efficacy of bone marrow-derived mesenchymal stem cells cultured in human platelet lysate. *J Clin Immunol*. 2011;31(6):1143-1156.

[205] Alimperti S, Lei P, Wen Y, Tian J, Campbell AM, Andreadis ST. Serum-free spheroid suspension culture maintains mesenchymal stem cell proliferation and differentiation potential. *Biotechnol Prog*. 2014;30(4):974-983.

[206] Ylostalo JH, Bartosh TJ, Tiblow A, Prockop DJ. Unique characteristics of human mesenchymal stromal/progenitor cells pre-activated in 3-dimensional cultures under different conditions. *Cytotherapy*. 2014;16(11):1486-1500.

[207] Gnecchi M, He H, Noiseux N, et al. Evidence supporting paracrine hypothesis for Akt-modified mesenchymal stem cell-mediated cardiac protection and functional improvement. *FASEB J*. 2006;20(6):661-669.

[208] Li W, Ma N, Ong L-L, et al. Bcl-2 engineered MSCs inhibited apoptosis and improved heart function. *Stem Cells*. 2007;25(8):2118-2127.

[209] Potier E, Ferreira E, Andriamanalijaona R, et al. Hypoxia affects mesenchymal stromal cell osteogenic differentiation and angiogenic factor expression. *Bone*. 2007;40(4):1078-1087.

[210] Lee RH, Seo MJ, Pulin A a., Gregory C a., Ylostalo J, Prockop DJ. The CD34-like protein PODXL and {alpha}6-integrin (CD49f) identify early progenitor MSCs with increased clonogenicity and migration to infarcted heart in mice. *Blood*. 2009;113:816-826.

[211] Zimmermann JA, Mcdevitt TC. Pre-conditioning mesenchymal stromal cell spheroids for immunomodulatory paracrine factor secretion. *Cytotherapy*. 2014;16(3):331-345.

[212] Adamopoulos IE, Mellins ED. Alternative pathways of osteoclastogenesis in inflammatory arthritis. *Nat Rev Rheumatol*. 2014;11(3):189-194.

[213] Simonet W., Lacey D., Dunstan C., et al. Osteoprotegerin: A Novel Secreted Protein Involved in the Regulation of Bone Density. *Cell*. 1997;89(2):309-319.

[214] Tsuda E, Goto M, Mochizuki S, et al. Isolation of a Novel Cytokine from Human Fibroblasts That Specifically Inhibits Osteoclastogenesis. *Biochem Biophys Res Commun*. 1997;234(1):137-142.

[215] Lacey D., Timms E, Tan H-L, et al. Osteoprotegerin Ligand Is a Cytokine that

Regulates Osteoclast Differentiation and Activation. *Cell*. 1998;93(2):165-176.

[216] Hattersley G, Owens J, Flanagan AM, Chambers TJ. Macrophage colony stimulating factor (M-CSF) is essential for osteoclast formation in vitro. *Biochem Biophys Res Commun*. 1991;177(1):526-531.

[217] Nakashima T, Hayashi M, Fukunaga T, et al. Evidence for osteocyte regulation of bone homeostasis through RANKL expression. *Nat Med*. 2011;17(10):1231-1234.

[218] Kartsogiannis V, Zhou H, Horwood N., et al. Localization of RANKL (receptor activator of NFκB ligand) mRNA and protein in skeletal and extraskeletal tissues. *Bone*. 1999;25(5):525-534.

[219] Grigoriadis A, Wang Z, Cecchini M, et al. c-Fos: a key regulator of osteoclast-macrophage lineage determination and bone remodeling. *Science (80-).* 1994;266(5184):443-448.

[220] Takayanagi H, Kim S, Koga T, et al. Induction and Activation of the Transcription Factor NFATc1 (NFAT2) Integrate RANKL Signaling in Terminal Differentiation of Osteoclasts. *Dev Cell*. 2002;3(6):889-901.

[221] Boyle WJ, Simonet WS, Lacey DL. Osteoclast differentiation and activation. *Nature*. 2003;423(6937):337-342.

[222] Bucay N, Sarosi I, Dunstan CR, et al. Osteoprotegerin-deficient mice develop early onset osteoporosis and arterial calcification. *Genes Dev*. 1998;12(9):1260-1268.

[223] Guerrini MM, Takayanagi H. The immune system, bone and RANKL. *Arch Biochem Biophys*. 2014;561:118-123.

[224] Yun TJ, Chaudhary PM, Shu GL, et al. OPG/FDCR-1, a TNF receptor family

member, is expressed in lymphoid cells and is up-regulated by ligating CD40. *J Immunol*. 1998;161(11):6113-6121.

[225] Wong BR, Josien R, Lee SY, et al. TRANCE (tumor necrosis factor [TNF]-related activation-induced cytokine), a new TNF family member predominantly expressed in T cells, is a dendritic cell-specific survival factor. *J Exp Med*. 1997;186(12):2075-2080.

[226] Josien R, Wong BR, Li HL, Steinman RM, Choi Y. TRANCE, a TNF family member, is differentially expressed on T cell subsets and induces cytokine production in dendritic cells. *J Immunol*. 1999;162(5):2562-2568.

[227] Josien R, Li HL, Ingulli E, et al. TRANCE, a tumor necrosis factor family member, enhances the longevity and adjuvant properties of dendritic cells in vivo. *J Exp Med*. 2000;191(3):495-502.

[228] Anderson DM, Maraskovsky E, Billingsley WL, et al. A homologue of the TNF receptor and its ligand enhance T-cell growth and dendritic-cell function. *Nature*. 1997;390(6656):175-179.

[229] Yun TJ, Tallquist MD, Aicher A, et al. Osteoprotegerin, a Crucial Regulator of Bone Metabolism, Also Regulates B Cell Development and Function. *J Immunol*. 2001;166(3):1482-1491.

[230] Kotake S, Udagawa N, Hakoda M, et al. Activated human T cells directly induce osteoclastogenesis from human monocytes: possible role of T cells in bone destruction in rheumatoid arthritis patients. *Arthritis Rheum*. 2001;44(5):1003-1012.

[231] Walsh MC, Choi Y. Biology of the RANKL-RANK-OPG System in Immunity,

Bone, and Beyond. *Front Immunol*. 2014;5:511.

[232] Oshita K, Yamaoka K, Udagawa N, et al. Human mesenchymal stem cells inhibit osteoclastogenesis through osteoprotegerin production. *Arthritis Rheum*. 2011;63(6):1658-1667.

[233] Walsh MC, Choi Y. Biology of the TRANCE axis. *Cytokine Growth Factor Rev*. 2003;14(3-4):251-263.

[234] Glass DA, Bialek P, Ahn JD, et al. Canonical Wnt Signaling in Differentiated Osteoblasts

[235] Goldring SR, Goldring MB. Eating bone or adding it: the Wnt pathway decides. *Nat Med*. 2007;13(2):133-134.

[236] Walsh MC, Choi Y. Biology of the RANKL-RANK-OPG System in Immunity, Bone, and Beyond. *Front Immunol*. 2014;5:511.

[237] Le Blanc K, Rasmusson I, Götherström C, et al. Mesenchymal stem cells inhibit the expression of CD25 (interleukin-2 receptor) and CD38 on phytohaemagglutinin-activated lymphocytes. *Scand J Immunol*. 2004;60(3):307-315.

[238] Takayanagi H, Ogasawara K, Hida S, et al. T-cell-mediated regulation of osteoclastogenesis by signalling cross-talk between RANKL and IFN-gamma. *Nature*. 2000;408(6812):600-605.

[239] Pietilä M, Lehtonen S, Tuovinen E, et al. CD200 Positive Human Mesenchymal Stem Cells Suppress TNF-Alpha Secretion from CD200 Receptor Positive Macrophage-Like Cells. Panepucci RA, ed. *PLoS One*. 2012;7(2):e31671.

[240] Jung SM, Kim KW, Yang C-W, Park S-H, Ju JH. Cytokine-Mediated Bone

Destruction in Rheumatoid Arthritis. *J Immunol Res*. 2014;2014:1-15.

[241] Walsh MC, Choi Y. Biology of the TRANCE axis. *Cytokine Growth Factor Rev*. 2003;14(3-4):251-263.

[242] Glass DA, Bialek P, Ahn JD, et al. Canonical Wnt Signaling in Differentiated Osteoblasts Controls Osteoclast Differentiation. *Dev Cell*. 2005;8(5):751-764.

[243] Jackson A, Vayssière B, Garcia T, et al. Gene array analysis of Wnt-regulated genes in C3H10T1/2 cells. *Bone*. 2005;36(4):585-598.

[244] Holmen SL, Zylstra CR, Mukherjee A, et al. Essential Role of -Catenin in Postnatal Bone Acquisition. *J Biol Chem*. 2005;280(22):21162-21168.

[245] Lee RH, Pulin A a, Seo MJ, et al. Intravenous hMSCs improve myocardial infarction in mice because cells embolized in lung are activated to secrete the anti-inflammatory protein TSG-6. *Cell Stem Cell*. 2009;5(1):54-63.

[246] Duijvestein M, Wildenberg ME, Welling MM, et al. Pretreatment with interferon-γ enhances the therapeutic activity of mesenchymal stromal cells in animal models of colitis. *Stem Cells*. 2011;29(10):1549-1558.

[247] Polchert D, Sobinsky J, Douglas G, et al. IFN-gamma activation of mesenchymal stem cells for treatment and prevention of graft versus host disease. *Eur J Immunol*. 2008;38:1745-1755.

[248] Carpenedo RL, Bratt-Leal AM, Marklein RA, et al. Homogeneous and organized differentiation within embryoid bodies induced by microsphere-mediated delivery of small molecules. *Biomaterials*. 2009;30(13):2507-2515.

[249] Purpura K a, Bratt-Leal AM, Hammersmith K a, McDevitt TC, Zandstra PW. Systematic engineering of 3D pluripotent stem cell niches to guide blood

development. *Biomaterials*. 2012;33(5):1271-1280.

[250] Bratt-Leal AM, Nguyen AH, Hammersmith K a., Singh A, McDevitt TC. A microparticle approach to morphogen delivery within pluripotent stem cell aggregates. *Biomaterials*. 2013;34:7227-7235.

[251] Goude MC, McDevitt TC, Temenoff JS. Chondroitin sulfate microparticles modulate transforming growth factor-β1-induced chondrogenesis of human mesenchymal stem cell spheroids. *Cells Tissues Organs*. 2014;199:117-130.

[252] Hettiaratchi MH, Miller T, Temenoff JS, Guldberg RE, McDevitt TC. Heparin microparticle effects on presentation and bioactivity of bone morphogenetic protein-2. *Biomaterials*. 2014;35(25):7228-7238.

[253] Saesen E, Sarrazin S, Laguri C, et al. Insights into the mechanism by which interferon-γ basic amino acid clusters mediate protein binding to heparan sulfate. *J Am Chem Soc*. 2013;135:9384-9390.

[254] Lortat-Jacob H, Kleinman HK, Grimaud JA. High-affinity binding of interferon-gamma to a basement membrane complex (matrigel). *J Clin Invest*. 1991;87:878-883.

[255] Lortat-Jacob H, Baltzer F, Grimaud JA. Heparin decreases the blood clearance of interferon-gamma and increases its activity by limiting the processing of its carboxyl-terminal sequence. *J Biol Chem*. 1996;271:16139-16143.

[256] Douglas MS, Rix DA, Dark JH, Talbot D, Kirby JA. Examination of the mechanism by which heparin antagonizes activation of a model endothelium by interferon-gamma (IFN-gamma). *Clin Exp Immunol*. 1997;107:578-584.

[257] Seto SP, Casas ME, Temenoff JS. Differentiation of mesenchymal stem cells in

heparin-containing hydrogels via coculture with osteoblasts. *Cell Tissue Res*. 2012;347:589-601.

[258] Krampera M. Mesenchymal stromal cell "licensing": a multistep process. *Leukemia*. 2011;25(9):1408-1414.

[259] Melief SM, Schrama E, Brugman MH, et al. Multipotent stromal cells induce human regulatory T cells through a novel pathway involving skewing of monocytes toward anti-inflammatory macrophages. *Stem Cells*. 2013;31(9):1980-1991.

[260] Cutler AJ, Limbani V, Girdlestone J, Navarrete C V. Umbilical Cord-Derived Mesenchymal Stromal Cells Modulate Monocyte Function to Suppress T Cell Proliferation. *J Immunol*. 2010;185(11):6617-6623.

[261] DelaRosa O, Lombardo E, Beraza A, et al. Requirement of IFN-gamma-mediated indoleamine 2,3-dioxygenase expression in the modulation of lymphocyte proliferation by human adipose-derived stem cells. *Tissue Eng Part A*. 2009;15:2795-2806.

[262] Vallés G, Bensiamar F, Crespo L, Arruebo M, Vilaboa N, Saldaña L. Topographical cues regulate the crosstalk between MSCs and macrophages. *Biomaterials*. 2015;37:124-133.

[263] Abdeen A a, Weiss JB, Lee J, Kilian K a. Matrix composition and mechanics direct proangiogenic signaling from mesenchymal stem cells. *Tissue Eng Part A*. 2014;20:2737-2745.

[264] Frazier TP, McLachlan JB, Gimble JM, Tucker H a., Rowan BG. Human Adipose-Derived Stromal/Stem Cells Induce Functional CD4\n +\n CD25\n +\n FoxP3\n

+\n CD127\n −\n Regulatory T Cells Under Low Oxygen Culture Conditions. *Stem Cells Dev*. 2014;23:968-977.

[265] Murphy WL, McDevitt TC, Engler AJ. Materials as stem cell regulators. *Nat Mater*. 2014;13:547-557.

[266] Ankrum JA, Dastidar RG, Ong JF, Levy O, Karp JM. Performance-enhanced mesenchymal stem cells via intracellular delivery of steroids. *Sci Rep*. 2014;4.

[267] Sudres M, Norol F, Trenado A, et al. Bone Marrow Mesenchymal Stem Cells Suppress Lymphocyte Proliferation In Vitro but Fail to Prevent Graft-versus-Host Disease in Mice. *J Immunol*. 2006;176:7761-7767.

[268] Constantin G, Marconi S, Rossi B, et al. Adipose-derived mesenchymal stem cells ameliorate chronic experimental autoimmune encephalomyelitis. *Stem Cells*. 2009;27:2624-2635.

[269] Le Blanc K, Frassoni F, Ball L, et al. Mesenchymal stem cells for treatment of steroid-resistant, severe, acute graft-versus-host disease: a phase II study. *Lancet*. 2008;371(9624):1579-1586.

[270] Wang D, Li J, Zhang Y, et al. Umbilical cord mesenchymal stem cell transplantation in active and refractory systemic lupus erythematosus: a multicenter clinical study. *Arthritis Res Ther*. 2014;16:R79.

[271] Renner P, Eggenhofer E, Rosenauer A, et al. Mesenchymal Stem Cells Require a Sufficient, Ongoing Immune Response to Exert Their Immunosuppressive Function. *Transplant Proc*. 2009;41:2607-2611.

[272] Baker M. Stem-cell drug fails crucial trials. *Nature*. 2009:1-4.

[273] Inoue S, Popp FC, Koehl GE, et al. Immunomodulatory effects of mesenchymal

stem cells in a rat organ transplant model. *Transplantation*. 2006;81:1589-1595.

[274] Chen X, Gan Y, Li W, et al. The interaction between mesenchymal stem cells and steroids during inflammation. *Cell Death Dis*. 2014;5:e1009.

[275] Ren J, Jin P, Sabatino M, et al. Global transcriptome analysis of human bone marrow stromal cells (BMSC) reveals proliferative, mobile and interactive cells that produce abundant extracellular matrix proteins, some of which may affect BMSC potency. *Cytotherapy*. 2011;13(6):661-674.

[276] Hsieh J-Y, Wang H-W, Chang S-J, et al. Mesenchymal stem cells from human umbilical cord express preferentially secreted factors related to neuroprotection, neurogenesis, and angiogenesis. *PLoS One*. 2013;8(8):e72604.

[277] Billing AM, Ben Hamidane H, Dib SS, et al. Comprehensive transcriptomic and proteomic characterization of human mesenchymal stem cells reveals source specific cellular markers. *Sci Rep*. 2016;6:21507.

[278] Delorme B, Ringe J, Pontikoglou C, et al. Specific lineage-priming of bone marrow mesenchymal stem cells provides the molecular framework for their plasticity. *Stem Cells*. 2009;27(5):1142-1151.

[279] Ren G, Su J, Zhang L, et al. Species variation in the mechanisms of mesenchymal stem cell-mediated immunosuppression. *Stem Cells*. 2009;27(8):1954-1962.

[280] Shultz LD, Brehm MA, Garcia-Martinez JV, Greiner DL. Humanized mice for immune system investigation: progress, promise and challenges. *Nat Rev Immunol*. 2012;12(11):786-798.

[281] Rongvaux A, Willinger T, Martinek J, et al. Development and function of human innate immune cells in a humanized mouse model. *Nat Biotechnol*.

2014;32(4):364-372.

[282] Chen P, Huang Y, Womer KL. Effects of mesenchymal stromal cells on human myeloid dendritic cell differentiation and maturation in a humanized mouse model. *J Immunol Methods*. 2015;427:100-104.

[283] Roemeling-van Rhijn M, Khairoun M, Korevaar SS, et al. Human Bone Marrow- and Adipose Tissue-derived Mesenchymal Stromal Cells are Immunosuppressive In vitro and in a Humanized Allograft Rejection Model. *J Stem Cell Res Ther*. 2013;Suppl 6(1):20780.

[284] Amarnath S, Foley JE, Farthing DE, et al. Bone marrow-derived mesenchymal stromal cells harness purinergenic signaling to tolerize human Th1 cells in vivo. *Stem Cells*. 2015;33(4):1200-1212.

[285] Tobin LM, Healy ME, English K, Mahon BP. Human mesenchymal stem cells suppress donor CD4(+) T cell proliferation and reduce pathology in a humanized mouse model of acute graft-versus-host disease. *Clin Exp Immunol*. 2013;172(2):333-348.

[286] Sun Y-Q, Zhang Y, Li X, et al. Insensitivity of Human iPS Cells-Derived Mesenchymal Stem Cells to Interferon-γ-induced HLA Expression Potentiates Repair Efficiency of Hind Limb Ischemia in Immune Humanized NOD Scid Gamma Mice. *Stem Cells*. 2015;33(12):3452-3467.

[287] Ling W, Zhang J, Yuan Z, et al. Mesenchymal stem cells use IDO to regulate immunity in tumor microenvironment. *Cancer Res*. 2014;74(5):1576-1587.

[288] Kappelman MD, Rifas-Shiman SL, Porter CQ, et al. Direct health care costs of Crohn's disease and ulcerative colitis in US children and adults. *Gastroenterology*.

2008;135(6):1907-1913.

[289] Strober W, Fuss I, Mannon P. The fundamental basis of inflammatory bowel disease. *J Clin Invest*. 2007;117(3):514-521.

[290] Dalal J, Gandy K, Domen J. Role of mesenchymal stem cell therapy in Crohn's disease. *Pediatr Res*. 2012;71(4 Pt 2):445-451.

[291] Wirtz S, Neurath MF. Mouse models of inflammatory bowel disease. *Adv Drug Deliv Rev*. 2007;59(11):1073-1083.

[292] Jurjus AR, Khoury NN, Reimund J-M. Animal models of inflammatory bowel disease. *J Pharmacol Toxicol Methods*. 2004;50(2):81-92.

[293] Wirtz S, Neufert C, Weigmann B, Neurath MF. Chemically induced mouse models of intestinal inflammation. *Nat Protoc*. 2007;2(3):541-546.

[294] Alex P, Zachos NC, Nguyen T, et al. Distinct cytokine patterns identified from multiplex profiles of murine DSS and TNBS-induced colitis. *Inflamm Bowel Dis*. 2009;15(3):341-352.

[295] Perše M, Cerar A. Dextran sodium sulphate colitis mouse model: traps and tricks. *J Biomed Biotechnol*. 2012;2012:718617.

[296] Allen AB, Zimmermann JA, Burnsed OA, et al. Environmental Manipulation to Promote Stem Cell Survival In Vivo: Use of Aggregation, Oxygen Carrier, and BMP-2 Co-Delivery Strategies. *J Mater Chem B*. 2016.

[297] Allen AB, Gazit Z, Su S, Stevens HY, Guldberg RE. In Vivo Bioluminescent Tracking of Mesenchymal Stem Cells Within Large Hydrogel Constructs. *Tissue Eng Part C Methods*. 2014.

[298] Anderson P, Souza-Moreira L, Morell M, et al. Adipose-derived mesenchymal

stromal cells induce immunomodulatory macrophages which protect from experimental colitis and sepsis. *Gut*. 2012:1-12.

[299] Gonzalez-Rey E, Chorny A, Delgado M. Therapeutic action of ghrelin in a mouse model of colitis. *Gastroenterology*. 2006;130(6):1707-1720.